# WATER USE, STORAGE AND TRANSFER IN TROPICAL BAMBOOS

The Dissertation Submitted in Partial Fulfillment for the
Academic Degree of "Doctor of Philosophy"
of the Faculty of Forest Sciences and Forest Ecology
of the Georg-August-Universität Göttingen

submitted by
Dongming Fang

from Hebei, China
Göttingen, 2017

# Abstract

Bamboos (Poaceae, Bambuseae) are abundant in the natural vegetation of tropical and subtropical regions. They have been used by humans for millennia, and multiple additional bamboo usages have been developed in recent decades. From much better-studied water use characteristics in dicot tree species, the water use patterns of bamboos could potentially vary substantially due to several aspects. Bamboos are monocotyledonous species and lack secondary growth, and vascular conduits of bamboo xylem thus have to remain functional throughout the ontogeny of a bamboo culm. The culm is mostly hollow and high in parenchyma content, which might lead to a high potential for stem water storage. Additionally, culms are often connected via rhizomes, which offers pathways for a redistribution of water among connected culms. In this study, we addressed water circulation patterns in bamboos with particular respect to (1) water use rates, (2) the role of the stem water storage, and (3) water transfer among culms. Applied methods include thermal sap flux measurements (thermal dissipation probes, TDP; and stem heat balance, SHB), deuterium tracing and modeling. We conducted lab and field experiments, and monitored water use in the field. Field studies were mainly carried out in southern China and on Java, Indonesia. Four bamboos species were studied (*Bambusa vulgaris*, *Dendrocalamus asper*, *Gigantochloa atroviolacea* and *Gigantochloa apus*) in parallel to several tree species for comparison.

To measure sap flux density of bamboos as precisely as possible, in the first step we calibrated the TDP method in the laboratory and the field. In both potted plant and field calibration experiments, we showed that the TDP method was suitable and reliable for sap flow measurements on bamboos after calibration. The potted plant experiment confirmed commonly reported underestimations of the TDP method as well as the accuracy of a second sap flux method, the stem heat balance technique. However, estimates with 1-cm-length TDP were significantly linearly correlated with those by the stem heat balance and a gravimetric method. From these linear relationships between estimates of the two methods, we subsequently derived species-specific calibration pa-

rameters for the TDP method for each of the four bamboo species in situ. The species-specific calibration parameters varied significantly among species, reflecting differences in wood thermal properties even though all four studied bamboo species are big, arborescent bamboos.

To gain a better understanding of the effects of wood thermal property on TDP measurements and accuracy, we examined changes in TDP-derived sap flux density with changing stem water content in bamboo culms. In a three-step approach, we conducted a culm dehydration experiment in the laboratory, monitored bamboos with TDP in situ and lastly implemented a steady-state thermal model. One central assumption of the TDP method is a constant wood thermal conductivity for determining maximum temperature differences between heated and reference probes of the TDP sensors. However, due to dynamics in bamboo culm water content, these assumptions may not always hold. In the dehydration experiment and numerical modeling simulations, we showed that wood thermal conductivity decreases with decreasing culm water content, which led to increasing maximum temperature differences and consequently to an underestimation of sap flux density if the change in water content was ignored. Keeping other controlling variables constant, we found that underestimations became particularly apparent 1) for large decreases of water content from nighttime to daytime, 2) at relatively low sap flux density, and 3) for relatively larger nighttime water content when the ratio of decline to the daytime was kept constant (e.g., by one half). Based on these insights, we provide a novel logistic-regression correcting equation using three parameters related to nighttime and daytime water content.

Bamboos were found to maintain relatively higher maximal sap flux density ($21.6$ - $70.5$ g cm$^{-2}$ h$^{-1}$) compared to nearby tree species ($10.5$ - $23.3$ g cm$^{-2}$ h$^{-1}$; *Gmelina arborea*, *Shorea leprosula* and *Hevea brasiliensis*). However, we did find evidence of diurnal hysteresis between sap flux density and transpirational driving variables (e.g., vapor pressure deficit and radiation), which indicated a decoupling from atmospheric processes and a rapid withdrawal of water from the stem during the morning hours. Observations with TDP at the top and bottom of selected bamboo culms manifested that stem water storage mechanisms supported only about 10% of daily transpiration of bamboos. Further, the relatively short water residence time in bamboo culms ($5.5$ - $6.3$ days) as derived from deuterium tracing methods also implied a rapid exchange of water between conducting pathways and storage compartments and thus a limited capacity for stem water storage in bamboos. Therefore, for the studied bamboo species, stem water storage mechanisms were shown to be of less

importance than we had assumed considering the significant percentages of parenchyma tissue in bamboo culms.

The prior study points to only small contributions of internal stem water storage to daily transpiration of bamboos. Nonetheless, the interconnected underground rhizome systems of bamboos can provide additional water transfer to cope with and balance water demand. The deuterium tracing applied in this study pointed to the existence of below-ground water transfer among culms within the same clumps. This mechanism provided significant transfer to newly sprouted culms. For newly sprouted culms, about 48% of daily water use may be supplied by established neighboring bamboo culms. When all established culms in a certain clump were removed, water use of newly sprouted culms could drop by about 80%. The dependency of newly sprouted culms from established culms largely disappeared after they started to produce leaves. However, after about four months since their emergence, newly sprouted culms kept active nighttime sap flow regardless of whether they were in leaves or not. To explore the mechanisms behind these somewhat unusual water use patterns, we focused on and discussed in detail potential driving forces as well as possible interactions with nutrient redistribution mechanisms.

At last, as a case study in a tropical dry forest in Ecuador, stem water storage estimated with the deuterium tracing method was assessed on a stem-succulent tree species (*Ceiba trichistandra*) and two coexisting evergreen species (*Capparis scabrida*, *Geoffroea spinosa*) and two other deciduous species (*Eriotheca ruizii*, *Erythrina velutina*). Unlike the relatively small stems of bamboos, stem-succulent trees are characterized by large, "swollen" trunks that can reach several meters in diameter. Large water storage ability of succulent stems was confirmed by the relatively longer water residence time (21.7 days) of a deciduous stem-succulent tree species (*C. trichistandra*) in contrast to the two evergreen species (on average 12.8 days; *C. scabrida*, *G. spinosa*) at the same sites. However, the water residence time of *C. trichistandra* (average diameter 76 cm) did not show significant differences to the two accompanying deciduous species (*E. velutina* and *E. ruizii*) with average diameters of 28 and 56 cm (water residence time 19 days). A literature review of woody species (n = 33) in which water residence time was estimated with deuterium tracing suggested, that residence time increases with plant diameter. The bamboos from the previous study in Java as well as the dry forest trees in Ecuador fit well into this picture, with the bamboos at the low diameter/short residence time end and the stem succulent *C. trichistandra* at the big diameter/long

residence time end. Additionally to its diameter-dependency, residence time was found to increase significantly with decreasing wood density.

In conclusion, the studied bamboos reached comparably high maximal sap flux densities. Culm water storage did not contribute substantially to daily transpiration. The residence time of water in bamboos culms was at the lower end of all available studies. The interconnected underground rhizome systems of bamboos were used for water transfer in particular to newly sprouted, leafless culms. Further exploring such underlying eco-hydrological mechanisms in greater detail will be a challenge for the years and studies to come.

# Table of contents

# Chapter 1

# Introduction

## 1.1 Water circulation within and between plants

Unidirectional water transport from the soil through plants to the atmosphere was thought to be the general framework when studying plant water use (Goldsmith, 2013; Philip, 1966). However, this framework has been gradually expanded by new findings, such as foliage water uptake (Goldsmith et al., 2013; Studer et al., 2015), inverse flow from the leaves to the soil (Eller et al., 2013; Goldsmith, 2013), soil water translocation by roots (Burgess et al., 2001b; Sakuratani et al., 1999; Smith et al., 1999) and water transfer among interconnected plants through roots (Adonsou et al., 2016) or rhizomes (Zhao et al., 2016). These water use characteristics, in combination with the frequently studied internal water storage (James et al., 2003; Meinzer et al., 2006; Yang et al., 2015) and the most studied transpiration, seem to constitute more complicated water circulation within and among plants. water circulation has been found to be important in stimulating and maintaining some physiological processes, e.g., maintaining transpiration with temporally stored water in stems (Goldstein et al., 1998; James et al., 2003), or relieving water shortage by water redistribution among interconnected plants (Adonsou et al., 2016; Zhao et al., 2016).

## 1.2 The meanings of water circulation for plants

Within plants, the internal water circulation can be formed by water transport (sap flow) towards canopy or the soil and by water exchange between conduits and storage compartments (James et al., 2003). In general, plant transpiration

is driven by micrometeorological factors (Bovard et al., 2005; Kume et al., 2007; O'Brien et al., 2004) and pulls up the water through the soil-plant-air continuum by forming water potential deficit. To satisfy the transpiration need, it is necessary to keep the conducting xylems in the stem efficient. However, the conducting xylems may face embolism danger when the transpiration need cannot be fulfilled by the limited soil water availability (Meinzer et al., 2010). Therefore, efficiency and safety of the xylems are essential for plants especially for large trees with relative long-distance water conducting pathways from the soil to leaves (Meinzer et al., 2010). Water storage is thought to be an important mechanism for plants to strengthen the xylem's safety when the transpiration demand and supply is imbalanced (Carrasco et al., 2015; Čermák et al., 2007a; Goldstein et al., 1998; Meinzer et al., 2006, 2010).

As an important part of internal water circulation, internal stored water is temporarily stored in plant tissues and can be withdrawn for physiological usage, e.g., transpiration due to the water potential deficits (Tyree and Yang, 1990). In woody plants, when high evaporative demand occurs, internally stored water may play an important role by temporarily supplying water to leaves; thereby maintaining high transpiration and carbon assimilation (Goldstein et al., 1998; Meinzer, 2002). As the most important storage reservoir for woody plants, the stem is thought to provide most of the available storage water for transpiration (Waring and Running, 1978; Waring et al., 1979) and thus has been paid more attention in the last few decades (Carrasco et al., 2015; Čermák et al., 2007b; Goldstein et al., 1998; Holbrook and Sinclair, 1992; Köcher et al., 2013; Meinzer et al., 2006, 2004; Phillips et al., 2003; Scholz et al., 2008; Waring and Running, 1978; Waring et al., 1979). The contribution of stem water storage to daily transpiration can range from 6 to 28% in subtropical trees (Carrasco et al., 2015) and reach even more than 50% in Scots pines (Waring et al., 1979).

Between plants and the environment (the atmosphere and the soil) and among plants, the outer water circulation can be composed of water uptake from the soil or foliage, water translocation, and water transfer among plants. This water circulation has been found to be important in stimulating and maintaining some physiological processes, e.g., redistributing water between root zones with different water status through roots (Burgess et al., 2001b; Sakuratani et al., 1999; Smith et al., 1999), or relieving water shortage by water redistribution among interconnected plants (Adonsou et al., 2016; Zhao et al., 2016). Unlike interaction between plants and the environmental factors, water redistribution and transfer among plants is more likely to occur within the

interconnected individuals of the same species (Adonsou et al., 2016). Water potential deficits between interlinked plants is considered as the driving power of the water transfer (Adonsou et al., 2016).

Compared with regular independent species, species with interconnected roots or rhizomes provide the possibility to directly share resource with each other (Baret and DesRochers, 2011). Resource allocation between interconnected individuals, which is called "physiological integration" (Caraco and Kelly, 1991; Kroon et al., 1996; Lau and Young, 1988), has been intensively investigated in herb species (Alpert and Mooney, 1986; Chapman et al., 1992; Kroon et al., 1996; Lau and Young, 1988; Stuefer et al., 1996). In contrast, only several tree species have been studied in recent years, e.g., lodgepole pine (Fraser et al., 2006), aspen (Baret and DesRochers, 2011), and poplar (Adonsou et al., 2016). In these studied herb or tree species, they found water, nutrients or carbohydrates can be transferred via connected roots or rhizomes. Transferred amounts and directions depended on the status of the donor and dependent individuals (Adonsou et al., 2016; Kroon et al., 1996). resource translocation can be increased when increasing the temporal variance in resource availability of the dependent individuals while decreased when increasing that of the donor individuals (Caraco and Kelly, 1991). Such resource integration would be critically important for new seedlings grown from the parental root systems (Baret and DesRochers, 2011) or for the young bamboo culms (Song et al., 2016).

Despite the studies mentioned above, the role and mechanism of water circulation still needs to be further explored, especially on species with potential water sharing (e.g., bamboos) or on species that must cope with water shortage diurnally or seasonally (e.g., species in dry forests). For these two types of species, maintaining efficient water transport in a safe range is vital to surviving. However, relative to the frequently studied phenological strategies (e.g., shedding leaves), internal and outer water circulation received less notice. Exploring and monitoring water circulation would deepen our understanding of plant physiology especially when plants confront water shortage diurnally or seasonally.

## 1.3 Internal and outer water circulation of bamboos

Thus far, most of the species studied on internal water circulation have been trees. Bamboos, widely spreading in the tropics or subtropics, receive far less attention. As fast-growing monocots, bamboos may have unique characteristics of water circulation due to their specific anatomy. First, unlike trees, bamboos have no radial growth, which means that the culms of bamboos remain at almost constant volumes and numbers of water conducting elements over the whole lifespan (Liese and Köhl, 2015). Such feature requires more safety mechanisms to maintain the xylem working, as the xylems of bamboos cannot be renewed like trees when they lose the conducting function due to embolism. Compared with trees, comparable (Dierick et al., 2010; Kume et al., 2010) or higher (Ichihashi et al., 2015; Mei et al., 2016) maximum sap flux densities were found in some bamboo species. Such high sap flux densities require not only an efficient conducting system but also a safety-guarantee system to avoid or repair possible embolism. Root pressure was thought to be an important safety mechanism to recover embolized bamboo xylems during the night and was observed to positively correlate with the height of the bamboos (Cao et al., 2012). This root pressure-height relation may mean some species without reliable, powerful safety mechanisms need to shorten the conducting pathways. Another safety mechanism could be the stem water storage capacity. Despite a relatively small sapwood area due to the hollow center, the bamboo stem may still provide considerable water storage room due to the abundant parenchyma (50%, Liese and Köhl (2015)). It was observed on *Bambusa vulgaris* that the sap flux densities at under-canopy level could maintain high rates much longer than at the base level, and this was attributed to the bamboo culm water storage (Yang et al., 2015). However, they did not give out how much the stem water storage can contribute to the transpiration of the bamboos. It would be necessary to quantify the contribution of the culm water storage for further understanding of the water circulation characteristics of bamboos.

Another distinctive characteristic of water circulation in bamboos is the water transfer among culms due to the rhizomes, which possibly provide passages for transporting water among culms (Liese and Köhl, 2015; Stapleton, 1998). It has been indicated that the nutrients can be translocated from the established mature culms to the freshly sprouted young culms during the shoot emerging and explosive-growing period (Li et al., 1998a,b; Song et al., 2016). During this nutrient-translocating period or even the whole life of the bamboos, water

transfer could be necessary as the nutrient-carrier. Thus far, as we know, only two studies have indicated the existence of water transfer among bamboos. Water transfer among culms has been implied in *Bambusa blumeana* by observing elevated $D_2O$ concentrations on the leaves of the neighbor culms which were in the same clump of the $D_2O$ labeled culms (Dierick et al., 2010). Another investigation on Moso bamboo (*Phyllostachys pubescens*) also implied water transfer by finding 20% less water use in the rhizome-cut culms than in the regular culms (Zhao et al., 2016). Long established or 1-year-old young culms rather than the freshly sprouted growing culms were studied. As the freshly sprouted culms have no or few leaves and less developed roots at the beginning of growing period, they may rely more on the connected mature culms for water transfer through rhizome. Therefore, water transfer needs to be further tested on more species with directly connected culms and with no destructive operation.

## 1.4 Internal water circulation of stem-succulent trees in tropical dry forest

In tropical dry forests, strengthening water storage capacity is one drought-coping strategy for trees, especially stem-succulent trees (Borchert, 1994). Compared to the deciduous and evergreen species in tropical dry forests, the most distinct characteristics of the stem-succulent trees are their large swollen stems, which can reach several meters of the diameters (Borchert, 1994; Chapotin et al., 2006b; Wickens, 1982). The large volumes of stems, with relatively low density (Borchert, 1994), can store water in the central pith, or bark and phellum or in the abundant parenchyma tissues, depending on the different species (Nilsen et al., 1990). In dry regions where they occupy together with their massive volumes with high water storage capacities, the stem-succulent trees have been long supposed to rely on water storage in the stems to cope the drought conditions (Baum, 1996; Wickens, 1982).

As the shallow-rooted species, stem-succulent trees are highly sensitive and dependent on the topsoil pulse water; which is controlled mainly by the rain in the natural conditions (Schwinning and Ehleringer, 2001). Therefore, in most of the dry season, stem-succulent trees keep leafless status until the end of the dry seasons and the onset of the rainy seasons (Chapotin et al., 2006a,b). Chapotin et al. (2006a,b) tested the hypothesis that the stem water

storage of stem-succulent trees exert more effect to buffer daily water deficits of deciduous baobab trees in the rainy season when they have leaves. The stem water storage was found to support leaf flushing rather than stomatal opening for transpiration at the end of the dry season (Chapotin et al., 2006a), and would play a limited role in supporting daily transpiration demand in the first two weeks of the rainy season (Chapotin et al., 2006b). On a daily scale, stem-succulent trees tend to keep xylem safe by regulating stomatal opening to maintain at relatively low transpiration rather than by support from the stem water storage (Chapotin et al., 2006b; Nilsen et al., 1990). Contrastly, the stem water storage was assumed to be used in long-term rather than daily scales, as indicated by the pattern of stem water content decreasing in the dry season while increasing with apparent nighttime refilling after rain events in the rainy season (Chapotin et al., 2006b). These observations raised the speculation that, to exert long-term effect, water entering into the stem from the soil could stay much longer in stem-succulent trees than in other deciduous or evergreen trees in the same arid habitats. Further assessment of water residence time in the stem would deepen our insight into the regulating mechanism of the stem water storage in stem-succulent trees.

## 1.5 Methods for the assessment of plant water circulation

### 1.5.1 Thermal dissipation probes (TDP)

Thermal dissipation probes (TDP) are widely used to measure sap flux density ($J_s$) in trees (Granier, 1985), due to the advantages of low-price, ease-to-install and simplicity (Lu et al., 2004). TDP's empiric equation for calculating $J_s$ was built upon three tree species (Granier, 1985), which may mean that the equation's parameters may not be applicable to all of the other species especially those with different wood properties. Several studies have suggested calibrating the method before studying new species (Lu et al., 2004; Vandegehuchte and Steppe, 2013; Wullschleger et al., 2011). To our knowledge, only few studies have applied the TDP method on bamboos so far (Dierick et al., 2010; Kume et al., 2010; Yang et al., 2015; Zhao et al., 2016). Three studies reported underestimation of bamboo sap flux density compared to stem heat balance (SHB; Dierick et al., 2010) or referenced gravimetric measure-

ments (GM; Kume et al., 2010; Zhao et al., 2016) when the TDP method was not calibrated.

With TDP at the top and base of stems, time delay between $J_s$ of these two positions has been used for assessing the daily dynamic of stem water storage in many tree species (Carrasco et al., 2015; Čermák et al., 2007a; Goldstein et al., 1998; James et al., 2003; Köcher et al., 2013; Meinzer et al., 2004; Phillips et al., 2009). As we know, there is only one case applying this method to bamboos (Yang et al., 2015). Without pointing out the direct quantized contribution of stem water storage to the transpiration as the other studies mentioned above, Yang et al. (2015) implied the afternoon contribution of stem water storage by comparing the different dynamic patterns of the $J_s$ at the top and bottom positions. Choosing qualitative and not quantitative analysis may base on the cautious consideration, as the applied 2-cm probes were not calibrated and the lengths of them may constrain the installation and measurement at the upper thin culms.

In contrast, the SHB method (Sakuratani, 1981) was suggested to be well suited for sap flux measurements on bamboos (Dierick et al., 2010). Bamboos are round and culms are hollow; hence heat loss in the form of heat storage inside culms is marginal so that steady thermal conditions as a central assumption of the method are met (Baker and Bavel, 1987). Therefore, to accurately measure bamboo water use and storage with TDP, calibrating TDP with reference methods (e.g., SHB or GM) on standing bamboos of more bamboo species should be conducted.

Except bias caused by the different wood properties between the new species and the equation-built species, water content ($\theta_{wood}$) dynamics may also introduce bias to the TDP measurements and are thus better to be analyzed and corrected for the related bias. Central to the calculation of $J_s$ is the maximum temperature difference between probes ($\Delta T_{max}$), and the $\Delta T_{max}$ is often referred to as "zero flow" conditions and reflects the wood thermal conductivity ($K_{wood}$). However, the depletion and recharge of water storage in stems can lead to substantial fluctuations of $\theta_{wood}$ (Nadler et al., 2008; Yang et al., 2015), which may influence $K_{wood}$ and subsequently the estimates of $J_s$. One study has analyzed such influence of $\theta_{wood}$ on $J_s$ with modeling the possible temperature change caused by $\theta_{wood}$ (Vergeynst et al., 2014). However, it is still not addressed on the direct quantitative impact of $\theta_{wood}$ to the TDP-estimated $J_s$.

### 1.5.2 Deuterium tracing

Deuterium tracing method has been applied for measuring sap velocity and water residence time in the stems of trees (Gaines et al., 2016; James et al., 2003; Meinzer et al., 2006), and for estimating daily water use rates (Calder, 1991; Dierick et al., 2010; Dye et al., 1992; Schwendenmann et al., 2010). In these studies, the $D_2O$ was first injected into the base stem of trees/bamboos (this operation is usually called labeling) and then the water which transpired from leaves in the labeled trees/bamboos were periodically sampled to trace the $D_2O$ movement (Calder, 1991). Subsequently, the $D_2O$ concentrations in the samples were used to estimate sap velocity, water residence time and daily water use rates (See details in Calder (1991) or Meinzer et al. (2006)). However, deuterium-derived water use rates were thought to be less reliable when two assumptions proposed by Calder (1991) for estimating the water use rates were violated (Schwendenmann et al., 2010). The two assumptions were: first, all the $D_2O$ injected into the base stem would be taken up and transpired out from leaves without tracer loss in other forms and second, the $D_2O$ is thoroughly mixed in the transpiration stream before water flowed into different regions of the crown (Calder, 1991). Compared with the other methods (e.g., thermal dissipation probe, TDP), both overestimation (Kalma et al., 1998; Marc and Robinson, 2004; Schwendenmann et al., 2010) and underestimation (Dye et al., 1992) on water use rates from deuterium tracing method were observed. On one bamboo species (*B. blumeana*), water use rates were found eight times higher with deuterium tracing method than with TDP method (Schwendenmann et al., 2010). The discrepancies could be attributed to several potential interference sources which may break the two assumptions, such as tracer loss due to retention of tracer in plants and water transfer among plants (Schwendenmann et al., 2010). Nevertheless, the discrepancies caused by the interference sources can also be estimated to explore the corresponding water circulation characteristics (e.g., water transfer). This process could be realized by monitoring tracer dynamics on leaves, stem and the interconnected plants to address the difference in water use rates simultaneously derived with deuterium tracing method and a reference method.

## 1.6 Aims of this study

The study aims were, to:

(1) calibrate TDP on potted bamboos with gravimetric and SHB method and in situ on standing bamboos with SHB method;

(2) compare bamboos and trees with respect to sap flux densities and its response to environmental factors;

(3) explore the effects of wood water content on sap flux densities derived with TDP by conducting a culm dehydration experiment, monitoring bamboos with TDP in situ, and implementing a steady-state thermal model;

(4) explore the role of stem water storage in bamboos;

(5) test for water transfer between bamboo culms with the deuterium tracing method, and exploring error sources of deuterium tracing method on bamboo water circulation;

(6) analyze water residence times as indicated by deuterium tracing in stem-succulent trees of a dry forest.

## 1.7   Author contribution

The dissertation is substantiated by five manuscripts (Chapter 2-6) at various stages of the publication process (i.e. "In preparation", "Advanced draft", "Published"). The status, as well as the contributions to each manuscript by the author of this dissertation (in the following simply refer to as "the author"), is indicated for each manuscript. Chapter 1 and 7 were solely compiled by the author.

Chapter 2: **Water use patterns of four tropical bamboo species assessed with sap flux measurements**
Tingting Mei[1*†], Dongming Fang[1†], Alexander Röll[1], Furong Niu[1], Hendrayanto[2], Dirk Hölscher[1]
*Manuscript status: Published in **Frontiers in Plant Science (2016). DOI: 10.3389/fpls.2015.01202**

The author contributed to field installation and maintenance of the equipment, data collection, and analysis, writing and revision of the manuscript. Particularly, the author conducted most of the data analysis and figure-making.

Chapter 3: **The influence of bamboo culm water content on sap flux measurements with thermal dissipation probes: observations and modeling**
Tingting Mei[1,3,4*†], Dongming Fang[1†], Alexander Röll[1], Dirk Hölscher[1]

*Manuscript status: Published in **Trees** (2017). DOI: 10.1007/s00468-017-1641-4*

The author contributed to field installation and maintenance of the equipment, data collection, and analysis, writing and revision of the manuscript. Mainly, the author was in charge of the modeling and conducted most of the data analysis and figure-making.

Chapter 4: **Deuterium tracing for assessing water circulation in bamboos**

Dongming Fang[1*], Tingting Mei[1,3,4], Alexander Röll[1], Hendrayanto[2], Dirk Hölscher[1]

*Manuscript status: Advanced draft.*

The author contributed to field installation and maintenance of the equipment, data collection, and analysis, writing and revision of the manuscript. Particularly, the author conducted all the data analysis and figure-making and wrote the preliminary draft of the manuscript.

Chapter 5: **Water transfer between bamboo culms in the period of sprouting**

Dongming Fang[1*], Tingting Mei[1,3,4], Alexander Röll[1], Dirk Hölscher[1]

*Manuscript status: Advanced draft.*

The author contributed to the experimental design, field installations, sample collections, data analysis and writing and revision for the manuscript. Particularly, the author conducted all the data analysis and figure-making and wrote the preliminary draft of the manuscript.

Chapter 6: **Water residence times in trees of a neotropical dry forest**

Sophie Graefe[1*], Dongming Fang[1], Philipp Butz[1], Dirk Hölscher[1]

*Manuscript status: In preparation.*

The author contributed to conduct all the data cleaning and analysis, collected data from reviewed literatures, and wrote the manuscript's method part relating deuterium data analysis and revised the manuscript.

# Chapter 2

# Water use patterns of four tropical bamboo species assessed with sap flux measurements

Tingting Mei[1][†][*], Dongming Fang[1][†], Alexander Röll[1], Furong Niu[1], Hendrayanto[2], Dirk Hölscher[1]

[1] Tropical Silviculture and Forest Ecology, Georg-August-Universität Göttingen, Germany.
[2] Department of Forest Management, Institut Pertanian Bogor, Indonesia

[†] The authors contributed equally to this work.

[*] Correspondence: Tingting Mei, Tropical Silviculture and Forest Ecology, Georg-August-Universität Göttingen, Büsgenweg 1, Göttingen, 37077, Germany. Email: tmei@gwdg.de

Running title: bamboo water use

# Abstract

Bamboos are grasses (Poaceae) that are widespread in tropical and subtropical regions. We aimed at exploring water use patterns of four tropical bamboo species (*Bambusa vulgaris*, *Dendrocalamus asper*, *Gigantochloa atroviolacea* and *Gigantochloa apus*) with sap flux measurement techniques. Our approach included three experimental steps: (1) a pot experiment with a comparison of thermal dissipation probes, the stem heat balance method and gravimetric readings using potted *B. vulgaris* culms, (2) an in situ calibration of thermal dissipation probes with the stem heat balance method for the four bamboo species, and (3) field monitoring of sap flux of the four bamboo species along with three tropical tree species (*Gmelina arborea*, *Shorea leprosula* and *Hevea brasiliensis*) during a dry and a wet period. In the pot experiment, it was confirmed that the stem heat balance method is well suited for bamboos but that thermal dissipation probes need to be calibrated. In situ, species-specific parameters for such calibration formulas were derived. During field monitoring we found that some bamboo species reached high maximum sap flux densities. Across bamboo species, maximal sap flux density increased with decreasing culm diameter. In the diurnal course, sap flux densities in bamboos peaked much earlier than radiation and vapor pressure deficit (VPD), and also much earlier than sap flux densities in trees. There was a pronounced hysteresis between sap flux density and VPD in bamboos, which was less pronounced in trees. Three of the four bamboo species showed reduced sap flux densities at high VPD values during the dry period, which was associated with a decrease in soil moisture content. Possible roles of internal water storage, root pressure and stomatal sensitivity are discussed.

**Keywords: calibration, environmental drivers, hysteresis, stem heat balance, thermal dissipation probes, trees, bamboos**

## 2.1  Introduction

Bamboos (Poaceae, Bambuseae) are abundant in the natural vegetation of tropical and subtropical regions. They have been used by people for millennia and are still used as food and construction materials. In addition, a large variety of bamboo usages have been developed in recent decades, for example for pulp, paper or clothing production (INBAR, 2014). The increasing economic

exploitation of bamboos goes along with a considerable expansion of bamboo plantations in some regions (Chen et al., 2009; FAO, 2010), which may lead to changes in ecological processes such as water use patterns (Komatsu et al., 2010; Uchimura, 1994). Some bamboo stands were reported to evaporate more water than tree-dominated forests (Ichihashi et al., 2015; Komatsu et al., 2010), but studies focusing on water use patterns of bamboos are still rare thus far (Dierick et al., 2010; Ichihashi et al., 2015; Komatsu et al., 2010; Kume et al., 2010; Pereira and Hosegood, 1962).

Water use patterns of bamboos and trees differ in several aspects. In contrast to trees, bamboos are monocotyledonous species and lack secondary growth (Zimmermann and Tomlinson, 1972). Therefore, vascular conduits of bamboo xylem have to remain functional throughout the ontogeny of a bamboo culm. Bamboos consequently have great ability to avoid cavitation (Cao et al., 2012; Cochard et al., 1994; Petit et al., 2014); root pressure mechanisms may contribute to repairing embolized conduits at night (Cao et al., 2012). Such features and structural traits of bamboos may also lead to particular water use patterns.

In general, plant water use is driven by micrometeorological factors and can be limited by soil water availability (Bovard et al., 2005; Kume et al., 2007; O'Brien et al., 2004); it is regulated by stomata opening and closing (Jarvis, 1989) and can be influenced by internal water storage mechanisms (Carrasco et al., 2015; Goldstein et al., 1998; Waring and Running, 1978). Xylem sap flux reflects these multiple factors. For some tree species, for example, hysteresis in the diurnal sap flux response to radiation and vapor pressure deficit (VPD) of the air have been reported (Goldstein et al., 1998; O'Brien et al., 2004). Sap flux measurements thus appear suitable to study the water use patterns of bamboos as well as their controlling environmental factors.

Thermal dissipation probes (TDP) are widely used to measure sap flux density ($J_s$) in trees (Granier, 1985). Several studies suggest calibrating the method before studying new species (Lu et al., 2004; Vandegehuchte and Steppe, 2013; Wullschleger et al., 2011). To our knowledge, only two studies have applied the TDP method on bamboos so far. Both reported an underestimation of bamboo sap flux compared to stem heat balance (SHB) and reference gravimetric measurements (GM) when the TDP method was not calibrated (Dierick et al., 2010; Kume et al., 2010). In contrast, the SHB method (Sakuratani, 1981) was suggested to be well suited for sap flux measurements on bamboos (Dierick et al., 2010). Bamboo culms are hollow; hence heat loss in the form of heat

storage inside culms is marginal, so that steady thermal conditions as a main assumption of the method are met (Baker and Bavel, 1987).

The aim of this study was to analyze water use patterns of tropical bamboo species and particularly the response of $J_s$ to the principal environmental drivers. First, we calibrated the SHB and the TDP method with reference GM in an experiment on potted culms of *Bambusa vulgaris*. We then measured $J_s$ in the field in four bamboo species including *B. vulgaris* with both the TDP and SHB method, and calibrated the TDP method with the SHB method. Herein, three factors which may influence the quality of the calibration were tested: time step of the data, formula specificity and calibration formula type. After calibration of the TDP method, we applied it to monitor $J_s$ in four bamboo and three tree species in a common garden in Bogor, Indonesia. Differences in the response of $J_s$ to fluctuations in environmental conditions were assessed. The study intends to contribute to expanding the yet limited knowledge on the eco-hydrological functioning of bamboos.

## 2.2 Materials and methods

### 2.2.1 Study sites and species selection

The pot calibration experiment was conducted in Guangzhou, China (23°26'13" N, 113°12'33" E, 13 m asl). The field calibration experiment and monitoring campaign were carried out in a common garden in Bogor, Indonesia (6°33'40" S, 106°43'27" E, 182 m asl). Average annual temperature in Bogor is 25.6 °C and annual precipitation is 3978 mm.

Relatively dry conditions with consecutive rainless days can occur between June and September. During this dry period, monthly precipitation is on average 40% lower than during the wet period (230 vs. 383 mm), and the number of consecutive dry days (rainfall < 1 mm) is twice that of the wet period (8 vs. 4 days, 1989 - 2008, Van Den Besselaar et al., 2015). During our study period (July 2012 to January 2013), differences between dry and wet period were more pronounced, i.e. 155 vs. 489 mm monthly precipitation, 14 vs. 2 consecutive dry days, and 0.29 vs. 0.39 $m^{-3}$ $m^{-3}$ daily soil water content. In Bogor, four bamboo species (*Bambusa vulgaris*, *Dendrocalamus asper*, *Gigantochloa atroviolacea*, *Gigantochloa apus*) with five culms per species and three tree species (*Gmelina arborea*, *Shorea leprosula* and *Hevea brasiliensis*, Table 2.1) with five stems per species were selected and their $J_s$

were monitored with the TDP method for seven months.

## 2.2.2 TDP construction and installation

To measure $J_s$ in trees and bamboos, we used self-made TDP (1 cm and 2 cm length, respectively). In sensor design and construction, we followed Wang et al. (2012). Each TDP sensor was comprised of a heating (downstream) and a reference (upstream) probe made of steel hypodermic needles. The probes were placed 10 cm apart (vertically). For bamboos and trees, TDP installation depths in culms and stems were 1 and 2 cm, respectively. After installation, each TDP was supplied with a constant current of 120 mA; the respective power outputs of 1 cm and 2 cm length TDP were 0.1 and 0.2 W. TDP signals were sampled every 30 s and stored as 10-min averages for the pot calibration experiment and as 1-min averages for all other experiments by data loggers and multiplexers (CR1000, AM16/32, Campbell Scientific Inc., USA).

## 2.2.3 Calibration of the TDP method

**Pot calibration experiment: TDP, SHB & GM**

Five culms of *B. vulgaris* (diameter 5.3 - 7.3 cm, height 2.2 - 3.2 m) with trimmed canopies were transplanted into plastic bags (diameter 30 cm, height 25 cm) six months before the calibration experiment. One day before the experiment, the five bamboos were transplanted into bigger plastic pots (diameter 50 cm, height 65 cm). The pots were filled with cobblestones and water and were then fully sealed with plastic cover and aluminum foil to prevent evaporation of water from the pots (Fig. 2.1 A). A scaled syringe tube was attached to each pot and connected into the pot through a U-type tube. At the beginning of the experiment, the water was added into the pot through the syringe tube to a fixed level (5 cm below the pot cover). Subsequently, water was added manually every 30 min to reach the pre-defined level. The weight of the added water was determined gravimetrically (GM). To measure $J_s$, each bamboo culm was equipped with 3 pairs of 1 cm length TDP which were evenly installed circumferentially, about 15 cm above the plastic cover. To minimize potential measurement errors induced by circumferential variations of $J_s$, the thermocouple wires of the three TDP were connected in paralFlel to get an average voltage signal for each bamboo culm (Lu et al., 2004). For a

Table 2.1 Structural characteristics of the studied bamboo and tree species (n = 5 per species; mean±SD).

|         | Species          | DBH (cm)  | BCWT (cm) | Height (m) |
|---------|------------------|-----------|-----------|------------|
| Bamboo  | *B. vulgaris*    | 7.0±0.3   | 1.3±0.1   | 17.9±0.8   |
|         | *G. apus*        | 8.6±0.4   | 1.2±0.2   | 16.2±2.7   |
|         | *D. asper*       | 11.9±1.9  | 2.4±0.2   | 21.1±0.9   |
|         | *G. atroviolacea*| 8.9±0.6   | 1.6±0.1   | 17.0±1.0   |
| Tree    | *H. brasiliensis*| 27.4±2.3  | -         | 25.2±3.0   |
|         | *G. arborea*     | 26.3±7.7  | -         | 26.5±2.3   |
|         | *S. leprosula*   | 20.7±4.8  | -         | 19.2±2.5   |

Note: DBH (Diamter at Breast Height); BCWT (Bamboo Culm Wall Thickness)

second $J_s$ estimate, a SHB gauge (SGB50 or SGA70, Dynagage Inc., USA) was installed about 1.5 m above the TDP. Both sensor types were protected by foil and the sensor signals were subsequently recorded as described in Section 2.2. For the comparison to reference gravimetric measurements (GM), 10-min TDP and SHB derived values were aggregated to half-hourly values.

To assess the performance of TDP and SHB in the pot experiments, $J_s$ derived from TDP and SHB ($J_{s\_TDP}$ and $J_{s\_SHB}$, respectively) on daily and 30-min scales were compared to GM derived $J_s$ ($J_{s\_GM}$) with paired t-tests. Additionally, the slopes of the respective linear fits between $J_{s\_TDP}$, $J_{s\_SHB}$ and $J_{s\_GM}$ were tested for significant differences from 1 with the test of homogeneity of slopes. The same statistical analyses were applied again later when testing for significant differences between $J_{s\_TDP}$ and $J_{s\_SHB}$ in the field calibration experiments.

**Field calibration experiment: TDP & SHB**

Five culms per bamboo species (*B. vulgaris*, *D. asper*, *G. atroviolacea*, *G. apus*) were selected for TDP measurements (Table 2.1), three to four of which were additionally measured with SHB for a field calibration of the TDP method. TDP sensors were installed at 1.3 m height, and SHB gauges (SGB50, SGA70, Dynagage Inc., USA) were installed about 2.5 m above the TDP. Simultaneous TDP-SHB measurements were conducted for a minimum of five days per culm (Fig. 2.1 B). Heat storage inside bamboo culms is assumed to be negligible, which was confirmed by installing thermocouple wires inside the measured segments of the respective bamboo culms to detect fluctuations in culm temper-

ature (Dierick et al., 2010). The observed fluctuations were marginal, which meant stable thermal conditions as a requirement of the SHB method were met.

### Parametrization for TDP calibration

We derived cross-sectional water conductive areas ($A_{\text{\_TDP}}$) from the culm wall thickness at the location of TDP sensor installation. In the pot calibration experiment, reference $J_s$ were calculated by dividing water flow rates (g h$^{-1}$, GM-derived) by $A_{\text{\_TDP}}$. In the field calibration experiment, reference $J_s$ were taken from the SHB measurements. The reference $J_s$ could subsequently be used to calibrate $J_{s\_\text{TDP}}$. Nighttime sap flux values were excluded in both calibration experiments.

In the field calibration, three factors were considered for obtaining a TDP calibration formula from reference (SHB) measurements: time step of the data, formula specificity and calibration formula type. To examine effects of varying time steps, the formulas were built and tested on data at varying intervals (1-, 10-, 30-, and 60-minute averages, respectively). The effects of formula specificity were examined by using common (i.e. all bamboo species pooled), species-specific and culm-specific formulas, respectively. Regarding the calibration formula type, two formulas were compared: one was nonlinear ($J_s = aK^b$) and generated by deriving new $a$ and $b$ parameters for the original Granier formula (1985). The second was a linear formula ($J_{s\_\text{SHB}} = c \times J_{s\_\text{TDP}}$) which was calculated from the linear relationship between $J_{s\_\text{TDP}}$ and $J_{s\_\text{SHB}}$.

To obtain stable calibration formulas, pooled data sets were randomly split in half for calibration and independent validation, respectively (Niu et al., 2015). First, for each time step (1-, 10-, 30-, and 60-minute, respectively), a data pool was built. Three culms of each bamboo species were randomly chosen, and for each, three days of data were randomly chosen from an initial common dataset. With these data pools, formula specificity was examined. For the common calibration, culms of all four species were selected for calibration. For species-specific and culm-specific calibration, only the data of the respective species or culms was selected. Next, the selected data was randomly split in half, for building the calibration formula and testing it, respectively. When testing the formula, the differences between $J_{s\_\text{SHB}}$ and calibrated $J_{s\_\text{TDP}}$ ($J_{s\_\text{TDP\_cali}}$, abnormal distribution, $P > 0.05$) were examined with the Wilcoxon Signed-Rank Test (no significant differences at $P > 0.05$). The process of randomly building and testing the formula was iterated 10,000 times. Final

calibration formula parameters were derived by averaging the parameters of those iterations which passed the Wilcoxon Signed-Rank Test ($P > 0.05$).

For an evaluation of the performance of the different formulas and the influence of the three factors (time scale, formula specificity and calibration formula type), differences in normalized Root-Mean-Square Errors (nRMSE) were assessed for each culm, species and formula factor, respectively. First, the RMSE for each day was derived with the $J_{s\_SHB}$ and $J_{s\_TDP\_cali}$ values, and the nRMSE was calculated by normalizing the RMSE with the observed daily range of $J_{s\_SHB}$ (difference between maximum and minimum $J_{s\_SHB}$). Then, the nRMSE were analyzed regarding the three formula factors (data time scale, formula specificity and calibration formula type) by ANOVA (Analysis of variance). Additionally, for each day, $J_{s\_TDP\_cali}$ with each formula type was tested for significant differences from $J_{s\_SHB}$ with the Wilcoxon Signed-Rank Test. The rates of passing the Wilcoxon Signed-Rank Test ($P > 0.05$ when no significant difference between TDP and SHB derived values) were assessed for each formula.

### 2.2.4   Field study

**Monitoring bamboo and tree sap flux**

Four calibrated bamboo species as well as three tree species (*G. arborea*, *S. leprosula* and *H. brasiliensis*) were monitored with the TDP method for seven months (July, 2012 to January, 2013). Five bamboo culms and five tree trunks per species were selected for the measurements. On bamboos, three pairs of TDP (10 mm in length) were installed evenly around each culm at 1.3 m height and connected in parallel (see Section 2.2 for details). On trees, two pairs of 20 mm TDP were installed in the trunk 1.3 m above the ground, in the North and South, respectively. $J_s$ for the two sensors were separately derived with the original calibration formula (Granier, 1985) and subsequently averaged to obtain values for each tree. For bamboos, $J_s$ derived with the original formula were calibrated with species-specific calibration parameters (from reference SHB field measurements) to obtain final $J_s$ values.

**Environmental measurements and analyses**

A micrometeorological station was set up in an open area. It was about 100 and 600 m away from the closer measurement sites (*D. asper*, *G. arborea*, *G. atroviolacea*, *G. apus*, *S. leprosula*) and farthest sites (*B. vulgaris*, *H. brasiliensis*), respectively. Air temperature ($T_a$, °C) and air relative humidity (RH, %) were measured with a temperature and relative humidity probe (CS215, Campbell) installed in a radiation shield. VPD (kPa) was calculated from $T_a$ and RH. Radiation (J m$^{-2}$ s$^{-1}$) was measured with a pyranometer (CS300, Campbell). Data were recorded with the previously described data loggers every minute.

In addition to the mentioned micrometeorological variables, soil moisture (SM, m$^{-3}$ m$^{-3}$) was measured with time domain reflectrometry sensors (TDR, CS616, Campbell) at 0 - 20 cm depth. As the clump of *D. asper* and the stand of *G. arborea* were next to each other, one TDR was positioned between them to measure soil moisture. Likewise, one sensor was used for measurements of *G. atroviolacea* and *G. apus*. One TDR each were used for the remaining species (*S. leprosula*, *B. vulgaris*, *H. brasiliensis*). TDR measurements ran in parallel to the sap flux field campaign and data were recorded with the described data loggers every minute.

For the day-to-day analysis of influences of fluctuations in environmental conditions (VPD, radiation, SM) on $J_s$ in the studied bamboo and tree species, daily accumulated $J_s$ (kg cm$^{-2}$ d$^{-1}$) were normalized by setting the highest daily observation of each species to 1 and the lowest to 0. For a more isolated analysis of potentially limiting influences of soil moisture on $J_s$, we focused on "dry period conditions" with consecutive rainless days, which occurred between June and September in the study area. During this period, monthly precipitation was only 32% of monthly wet period precipitation (155 vs. 489 mm), and the number of consecutive dry days (rainfall < 1 mm) was 7 times higher than during the wet period (14 vs. 2 days). Dry period conditions are also characterized by higher VPD (average daily VPD > 0.74 kPa on 92% of the days). 0.74 kPa was chosen as the threshold to distinguish between dry and wet period because it constituted the mean maximum ("turning point") in the fitted $J_s$ response functions to VPD in three of the four studied bamboo species (except *D. asper*, see Fig. 2.4 B).

For the diurnal analysis of influences of fluctuations in environmental conditions on $J_s$, time lags between $J_s$ and micrometeorological drivers (radiation and VPD) were calculated as the time difference between the respective occurrences of maximal $J_s$ ($J_{s\_max}$) and maximal radiation and VPD. T-tests

were used to test time lags for significant differences from 0 min. 30-min $J_s$ values (average values of three selected sunny days) of each species were plotted against radiation and VPD to examine occurrences of hysteresis. The respective areas of hysteresis were compared between bamboos and trees with t-tests.

All data analyses were performed with SAS 9.3 (SAS Institute Inc., 2013).

## 2.3    Results

### 2.3.1    Calibration of the TDP method for bamboos

**Pot calibration experiment: TDP, SHB & GM**

In the pot calibration experiment with *B. vulgaris*, SHB yielded similar absolute values of $J_s$ as GM on daily and 30-min scales ($P > 0.05$). The slope of the linear fit between SHB and GM on the 30-min scale was 0.98 ($R^2 = 0.93$, $P < 0.01$). It did not significantly differ from 1 ($P > 0.05$, Fig. 2.2 A). In contrast to this, TDP estimates, with the original parameters of the calibration formula (Granier, 1985), differed substantially from GM values at both the daily (60% underestimation of accumulated $J_s$, $P < 0.01$) and 30-min scale (56% underestimation, $P < 0.01$). The slope of the linear fit between TDP and GM on the 30-min scale was 0.44 ($R^2 = 0.84$, $P < 0.01$). It was significantly different from 1 ($P < 0.01$, Fig. 2.2 A).

After applying the TDP calibration parameter for *B. vulgaris* derived from the pot experiment ($c = 2.28$), the 30-min $J_{s\_TDP}$ were in line with those from GM. The slope was not significantly different from 1 ($P > 0.05$, Fig. 2.2 B). When applying the calibration parameters derived for *B. vulgaris* from the SHB field calibration experiment ($c = 2.79$), $J_{s\_TDP}$ was 19% higher than $J_{s\_GM}$ ($P < 0.01$, Fig. 2.2 B).

## 2.3.2    Field calibration experiment: TDP & SHB

Formula type and data time step had no significant influence on the performance of the calibration formula, but it mattered whether culm- or species-specific or a common calibration formula was used (Appendix Table A.1; Appendix Table A.2). Based on the nRMSE and the passing rate of the Wilcoxon test ($P > 0.05$) between calibrated $J_{s\_TDP}$ and $J_{s\_SHB}$, culm-specific
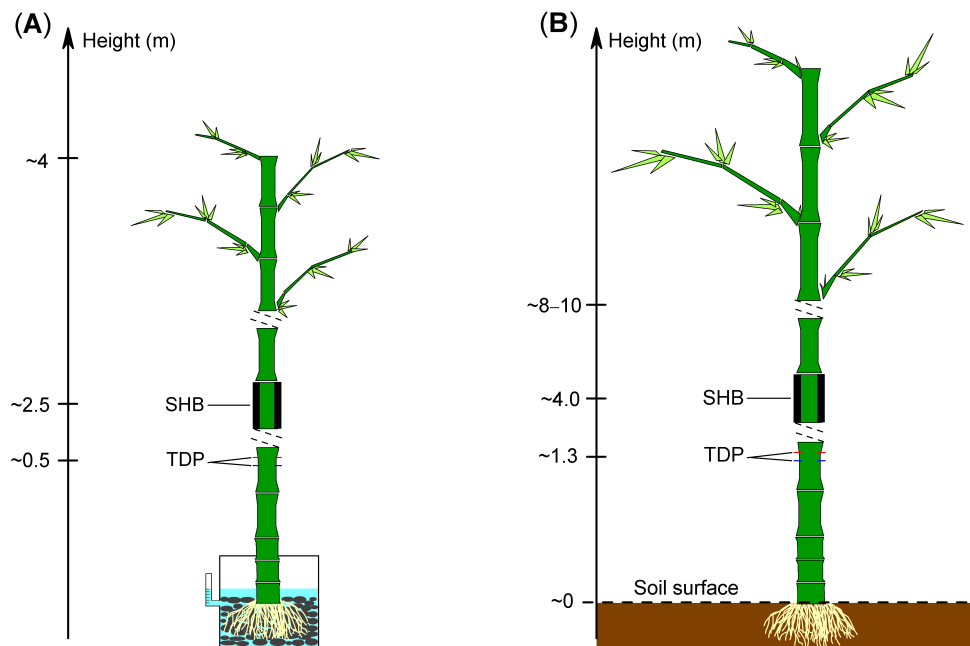
Fig. 2.1 Installation of thermal dissipation probe (TDP) and stem heat balance (SHB) sensors on bamboo culms for the calibration experiments on potted plants (A) and for field calibration (B).
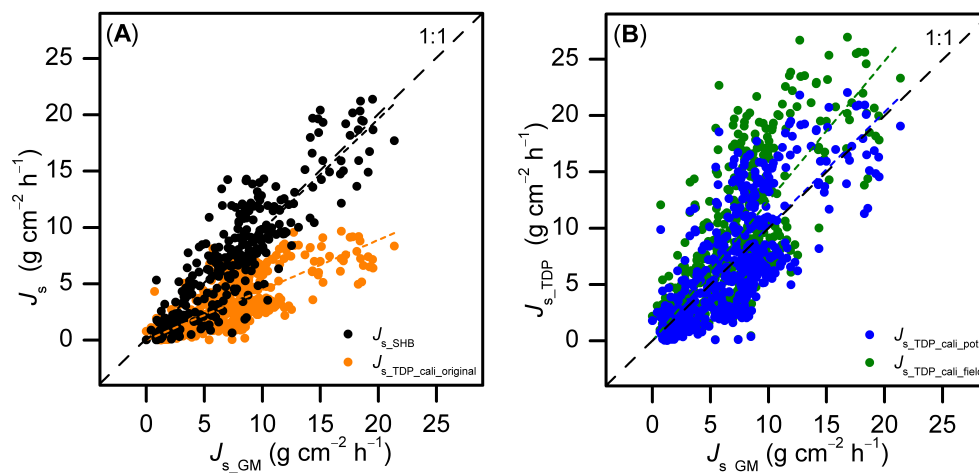


Fig. 2.2 Half-hourly sap flux density ($J_s$) measured with thermal dissipation probes (TDP) and stem heat balance (SHB) sensors on five potted *Bambusa vulgaris* culms plotted against GMderived reference sap flux densities ($J_{s\_GM}$) before (A; $J_{s\_TDP\_cali\_original}$: $Y = 0.44X$, $R^2 = 0.84$, $P < 0.01$; $J_{s\_SHB}$: $Y = 0.98X$, $R^2 = 0.93$, $P < 0.01$) and after (B; $J_{s\_TDP\_cali\_field}$: $Y = 1.24X$, $R^2 = 0.84$, $P < 0.01$; $J_{s\_TDP\_cali\_pot}$: $Y = 1.01X$, $R^2 = 0.84$, $P < 0.01$) species-specific calibration and field calibrations of the TDP method. Pooled data from 2 to 5 days of simultaneous TDP, SHB, and gravimetric measurements (GM).

Table 2.2 Values of the parameter c of different bamboo calibrations (species-specific/common) for TDP sap flux estimates.

| Formula specificity | Species | $c$ | Formula nRMSE | | $P$ |
| --- | --- | --- | --- | --- | --- |
| | | | Species-specific | common | |
| Species | *B. vulgaris* | $2.79{\pm}0.13^{a}$ | 0.10 | 0.11 | 0.07 |
| | *G. apus* | $3.32{\pm}0.08^{b}$ | 0.10 | 0.12 | 0.06 |
| | *D. asper* | $2.42{\pm}0.06^{c}$ | 0.18 | 0.18 | 0.97 |
| | *G. atroviolacea* | $2.53{\pm}0.11^{d}$ | 0.12 | 0.13 | 0.81 |
| Common | | $2.74{\pm}0.07^{e}$ | | | |

Note: Significant differences between species-specific and common c estimates (Turkey's test, $P < 0.01$) are indicated by superscripted letters. $P < 0.05$ indicate significant differences between Normalized Root-Mean-Square Errors (nRMSE) of species-specific and common formula.

formulas performed better than species-specific and common formulas. In our study, there was no statistically significant difference between the species-specific and the common calibration parameters (Table 2.2, $P > 0.05$). For two of the four studied bamboo species (*G. apus* and *B. vulgaris*), however, using species-specific formulas slightly improved the quality of predictions as compared to applying the common formula ($P = 0.06$ and $0.07$, respectively, Table 2.2). These two bamboo species had lower nRMSE and higher passing rates than *D. asper* and *G. atroviolacea* (Appendix Table A.2). The linear calibration parameters of the four bamboo species were significantly different from each other ($P < 0.01$). The linear calibration parameters, the slopes of $J_{s\_TDP}$ vs. $J_{s\_SHB}$, were examined with the test of homogeneity of slopes and were found to differ significantly from each other ($t > 0.01$).

Before calibration, $J_{s\_TDP}$ was on average 66% and 63% lower than SHB-derived reference values on the daily and 30-min scales, respectively ($P < 0.01$). This deviation was reduced to 10% and 8% underestimations ($P < 0.01$) when using species-specific calibration parameters (Table 2.2). On average, for $77{\pm}6\%$ of the days that were included in the analysis, the species-specific post-calibration 30-min $J_{s\_TDP}$ values were not significantly different from the respective reference $J_{s\_SHB}$ (Wilcoxon Signed-Rank test, $P > 0.05$).
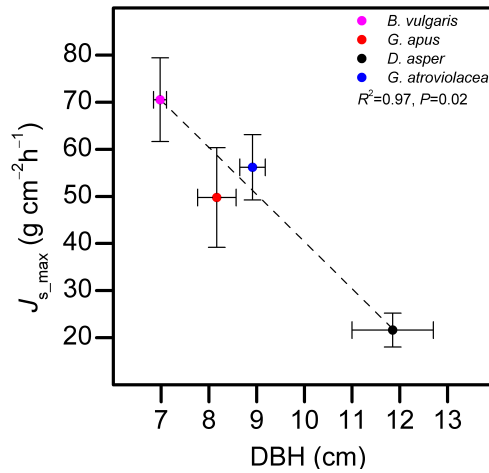
Fig. 2.3 Relationship between diameter at breast height (DBH) of bamboo culms and maximum observed sap flux density ($J_{s\_max}$) in four bamboo species. Horizontal error bars indicate DBH standard errors, vertical bars standard errors of $J_{s\_max}$. Data of five culms pooled per species, average of the highest 10% of daily $J_{s\_max}$ values of each culm used for the analysis.

### 2.3.3   Field study

**Monitoring bamboo and tree sap flux**

$J_{s\_max}$ in the studied bamboo species (averages from five individuals per species) were 70.5, 21.6, 49.7 and 56.2 g $cm^{-2}$ $h^{-1}$ for *B. vulgaris*, *D. asper*, *G. apus* and *G. atroviolacea*, respectively. In trees, corresponding values were 17.7, 10.5 and 23.3 g $cm^{-2}$ $h^{-1}$ for *H. brasiliensis*, *G. arborea* and *S. leprosula*, respectively. Across bamboo species, $J_{s\_max}$ decreased with increasing culm diameter ($R^2 = 0.97$, $P = 0.02$, Fig. 2.3).

**Environmental measurements and analyses**

The normalized daily accumulated $J_s$ of all studied species increased with increasing daily integrated radiation. This relationship did not fully hold up for accumulated $J_s$ and average daily VPD. In several species, daily $J_s$ increased with increasing VPD only to a certain VPD threshold (approx. 0.74 kPa, Fig. 2.4); after this threshold, accumulated $J_s$ decreased with further increasing VPD. Such conditions of high VPD were characteristic of the dry period. For days with VPD > 0.74 kPa, daily accumulated $J_s$ of most studied species (except in *D. asper* and *G. arborea*) declined with decreasing soil moisture content ($R^2 = 0.39$, 0.44, 0.4 ,0.52 and 0.55 for *B. vulgaris*, *G. apus*,
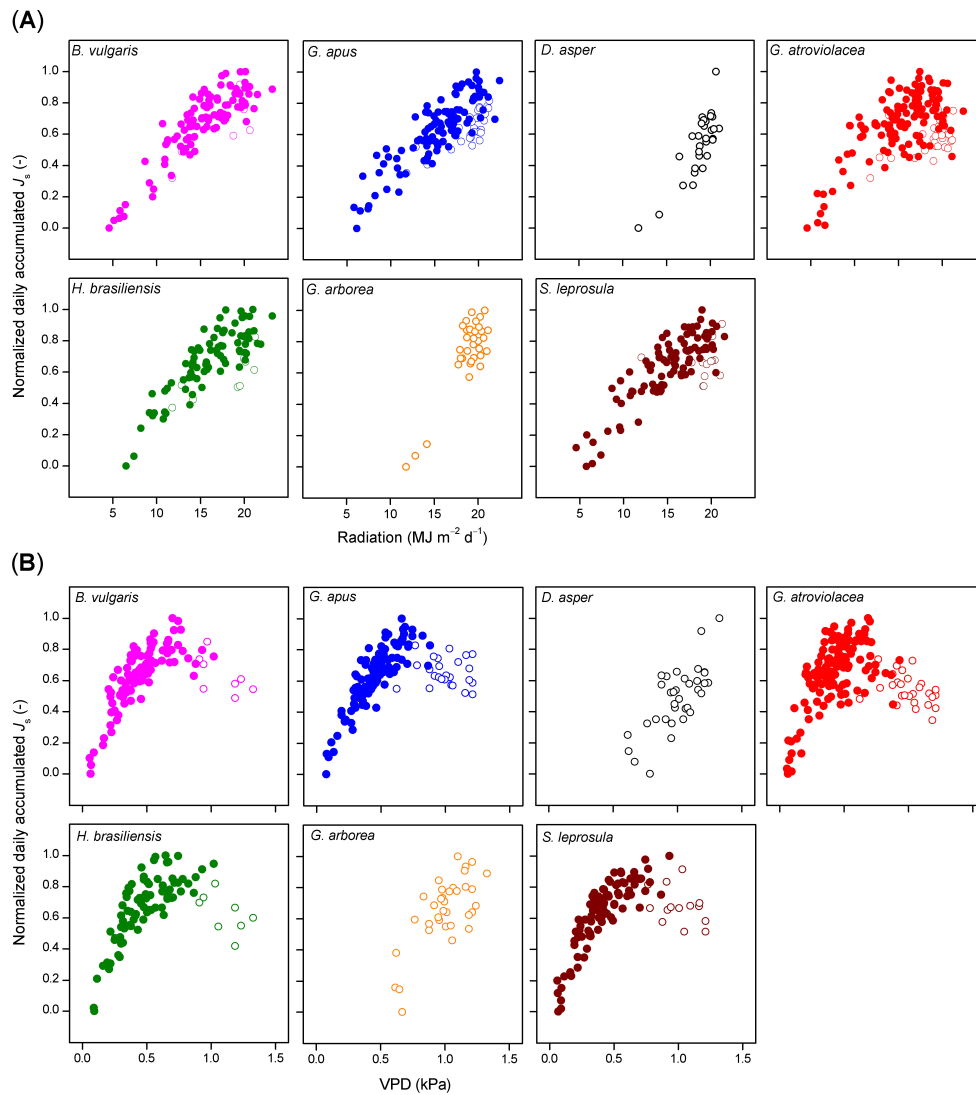
Fig. 2.4 Normallized daily accumulated sap flux density ($J_s$) plotted against absolute values of (A) intergrated daily radiation and (B) average daily vapor pressure deficit (VPD). Daily values of four bamboo (upper row) and three tree species (lower row); data from 7 months of measurements (July 2012-January 2013) encompassing both wet (filled circles) and dry (open circles) periods (except for *Dendrocalamus asper* and *Gmelina arborea*, mainly dry period). Daily averages derived from measurements of five culms per species.
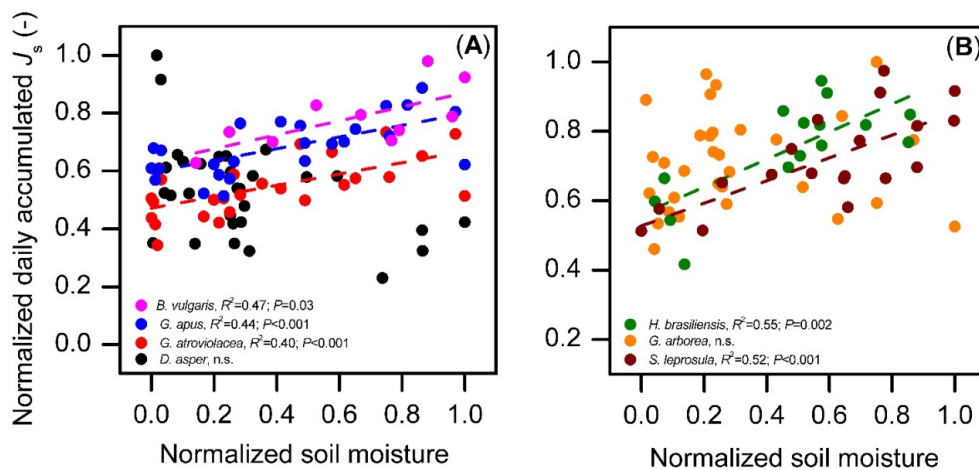
Fig. 2.5 Normalized daily accumulated sap flux density ($J_s$) of four bamboo species (A) and three tree species (B) in the "dry period" (characterized with mean daily VPD > 0.74 kPa) plotted against normalized mean daily soil moisture content (SM). There was a significant linear relationship between $J_s$ and SM ($P < 0.05$) for all species except *D. asper* and *G. arborea*. Normalized values do not reach 1.0 for all species in the figure as the normalization was performed by setting the maximum value of the full measurement period of each species (including wet period) to one, while the figure displays only values in dry period. Daily averages derived from measurements on five culms per species, data of at least 10 dry period days per species.

*G. atroviolacea*, *S. leprosula* and *H. brasiliensis* respectively; $P < 0.05$, Fig. 2.5 A & B).

Diurnal peaks in $J_s$ in the studied bamboo species occurred relatively early (on average at about 11 am), which was significantly earlier than the peaks of radiation and VPD (20 - 82 min and 131 - 206 min, respectively). In the studied tree species, maximal hourly $J_s$ values were observed after the peak of radiation (3 - 97 min), but still before (51 - 108 min) VPD peaked. All time lags were significantly different from zero minutes ($P < 0.01$; Table 2.3), except for the time lag to radiation for the tree species *S. leprosula* ($P > 0.05$).

Diurnally, some of the studied species showed pronounced hysteresis of hourly $J_s$ to radiation and VPD. Direction of rotation (i.e. order of observations) was counter-clockwise for radiation (Fig. 2.6 A) and clockwise for VPD (Fig. 2.6 B). The area of the hysteresis to VPD was on average 32% larger in bamboos than in trees, while the area of hysteresis to radiation was on average 50% smaller in bamboos ($P < 0.01$).
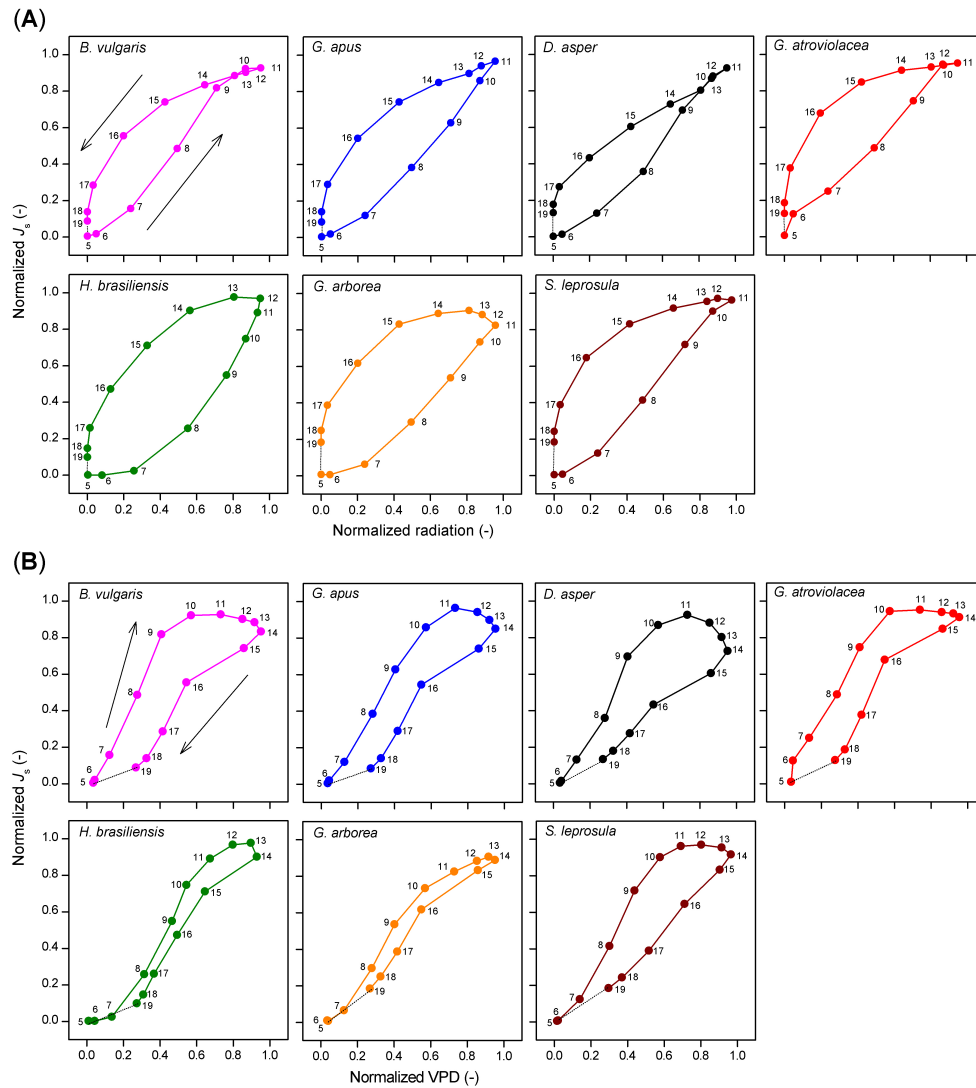
**(A)**



**(B)**



Fig. 2.6 Normalized hourly sap flux density ($J_s$) plotted against (A) normalized hourly radiation and (B) VPD. Data of four bamboo (upper row) and three tree species (lower row). Hourly averages derived from simultaneous measurements on five culms per species and by averaging the values of three sunny days to minimize influences of weather. The numbers in the sub-figures indicate the respective time of the day.

Table 2.3 Time lags between diurnal peaks of radiation and VPD and peaks of $J_s$ in studied bamboos and trees.

| Species | $N$ | Time lag with radiation (min) | Time lag with VPD (min) |
|---|---|---|---|
| *B. vulgaris* | 5 | 82±62 | 171±63 |
| *G. apus* | 5 | 41±57 | 206±57 |
| *D. asper* | 4 | 20±61 | 131±53 |
| *G. atroviolacea* | 5 | 64±30 | 170±35 |
| Bamboo_mean | 19 | 51[A] | 169[A] |
| *H. brasiliensis* | 5 | -37±12[a] | 51±9 |
| *G. arborea* | 5 | -97±87[b] | 67±87 |
| *S. leprosula* | 5 | -3±25[a] | 108±20 |
| Tree_mean | 15 | -46[B] | 75[B] |

Note: Positive values indicate a peak of radiation/VPD after the peak of $J_s$, negative values indicate a peak before $J_s$; $N$, culms/trunks per species averaged (mean±SD). Significant differences in bamboo/tree mean time lags are indicated by different superscripted letters (Turkey's test, $P < 0.01$). Significant differences between species are indicated by capital letters ($P < 0.01$).

## 2.4   Discussion

### 2.4.1   Calibration experiments

In the pot calibration experiment, SHB yielded similar results as reference GM measurements. Bamboos seem well suited for the SHB method (Dierick et al., 2010) due to their round shape and smooth and barkless surface, which allows for tight contact with the gauges. Additionally, the hollow center and thin culm walls result in relatively low energy losses to heat storage so that the heat balance conditions required for the SHB method are met. "Zero sap flux" conditions to obtain the heat conductivity of the sheath ($K_{sh}$, Sakuratani, 1981) as a further requirement of the SHB method are difficult to determine in situ due to potential root pressure induced night time sap flux in bamboos (Cao et al., 2012); however, using $K_{sh}$ derived from field conditions of very low night-time sap flux likely introduced only negligible errors into the calculation of daytime sap flux (Grime and Sinclair, 1999). As we observed very low sap flux over several hours during our experiments (e.g., about 1 g cm$^{-2}$ h$^{-1}$ during the pot experiment), our obtained $K_{sh}$ were likely reliable.

In contrast to SHB, the TDP method was found to substantially underestimate $J_s$ of bamboos in the pot and field calibration experiments. Underesti-

mations by TDP were also reported in two other bamboo species: respective average underestimations of 13% for *Bambusa blumeana* (Dierick et al., 2010) and 31% for *Phyllostachys pubescens* (Moso bamboo, Kume et al., 2010) were reported. Reasons for the observed underestimations could lie in the distinct hydraulic and physiological features of bamboos. Diurnal variations of stem water storage, for example, could affect the accuracy of TDP measurements (Vergeynst et al., 2014). Bamboos have approx. 50% parenchyma in culm walls (Dransfield and Widjaja, 1995), which potentially provides large water reservoirs. The depletion and refilling of the stem during the day and night, respectively, could cause diurnal fluctuations in culm thermal diffusivity. Higher water content during the night could lead to a lower maximum temperature difference ($\Delta T_{max}$) between heated and reference probe under "zero sap flux" conditions. Likewise, lower water content during the day could lead to higher observed $\Delta T$ values. As $\Delta T_{max}/\Delta T$ constitutes the basis for calculations of daytime $J_s$, substantial underestimations of $J_s$ could be introduced when using the original calibration parameters (Granier, 1985; Vergeynst et al., 2014). This hypothesis was assessed further by comparing the linear calibration parameters of *B. vulgaris* from the pot and the field calibration experiment ($c = 2.28$ and $2.79$, respectively). In the pot experiment, the bamboos were always supplied with plenty of water, so that the variability of the culm water content was likely smaller than under field conditions. Effects of varying stem water content on $\Delta T_{max}/\Delta T$ are thus likely much smaller in the pot experiment, which may explain why pot and field calibration experiment yield different parameters for the linear calibration of the same species (*B. vulgaris*). Another potential factor for the divergence could be that the maximum observed $J_s$ in the field (about 70 g cm$^{-2}$ h$^{-1}$) was much larger than in the pot experiment (about 20 g cm$^{-2}$ h$^{-1}$). Higher daytime sap flux (and thus transpiration) may cause a quicker depletion of the potential culm water storage, which consequently leads to a higher variability of culm water content between night and day.

We expected the calibration formula type (linear vs. nonlinear) and data time step to have an impact on the performance of TDP predictions. However, both were not as important as the factor formula specificity. Even though species-specific calibration formulas generally did not perform significantly better than the common formula, species-specific formulas tended to show slightly better performance (Table 2.1) for two of the studied species (*G. apus* and *B. vulgaris*). Also, the calibration parameters were significantly different among the four studied bamboo species (Table 2.2). Confronting this insight

with results from sap flux studies on other bamboo species (Dierick et al., 2010; Kume et al., 2010), differences among species become even more apparent. We thus used the derived species-specific formulas for further analysis. The observed differences among species may be indicative of highly heterogeneous wood anatomical properties among bamboo species. For example, size and shape of vascular bundles and parenchyma of 15 bamboo species were reported to be highly variable (de Agrasar and Rodríguez, 2003). For two further bamboo species (*Chusquea ramosissima* and *Merostachys claussenii*), it was suggested that differences in number of vascular bundles per unit area (1000 vs. 225 per cm$^2$) and vessel length ($\approx$ 1 m vs. 20 cm) could lead to differences in xylem hydraulic conductivity (Saha et al., 2009). Differences in wood anatomical properties may also lead to heterogeneous heat conductive properties, which potentially affects applicability and accuracy of sap flux measurements and particularly of the TDP method (Wullschleger et al., 2011).

In our study, culm-specific formulas performed better at predicting $J_s$ than species-specific and common calibration formulas (Appendix Table A.1 and A.2). This result indicates heterogeneity in conductive properties among culms of the same species. Potential reasons could lie in the age and the ontogeny of individual culms. Even though we carefully selected culms of similar age (approx. two years old), the exact age of individual bamboo culms within a given clump is difficult to assess. As all monocot species, bamboos lack secondary growth (Zimmermann and Tomlinson, 1972), so culm diameters are not related to culm age. Additionally, over the ontogeny of a certain culm, events and processes such as conductive circuit failure (drought- or metabolism-related; Cochard et al., 1994; Liese and Weiner, 1996), lignification (Lin et al., 2002) or increasing hydraulic limitations with height (Cao et al., 2012; Renninger and Phillips, 2010) could result in overall reduced hydraulic conductivity and thus lower sap flux densities with increasing culm age. However, these processes remain difficult to assess from the outside of the culm; further studies linking the age and ontogeny of bamboos to (TDP-derived) sap flux and water use patterns are suggested.

### 2.4.2 Water use patterns of bamboos and trees

Half-hourly $J_{s\_max}$ in the four studied bamboo species ranged from 21.6 to 70.5 g cm$^{-2}$ h$^{-1}$ and were (on average) almost two times greater than in the studied tree species. The observed range for both bamboos and trees falls into

the range of $J_{s\_max}$ values reported for tropical tree species in a variety of sap flux studies (Meinzer et al., 2001; O'Brien et al., 2004). For *D. asper*, the $J_{s\_max}$ (21.6 g cm$^{-2}$ h$^{-1}$) was similar to values reported for *Bambusa blumeana* culms (25.7 g cm$^{-2}$ h$^{-1}$, Dierick et al., 2010) and Moso bamboos (approx. 20 g cm$^{-2}$ h$^{-1}$, Kume et al., 2010) of similar size. Our four studied bamboo species showed significant differences in $J_{s\_max}$, which were negatively correlated with species-specific differences in DBH (Fig. 2.3). Consistent with this, in a study on 27 tropical tree species, the negative correlation between $J_{s\_max}$ and DBH was also observed (Meinzer et al., 2001). It was assumed to be related to a decline of the leaf area to sapwood area ratio with increasing DBH. This was also observed in a study on *Eucalyptus grandis* trees (Dye and Olbrich, 1993). In our study, we harvested leaves of three bamboo species (*B. vulgaris*, *D. asper*, and *G. apus*) and found that the leaf weight to sapwood area ratio was positively correlated with $J_{s\_max}$ ($R^2 = 0.45$, $P < 0.05$). However, studies connecting such anatomical and eco-hydrological properties of bamboos are yet scarce (Saha et al., 2009).

On the day-to-day level, accumulated $J_s$ of both the studied bamboo and tree species were significantly correlated with radiation and VPD (Fig. 2.4). During the long wet period, accumulated $J_s$ linearly increased with higher integrated radiation and average daily VPD. Likewise, linear relationships in the day-to-day behavior of $J_s$ to micrometeorological drivers have been reported for some tropical bamboo and several dicot tree species (Dierick and Hölscher, 2009; Köhler et al., 2009). During the dry period characterized by higher radiation and VPD (13% and 100% higher, respectively) than during the wet period, however, the observed linear relationship to VPD did not hold. Higher average daily VPD ("dry period conditions") led to decreases in accumulated $J_s$ of several studied species (Fig. 2.4 B). Similar decreases after a certain peak value have been reported for some previously studied tree species (Jung et al., 2011; Kubota et al., 2005), but in most species studied so far, higher average daily VPD leads to increases in accumulated $J_s$ or water use (Hernández-Santana et al., 2008; Horna et al., 2011; Kume et al., 2007; Peters et al., 2010; Tang et al., 2006; Wullschleger and Norby, 2001). This was also reported for Moso bamboo (Komatsu et al., 2010). The observed decreasing accumulated $J_s$ in bamboos under high VPD in our study were related to a reduction of soil moisture in the dry period (for three of the four bamboo and two of the three studied tree species). During the dry period, VPD was generally much higher than during the wet period. Soil moisture may become a limiting factor after several days without rainfall in the dry period.

Accumulated $J_s$ decreased strongly and linearly with decreasing soil moisture under "dry period conditions" (i.e. VPD > 0.74 kPa) for all studied bamboo (except *D. asper* ) and tree species (except *G. arborea* , Fig. 2.5). Similarly, in a throughfall reduction experiment in Indonesia, declines of monthly $J_s$ of Cacao and *Gliricidia sepium*  were found to linearly correlate with reduced soil moisture (Köhler et al., 2010). Such sensitivity of daily $J_s$ to fluctuating soil moisture may be related to a relatively shallow rooting depth (Kume et al., 2007).

Regarding the diurnal course of $J_s$, the studied bamboo species showed earlier peaks than radiation and VPD, and also earlier than the respective peaks of the studied tree species. In contrast to this, previous studies on tropical trees reported rather small time-lags between peaks of $J_s$ and radiation and VPD, respectively (Dierick and Hölscher, 2009; Horna et al., 2011; Köhler et al., 2009). Pre-noon peaks of $J_s$ have only been described for few species thus far, for example, *Acer rubrum* (Johnson et al., 2011) and oil palms (Niu et al., 2015). The early diurnal peaks of $J_s$ result in substantial hysteresis of $J_s$ particularly to VPD. For another monocot species, oil palm, it has been suggested that such pre-noon peaks of $J_s$ and the resulting large hysteresis to VPD could be indicative of internal trunk water storage and/or root pressure mechanisms (Niu et al., 2015; Röll et al., 2015). Early peaks of $J_s$ could be due to a pre-noon contribution of internal water storage to bamboo transpiration. Likewise, the decoupling of hourly $J_s$ particularly from VPD in the afternoon, i.e. the drop in bamboo $J_s$ (after an early peak) despite further rising VPD, could be connected to the reduced water availability for leaves after the depletion of internal water storage at a certain time of the day. The depletion of stored stem water may be compensated for during the night by root pressure mechanisms (Cao et al., 2012; Yang et al., 2012). Other potential reasons for the diurnally relatively early decline of bamboo $J_s$ and the consequent decoupling of the sap flux response from micrometeorological drivers could be a decline in leaf hydraulic conductance in the afternoon hours, which could contribute to prevent stem water potential loss and subsequent xylem cavitation (Saha et al., 2009; Yang et al., 2012).

## 2.5 Conclusion

Adjusting and applying the TDP method for sap flux measurements on four bamboo species pointed to substantial differences in water use patterns between the studied bamboos and three tree species studied. Bamboos had higher $J_s$, and respective hourly maxima were reached earlier in the day than in tree species. This resulted in strong diurnal hysteresis, particularly to VPD, and in significant time lags between the peaks of $J_s$ in bamboos and the respective peaks of radiation and VPD. Both may point to a strong contribution of internal water storage mechanisms to bamboo transpiration. We found substantial differences in the day-to-day $J_s$ response of most studied bamboo and tree species to fluctuations in environmental conditions between the dry and the wet period. Reduced $J_s$ under conditions of high VPD in the dry period could largely be explained by limiting soil moisture content. The regulation of bamboo water use thus seems to involve mechanisms at the leaf-, culm- and root- level. However, these mechanisms yet remain to be inter-connected convincingly.

# Chapter 3

# The influence of bamboo culm water content on sap flux measurements with thermal dissipation probes: observations and modeling

Tingting Mei[1,2,3†*], Dongming Fang[1†], Alexander Röll[1], Dirk Hölscher[1]

[1] Tropical Silviculture and Forest Ecology, Georg-August-Universität Göttingen, Germany.
[2] State Key Laboratory of Subtropical Silvilculture, Zhejiang Agriculture and Forestry University, Lin'an 311300, Zhejiang province, China.
[3] Zhejiang Provincial Key Laboratory of Carbon Cycling in Forest Ecosystems and Carbon Sequestration, Zhejiang Agriculture and Forestry University, Lin'an 311300, Zhejiang province, China.

[†] The authors contributed equally to this work.

[*] Correspondence:
Tingting Mei, Tropical Silviculture and Forest Ecology, Georg-August-Universität Göttingen, Büsgenweg 1, Göttingen, 37077, Germany. Email: tmei@gwdg.de

# Abstract

Bamboos and other plants may substantially rely on stem water storage for transpiration. Fluctuations in wood water content ($\theta_{wood}$) may lead to errors when estimating transpiration based on sap flux ($J_s$) measurements with the widely used thermal dissipation probe (TDP) method. To test the effects of $\theta_{wood}$ on $J_s$, we conducted a culm dehydration experiment, monitored bamboos with TDPs, and implemented a steady-state thermal model. Central to the calculation of $J_s$, and thus a major potential source of error, is the maximal temperature difference between probes ($\Delta T_{max}$) which is often referred to as "zero sap flow" condition. In the culm dehydration experiment, we observed that $\Delta T_{max}$ decreased when $\theta_{wood}$ increased. In long-term field monitoring, $\Delta T_{max}$ decreased when soil moisture content increased, potentially indicating changes in $\theta_{wood}$ and a seasonal decrease in stem water storage. The steady-state model reproduced the $\theta_{wood}$ to $\Delta T_{max}$ relationship of the dehydration experiment and underlined a considerable sensitivity of $J_s$ estimates to $\theta_{wood}$. Fluctuations in $\theta_{wood}$ may lead to substantial underestimation of $J_s$, and subsequently of transpiration, in commonly applied estimation schemes. However, our model results suggest that such underestimation can be quantified and subsequently corrected for with our correction equations when key wood properties are known. Our study gives insights into the relationship between $\theta_{wood}$ and TDP-derived $J_s$ and examines potential estimation biases.

**Keywords: calibration, culm water storage, soil moisture content, steady-state thermal model, transpiration, zero sap flow**

## 3.1   Introduction

Plant stems are the pathways of soil water to the leaves for transpiration (Tyree and Sperry, 1988). Measuring sap flow in stems and up-scaling it to plant transpiration can be conducted with several different sap flow methods such as the stem heat balance method, the heat pulse method or the thermal dissipation method (Smith and Allen, 1996). Among these methods, the thermal dissipation probe (TDP) method (Granier, 1985) is most widely used one. Its advantages include its relatively low cost as well as relatively easy sensor construction and installation (Lu et al., 2004). The empirical TDP formula for the calculation of sap flux density ($J_s$, g m$^{-2}$ s$^{-1}$) was first put forward

by Granier (1985); $J_s$ is expressed as a function of the temperature difference ($\Delta T$) between a heating probe and a reference probe: $J_s = 119 \times (\Delta T_{max}/\Delta T - 1)^{1.231}$, where $\Delta T_{max}$ is the $\Delta T$ under zero flow condition, which is commonly substituted by the diurnal nighttime maximum $\Delta T$ (Granier, 1987).

As Granier's formula was derived from an empirical relationship of three tree species (*Pseudotsuga menziesii*, *Pinus nigra* and *Quercus pedunculate*; Granier 1985) rather than being based on wood physical properties (Wullschleger et al., 2011), the TDP method has been reported to substantially over- or underestimate $J_s$ in various studies (Bush et al., 2010; Clearwater et al., 1999; Steppe et al., 2010). Potential reasons for observed divergences include non-uniform sap flow along the sensor (Clearwater et al., 1999), lacking compensation for the "wound effect" (Wullschleger et al., 2011) and gradients in temperature along the stem (Do and Rocheteau, 2002). Further, the effects of variations in wood water content ($\theta_{wood}$) of the stem on the accuracy of TDP measurements have been the subject of investigation (Lu et al., 2004; Tatarinov et al., 2005; Vergeynst et al., 2014). Generally, the depletion and recharge of water storage in stems can lead to substantial fluctuations of $\theta_{wood}$ (Nadler et al., 2008; Yang et al., 2015), which may influence wood thermal conductivity ($K_{wood}$) and subsequently estimates of $J_s$. Based on theoretical analysis of the temperature-$\theta_{wood}$ relationship (Carslaw and Jaeger, 1959) and a laboratory dehydration experiment on tree stem segments (Vergeynst et al., 2014), it was demonstrated that $\theta_{wood}$ influenced $K_{wood}$ around TDP probes and caused underestimations of daytime $J_s$. These underestimations were attributed to selecting one single $\Delta T_{max}$ (usually at night) to calculate hourly $J_s$ for the whole day (Granier, 1987) while ignoring potentially differing $K_{wood}$ between nighttime and daytime. Additionally, the influence of $\theta_{wood}$ on $\Delta T_{max}$ may differ with soil water conditions, as previous studies found that $\theta_{wood}$ in trees and palms fluctuates with $\theta_{soil}$ on the longer (i.e. monthly, seasonal) term (Constantz and Murphy, 1990; Holbrook et al., 1992; Wullschleger et al., 1996). Further, on rainy days, trunk $\theta_{wood}$ was reported to be significantly increased, and subsequently decreased during the following sunny days (Constantz and Murphy, 1990; Holbrook et al., 1992; Wullschleger et al., 1996), which may further influence $K_{wood}$ around TDP probes, and thus $\Delta T_{max}$. Ignoring these influences could lead to a potential misinterpretation of the patterns or values of TDP-derived $J_s$.

In a previous study on bamboo water use, underestimated $J_s$ by TDP was observed when using the original parameters of the calibration equation (Granier, 1985), while newly calibrated, species-specific equation parame-

ters significantly improved the accuracy of the estimation (Mei et al., 2016).
Among the potential reasons for the underestimation by the TDP approach on
bamboos is the thus-far neglected influence of dynamics in $\theta_{wood}$. Bamboo
culms have a large percentage of parenchyma ($\approx 50\%$, Liese and Köhl, 2015),
which provides a potential "buffering" reservoir for transpiration. With the
withdrawal from and refilling of water to this reservoir, $\theta_{wood}$ may fluctuate
accordingly, which can induce changes in culm circumference (Yang et al.,
2015). Changes in $\theta_{wood}$ in bamboo culms may at least partly be responsible
for underestimations of $J_s$ by influencing $K_{wood}$ of the culm and consequently
$\Delta T_{max}$.

However, the mentioned factors are rather difficult to assess under field con-
ditions and are commonly ignored in TDP studies on bamboos and trees, which
is mainly due to practical constraints and the difficulty of measuring the dynam-
ics of temperature around the TDP sensors. One promising approach could be
series of controlled numerical simulations of $\theta_{wood}$ encompassing different sce-
narios. Such numerical simulations have previously been successfully applied
to investigate the uncertainty of factors such as wood thermal conductivity,
non-homogeneity of radial sap flow profiles or external temperature gradients
on thermal-based methods including the TDP approach (Tatarinov et al., 2005)
and to analyze the influence of wood and probe properties (Wullschleger et al.,
2011) and of heat storage capacity (Hölttä et al., 2015) on the accuracy of TDP
estimates.

Partially based on such series of numerical simulations, we hypothesized
that the change of $K_{wood}$, responding to diurnal and seasonal fluctuations of
$\theta_{wood}$, induces estimation biases in $\Delta T_{max}$ and thus in TDP-derived daytime
$J_s$; this may (partly) be responsible for the mentioned underestimations of $J_s$.
Therefore, the objectives of our study were 1) to test on bamboo segments in a
laboratory dehydration experiment whether $\Delta T_{max}$ is affected by decreasing
$\theta_{wood}$, and to explore if $\Delta T_{max}$ in bamboos is influenced by changes in $\theta_{soil}$
under field conditions, and 2) to quantify and if necessary correct for potential
deviations of $J_s$ in bamboo culms with a steady-state thermal model. Our study
is intended as a methodological baseline study to evaluate and improve the
accuracy of TDP measurements on bamboos.

## 3.2  Methods

### 3.2.1  Culm $\theta_{wood}$, $\theta_{soil}$ and $\Delta T_{max}$

To test if $\Delta T_{max}$ is affected by changes in $\theta_{wood}$ in bamboos, we applied three different approaches: 1) a dehydration experiment on freshly cut culm segments of *Gigantochloa apus*, 2) long-term field monitoring of $\theta_{soil}$ and daily TDP-derived $\Delta T_{max}$ on culms of three bamboo species (*Bambusa vulgaris*, *Dendrocalamus asper*, *G. apus*), and 3) numerical simulation experiments with a steady-state thermal model based on the geometry and physical characteristics of a segment of *B. vulgaris*.

**Laboratory dehydration experiment**

Similar to previously conducted dehydration experiments on tree segments (Vergeynst et al., 2014), we performed dehydration experiments on freshly cut culm segments of *G. apus*; our laboratory experiments took place in May 2013. Before the actual experiments, a freshly sprouted culm of *G. apus* (diameter 7.3 cm) was cut before sunrise in the common garden of Bogor Agriculture University, Bogor, Indonesia. From the cut culm, three segments (each 20 cm in length) were collected and immediately transported to the laboratory inside a sealed plastic bag to prevent water loss. In the laboratory, the segments were soaked in 40 mM KCl solution for 24 hours to ensure that they reached saturation moisture content. After that, water on the surface of the segments was removed with tissues, while the two ends of each segment were sealed with glue. This ensured that they subsequently only and uniformly dehydrated from the outer culm surfaces.

At a first step of the actual dehydration experiment, the fresh weight of each segment ($w_{fresh}$, g) was obtained with a balance with 0.01 g resolution (KB2400-2N, KERN & SOHN GmbH, Balingen, Germany). Each segment was then laid down horizontally and a pair of 1 cm-long TDP was installed in the culm wall (Mei et al., 2016). The heating and reference probes were placed 10 cm apart, at 5 cm distance to each end of the segment.

As a second step, cycles of three-hour probe powering and subsequent two-hour dehydration periods were conducted repeatedly over the duration of five days. During the powering phase, the heating probe of the TDP sensors was continuously powered with 0.1 W in order to obtain stable $\Delta T_{max}$ readings. During this interval, room temperature was kept constant at about 20 °C and

laboratory conditions prevailed (constant light, only a little air circulation); the segments thus dehydrated only marginally during this time. During the following two-hour dehydration period, the power of the heating probe was turned off and the segments were placed under an electric fan to artificially accelerate the dehydration process. The segments were further continuously turned to ensure uniform dehydration. At the end of each two-hour period, TDP sensors were removed and the segments were weighted. By continuously repeating the powering-dehydration cycles, data pairs of $w_{\text{fresh}}$ vs. $\Delta T_{\text{max}}$ were produced and recorded.

After the end of the dehydration experiments, the segments were oven dried at 100 °C for 48 hours to get their dry weight ($w_{\text{dry}}$, g). With the $w_{\text{dry}}$ and $w_{\text{fresh}}$ of each powering-dehydration cycle, the $\theta_{\text{wood}}$ (kg kg$^{-1}$) was calculated as ($w_{\text{fresh}}$ - $w_{\text{dry}}$)/ $w_{\text{dry}}$. Subsequently, the relationship between $\theta_{\text{wood}}$ and $\Delta T_{\text{max}}$ was examined.

### Field monitoring of $\theta_{\text{soil}}$ and $\Delta T_{\text{max}}$

To explore whether, and if so how, $\Delta T_{\text{max}}$ in bamboo culms was influenced by the $\theta_{\text{soil}}$ under field conditions, we monitored daily TDP-derived $\Delta T_{\text{max}}$ on three culms each of *D. asper* and *G. apus* and on four culms of *B. vulgaris* for seven months (July 2012 to April 2013). Simultaneously, $\theta_{\text{soil}}$ at 20 cm depth was monitored at the respective study sites with time domain reflectometry sensors (TDR, CS616, Campbell). For a detailed description of the installation process refer to Mei et al. (2016). Subsequently, the relationship between $\Delta T_{\text{max}}$ and daily mean $\theta_{\text{soil}}$ was examined.

### $\theta_{\text{wood}}$ and thermal conductivity for the numerical model

As the theoretical basis of the following numerical model, the relationship of thermal conductivity of wood ($K_{\text{wood}}$) and $\theta_{\text{wood}}$ was applied following Vandegehuchte and Steppe (2012), who introduced a corrected thermal conductivity for axial directions ($K_{\text{axial}}$, W m$^{-1}$ K$^{-1}$; Eq. 3.1):

$$K_{axial} = K_w(\theta_{wood} - \theta_{wood-FSP})\frac{\rho_{dry}}{\rho_w} + 0.04186 \times (21.0 - 20.0 \times F_{v-FSP})$$

(3.1)

Where $K_{\text{w}}$ is thermal conductivity of water (0.6 W m$^{-1}$ K$^{-1}$), $\theta_{\text{wood-FSP}}$ is $\theta_{\text{wood}}$ at the fiber saturation point (%), $\rho_{\text{dry}}$ and $\rho_{\text{w}}$ are the respective densities
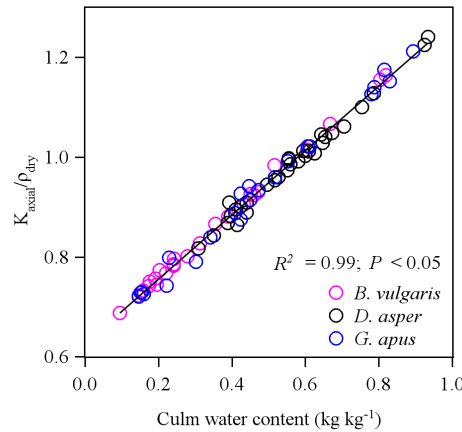
Fig. 3.1 The relationship between the ratio of thermal conductivity in the axial direction ($K_{axial}$) to culm dry density ($\rho_{dry}$) and culm water content. The relationship was derived by Eq. 3.1.

of dry wood and water (1000 kg m$^{-3}$) and $F_{v\text{-FSP}}$ is the void fraction of wood at the fiber saturation point. $\theta_{wood\text{-FSP}}$ and $F_{v\text{-FSP}}$ were calculated with several different approaches, using $\rho_{dry}$ and $\rho_w$ (see details in Appendix Chapter 3).

To obtain $\rho_{dry}$ of bamboo culms, all culms of the three species that were monitored in our study were harvested at 6:00 am on 15, 16 and 28 April 2013. Segments were obtained every two meters on the respective culms. The segments were immediately transported to the laboratory in sealed plastic bags. The fresh volumes ($v_{fresh}$, cm$^3$) of the segments were derived by measuring lengths and inner and outer radiuses of the cylindrical segments; additionally, the $w_{fresh}$ of each segment was established. After that, the segments were dried in an oven at 100 °C for 48 hours to get their $w_{dry}$. Subsequently, $\rho_d$ could be calculated as $w_{dry}/v_{fresh}$.

With the mentioned variables ($\rho_{dry}$, $\rho_w$, $\theta_{wood\text{-FSP}}$ and $F_{v\text{-FSP}}$), we calculated series of $K_{axial}$ with $\theta_{wood}$ ranging from 0.1 to 1 kg kg$^{-1}$ (in incremental 0.1 kg kg$^{-1}$ steps); the thermal conductivity in the transverse direction ($K_t$) was set to half the value of the $K_{axial}$ (Wullschleger et al., 2011). The linear relationship between the $K_{axial}$ and $\theta_{wood}$ of the bamboo culms was derived (Fig. 3.1), and this relationship was applied in the following numerical steady-state thermal model to set the corresponding parameters.

**Steady-state thermal model**

To test if $\Delta T_{max}$ decreased with increasing $\theta_{wood}$ in bamboos, numerical simulations of temperature distributions were performed with a steady-state thermal model (Academic version, CFX 17.0, ANSYS Inc., Pennsylvania, USA). The simulations were conducted on a 3D anisotropic grid by numerically solving the steady-state energy balance equation (Eq. 3.2):

$$-\lambda \nabla^2 T + c_w Q_w \nabla T = q \tag{3.2}$$

Where $q$ is the heat input of a grid (W m$^{-3}$), $T$ is the temperature of a grid (K), $\lambda$ is matrix of thermal conductivity (W $^{-1}$ K$^{-1}$), $\nabla$ is vector differential operator, $c_w$ is the specific heat of water (J kg$^{-1}$ K$^{-1}$) and $Q_w$ is the sap flow vector (kg m$^{-2}$ s$^{-1}$). To explore the relationship between $\theta_{wood}$ and $\Delta T_{max}$, $Q_w$ was set to zero sap flow when aiming to simulate $\Delta T_{max}$ (See detailed parameters in Table 3.1).

In order to simplify the simulation, the geometry of the model was based on a simplified 3D bamboo segment, i.e. a cuboid with 20 cm height, 6.65 cm width, and 1 cm depth, ignoring the curvature of the stem surface. The heating probe of the TDP sensor was modeled as an aluminum tube with its actual dimensions, i.e. 0.235 cm in diameter and 1 cm in length (Mei et al., 2016); it was inserted through into the 1 cm wide simulated culm wall of the cuboid, in the center of the segment (Wullschleger et al., 2011). Resembling the (actual) field methodology, the unheated reference probe was positioned 10 cm upstream from the heating probe. Along the length of the heating probe, the temperature was assumed to be fairly uniform (Wullschleger et al., 2011), and wood physical properties along the probe were also assumed to be uniform. The steady state simulations were thus simplified for both the front and back surfaces of the segment. Generally, a 2 mm (quadratic) mesh was used for the thermal steady state model. To better fit the round shape of the heating probe, mesh type was set to quad/tri for the contact area between the heating probe and the surrounding wood.

The boundary conditions of the segment surfaces included inlet, outlet, probe, symmetric surfaces (front and back) and wall. The inlet surface was located on the upstream side and the water came into the segment from the inlet. The outlet surface was located on the downstream side and the pressure was set to 0 Pa. The heating probe was located in the center of the bamboo segment and was powered with 1444 W m$^{-2}$ (the input power divided by the surface area of the aluminum tube). The front and back surfaces of the wood

Table 3.1 Parameters for the ANSYS numerical simulation

| Parameters | Values | Reference |
|---|---|---|
| Specific heat capacity of fresh wood | 1644 J kg$^{-1}$ K$^{-1}$ | Measured |
| Dry wood density | 956 kg m$^{-3}$ | Measured |
| Heating probe power | 1444 W/m$^2$ | Measured |
| Probe length | 1 cm | Measured |
| Ambient temperature | 300 K/26.85 °C | Set |

domain were set as symmetric, which means any plane between the front and back surfaces has same physical and thermal properties. The left and right sides of the bamboo segment were defined as walls with no water flowing out of the segment. The initial temperatures on all segment surfaces and of sap water were set to 300 K (26.85 °C) by default in the ANSYS model.

## 3.2.2 The influence of $\theta_{wood}$ on $J_s$ simulated in ANSYS

To simulate the influence of varying $\theta_{wood}$ on TDP-derived $J_s$ in bamboo culms, we simulated the $\Delta T$ between probes in a series of numerical simulations of $J_s$ and $\theta_{wood}$. We incrementally increased $J_s$ from 0 to 30 g cm$^{-2}$ h$^{-1}$ in 5 g cm$^{-2}$ h$^{-1}$ steps and $\theta_{wood}$ from 0.1 to 1 kg kg$^{-1}$ in 0.1 kg kg$^{-1}$ steps, and thus got a series of $\Delta T$ under each combination of $J_s$ and $\theta_{wood}$. The $\Delta T$ of each possible combination at zero $J_s$ was used as $\Delta T_{max}$. The settings of geometry, meshing and change of $K_{axial}$ against $\theta_{wood}$ followed the previously described model description (see the section "$\theta_{wood}$ **and thermal conductivity for the numerical model**").

Two scenarios were simulated: 1) relative to a fixed nighttime $\theta_{wood}$ ($\theta_{wood\_night}$, e.g., 1 kg kg$^{-1}$), where the daytime $\theta_{wood}$ ($\theta_{wood\_daytime}$) was reduced in 0.1 kg kg$^{-1}$ steps until its minimum 0.1 kg kg$^{-1}$; in total, 45 pairs of $\theta_{wood\_night}$ and $\theta_{wood\_daytime}$ were simulated; 2) based on different $\theta_{wood\_night}$ (0.3, 0.6 and 0.9 kg kg$^{-1}$), where $\theta_{wood\_daytime}$ was reduced by a constant ratio (i.e. half of $\theta_{wood\_night}$). The first scenario was simulated to explore the influence of changes in $\theta_{wood}$ between daytime and nighttime ($\Delta\theta_{wood}$) on diurnal (daytime) $J_s$. The second scenario compared the varying influence of $\Delta\theta_{wood}$ on daytime $J_s$ among the days with different $\theta_{wood\_night}$ but with the same relative reduction during the daytime. The second scenario likely occurs e.g., between different seasons (dry vs. wet season) or among days with different weather conditions (e.g., sunny vs. rainy days).

For a set $\theta_{wood\_daytime}$ (e.g., $\theta_{wood\_daytime}$ = 1 kg kg$^{-1}$), the derived $\Delta T$ were used to calculate $J_s$ in two ways: (1), $J_s$ was calculated with $\Delta T_{max}$ derived from $\theta_{wood\_night}$ values equal to the set $\theta_{wood\_daytime}$; (2), a biased $J_s$ ($J_{s\_bias}$) was calculated with a $\Delta T_{max}$ derived from a $\theta_{wood\_night}$ that was higher than the set $\theta_{wood\_daytime}$ (e.g., $\theta_{wood\_night}$ = 0.9 kg kg$^{-1}$). The respective relative changes of $J_s$ ($\Delta J_s$) were calculated as $\Delta J_s = (J_{s\_bias} - J_s)/J_s$. To determine the influence of using different (e.g., biased vs. un-biased) $\Delta T_{max}$ on daily accumulated $J_s$, the relationship between $\Delta J_s$ and $\Delta\theta_{wood}$ was then applied to one culm of *B. vulgaris* on a sunny day as a case study.

### 3.2.3 Correcting $J_{s\_bias}$

To correct the $J_{s\_bias}$, in a first step, we compared $\Delta J_s$ to $J_{s\_bias}$ for each combination of $\theta_{wood\_daytime}$ and the mismatched $\theta_{wood\_night}$ by applying a continuous logistic equation with three variables ($\Delta J_{s\_max}$, $\Delta J_{s\_0}$, $r$) in Eq.3.3:

$$\Delta J_s = \Delta J_{s\_max}/(1+(\frac{\Delta J_{s\_max}}{\Delta J_{s\_0}}-1)\times e^{-r\times J_{s\_bias}}) \tag{3.3}$$

Where $\Delta J_{s\_max}$ is the maximum $\Delta J_s$; note that as $\Delta J_s$ is negative value, $\Delta J_{s\_max}$ is the value closest to 0 and means the least relative change between $J_{s\_bias}$ and $J_s$; $\Delta J_{s\_0}$ is the $\Delta J_s$ when $J_{s\_bias}$ is 0; $r$ is the maximum increasing rate of $\Delta J_s$, for each $\Delta J_s$ and per unit of increase in $J_{s\_bias}$ (g cm$^{-2}$ h$^{-1}$)$^{-1}$, in analogy to the maximum rate of population increasing per capita per year in logistic regression of population growth (Balakrishnan, 1992).

As a second step, the three parameters of Eq. 3.3 ($\Delta J_{s\_max}$, $\Delta J_{s\_0}$, $r$), for all combinations that passed the logistic regression, were fitted with $\theta_{wood\_daytime}$ and the mismatched $\theta_{wood\_night}$ by linear regression. Then we replaced the three parameters in Eq. 3.3 with $\theta_{wood\_daytime}$ and the mismatched $\theta_{wood\_night}$, so that the $\Delta J_s$ was instead represented as a function of $\theta_{wood\_daytime}$, the mismatched $\theta_{wood\_night}$ and $J_{s\_bias}$. The thus derived $\Delta J_s$ was subsequently used to correct $J_{s\_bias}$ (Eq. 3.4):

$$\begin{aligned} J_{s\_corrected} &= J_{s\_bias}\times(1+\Delta J_s) \\ &= J_{s\_bias}/(1+\Delta J_{s\_max}/(1+(\frac{\Delta J_{s\_max}}{\Delta J_{s\_0}}-1)\times e^{-r\times J_{s\_bias}})) \end{aligned} \tag{3.4}$$

For all data analysis and plotting presented in our study, we used SAS 9.3 (SAS Institute Inc., Cary, NC, USA, 2013).

## 3.3  Results

### 3.3.1  $\Delta T_{max}$ and $\theta_{wood}/\theta_{soil}$

In the laboratory dehydration experiment, the three freshly sprouted bamboo segments of *G. apus* showed differences in $\theta_{wood}$ vs. $\Delta T_{max}$ patterns. Nonetheless, all three segments showed significant negative linear correlations between $\Delta T_{max}$ and $\theta_{wood}$ ($R^2 = 0.56$, 0.68 and 0.93 for the segment 1, 2 and 3, respectively, $P < 0.05$; Fig. 3.2 a). The negative linear relationship was also observed for simulated $\theta_{wood}$ and $\Delta T_{max}$ derived from the ANSYS model ($R^2 = 0.96$, $P < 0.05$; Fig. 3.2 b).

In the field monitoring, daily mean $\theta_{soil}$ was found to have a significant negative linear relationship ($P < 0.05$) with daily $\Delta T_{max}$ on all three bamboo species (*D. asper*, *G. apus*, *B. vulgaris*; Fig. 3.3). The slope of the $\Delta T_{max}$-$\theta_{soil}$ regression line was larger for *B. vulgaris* (-3.55) than for *D. asper* (-1.91) and *G. apus* (-2.14).

### 3.3.2  The influence of $\theta_{wood}$ on $J_s$

Keeping other controlling variables constant, large relative underestimation became apparent 1) for large decreases of $\theta_{wood}$ from nighttime to daytime, 2) at relatively low $J_s$, and 3) for relatively larger nighttime $\theta_{wood}$ when the ratio of decrease from daytime $\theta_{wood}$ was kept constant (e.g., by half).

Using the ANSYS model for series of numerical simulations of $\theta_{wood}$ and $J_s$, we found that TDP underestimated daytime $J_s$ calculated with nighttime $\Delta T_{max}$ when $\theta_{wood}$ was lower during the day than during the night. For a given nighttime $\theta_{wood}$ (e.g., 1 kg kg$^{-1}$), lower daytime $\theta_{wood}$ (e.g., 0.1 kg kg$^{-1}$) led to larger underestimation of $J_s$ of up to 44% (Fig. 3.4). The $\Delta J_s$ (%) was larger at lower $J_s$, and it gradually became smaller and approached to a stable value with increasing $J_s$. For example, the $\Delta J_s$ was 18.6% at 5 g cm$^{-2}$ h$^{-1}$ while being only 9.4% at 30 g cm$^{-2}$ h$^{-1}$, when $\theta_{wood}$ was decreased from 1 kg kg$^{-1}$ (nighttime) by 0.3 kg kg$^{-1}$ in the daytime (Fig. 3.4). Even though relative errors were smaller at higher daytime $J_s$, they were responsible for most of the underestimation of daily accumulated $J_s$. Numerical simulations
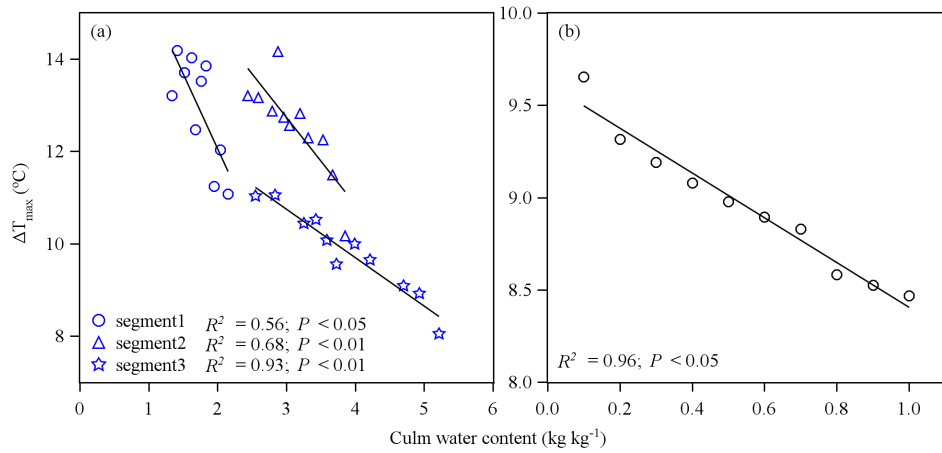
Fig. 3.2 The maximum temperature difference between the probes of TDP
($\Delta T_{max}$) in relation to the water content in culm segments of a freshly sprouted
*G. apus* in (a) the dehydration experiment and (b) the ANSYS simulation
experiment. Different symbols indicate different segments. The unit of culm
water content (kg kg$^{-1}$) indicates kg water in the culm per kg dry weight.



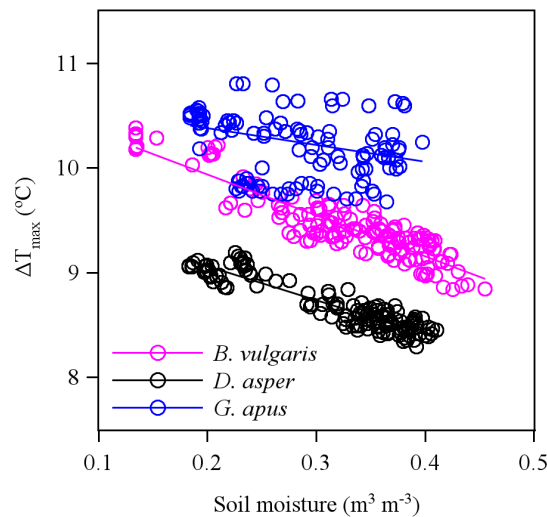Fig. 3.3 The daily maximum temperature difference between the probes of
TDP ($\Delta T_{max}$) in relation to daily mean soil moisture for three bamboo species
(*B. vulgaris*: $Y = -3.55X + 10.54$, $R^2 = 0.63$, $P < 0.01$; *D. asper*: $Y = -1.91X +
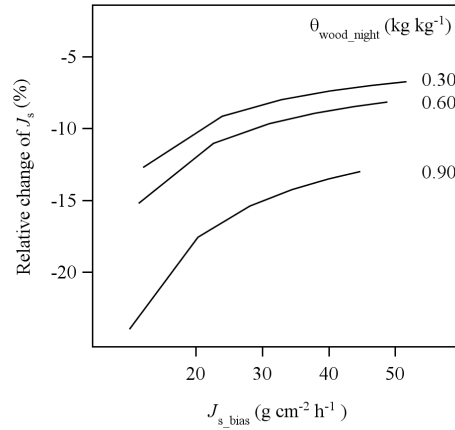9.21$, $R^2 = 0.54$, $P < 0.01$; *G. apus*: $Y = -2.14X + 11.10$, $R^2 = 0.37$, $P < 0.01$).
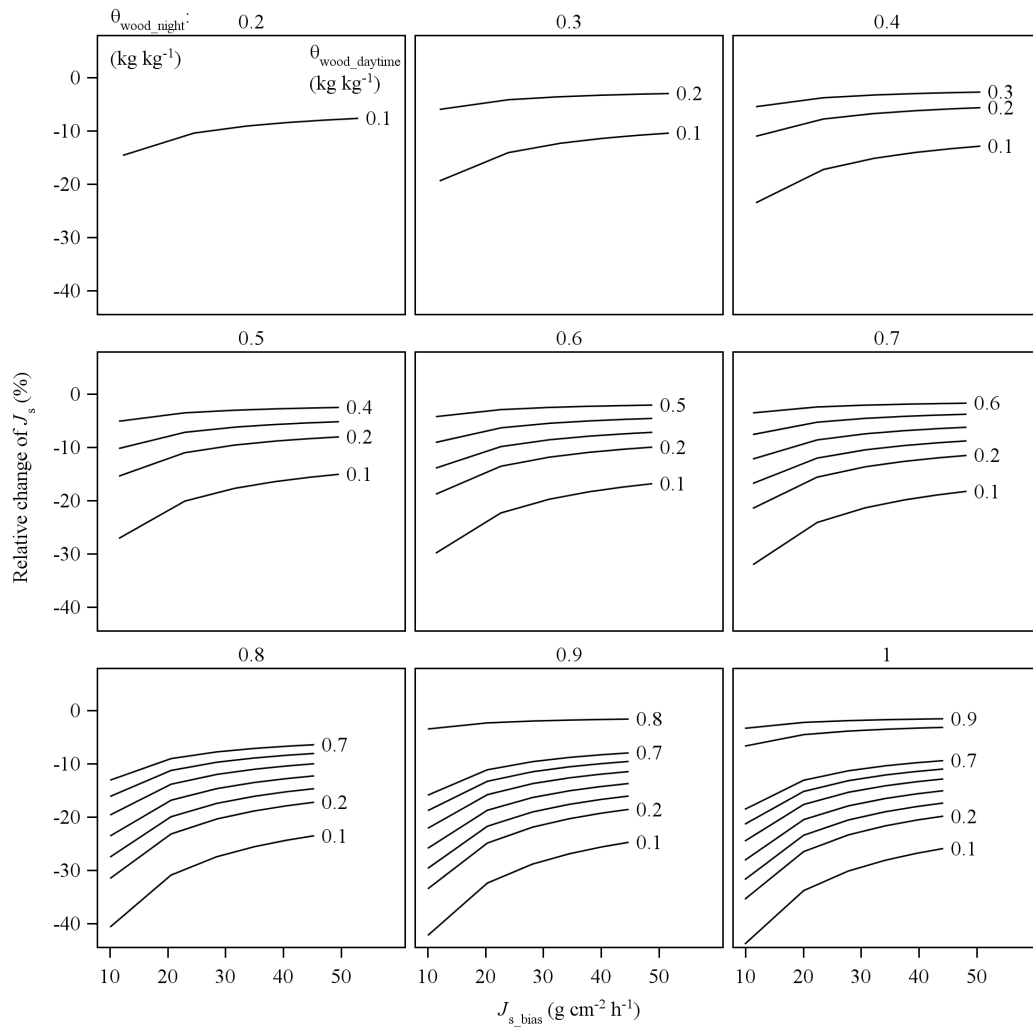
Fig. 3.4 The simulated relative change of daytime sap flux density ($J_s$) in percentage (%) at different absolute $J_s$ calculated with the mismatched $\Delta T_{max}$ ($J_{s\_bias}$, g cm$^{-2}$ h$^{-1}$). The value on the top of each sub-figure is the night water content ($\theta_{wood\_night}$, kg kg$^{-1}$), and the values at the ends of the lines are daytime water content ($\theta_{wood\_daytime}$, kg kg$^{-1}$). The provided data based on numerical simulations with the ANSYS model.
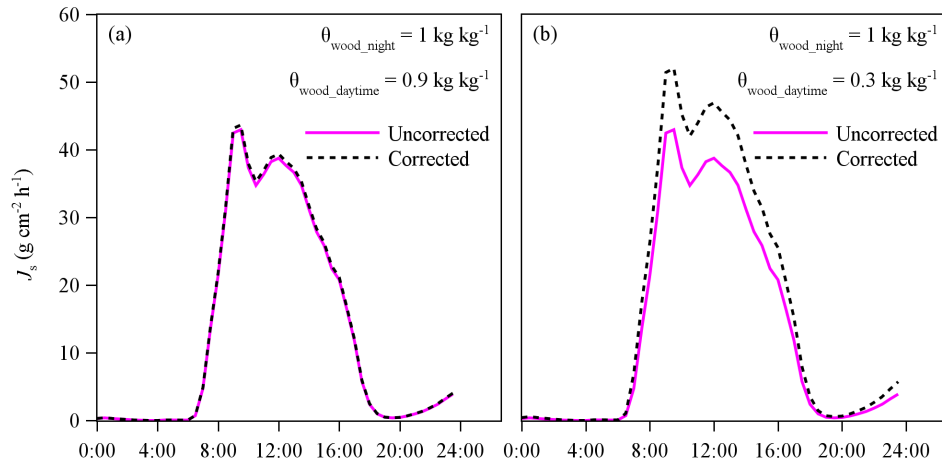
Fig. 3.5 The corrected sap flux density ($J_s$) for different daytime culm wood water content ($\theta_{wood}$, kg kg$^{-1}$), (a) $\theta_{wood}$ = 0.9 and (b) $\theta_{wood}$ = 0.3. Simulations based on field monitoring data of a *B. vulgaris* on 17 September 2012. Numerical simulations with the ANSYS model for daytime $\theta_{wood}$ of 0.9, 0.3 kg kg$^{-1}$ reduced from a 1 kg kg$^{-1}$ nighttime $\theta_{wood}$ result in underestimation of daily accumulated $J_s$ by 2%, 19%, respectively.

with the ANSYS model for reductions of $\theta_{wood\_daytime}$ by 0.1 and 0.7 kg kg$^{-1}$ (corresponding to 0.9 and 0.3 kg kg$^{-1}$ $\theta_{wood\_daytime}$) from 1 kg kg$^{-1}$ $\theta_{wood\_night}$ resulted in underestimations of daily accumulated $J_s$ by 2% and 19%, respectively (Fig. 3.5). For example, the relative errors caused at $J_s$ over 30 g cm$^{-2}$ h$^{-1}$ constituted as much as 64% of the total underestimation of daily water use (Fig. 3.5).

For hypothetical reductions of $\theta_{wood\_night}$ (0.3, 0.6, 0.9 kg kg$^{-1}$) to half of their respective values in the daytime (i.e. 0.15, 0.3 and 0.45 kg kg$^{-1}$), the highest (> 25%) underestimation of daytime $J_s$ were simulated for scenarios with high $\theta_{wood\_night}$ (i.e. 0.9 kg kg$^{-1}$) under conditions of low $J_s$ (e.g., 5 g cm$^{-2}$ h$^{-1}$). With increasing $J_s$, the underestimation became smaller (e.g., < 15% at 30 g cm$^{-2}$ h$^{-1}$), particularly for lower (i.e. 0.3, 0.6) $\theta_{wood\_night}$ (e.g., < 10% at 30 g cm$^{-2}$ h$^{-1}$, Fig. 3.6).

### 3.3.3   Correcting $J_{s\_bias}$

Among the 45 combinations of $\theta_{wood\_night}$ and $\theta_{wood\_daytime}$ (Fig. 3.4), there are 21 whose $\Delta J_s$ (negative percentage) and $J_{s\_bias}$ converged when applying a logistic regression. Two of the three parameters ($\Delta J_{s\_max}$ and $\Delta J_{s\_0}$) derived in these 21 logistic regressions were linearly related with both $\theta_{wood\_night}$ and

Fig. 3.6 The simulated relative change of daytime sap flux density ($J_s$) in percentage (%) at different absolute $J_s$ calculated with the mismatched $\Delta T_{max}$ ($J_{s\_bias}$, g cm$^{-2}$ h$^{-1}$). Relationships are provided for different nighttime stem water contents ($\theta_{wood\_night}$, 0.3, 0.6 and 0.9 kg kg$^{-1}$), assuming a constant reduction (i.e. by half) in the ratio between nighttime and daytime $\theta_{wood}$. Provided data based on numerical simulations with the ANSYS model.

$\theta_{wood\_daytime}$ (Eq. 3.5 and 3.6), while $r$ was corrected with $\theta_{wood}$ (Eq. 3.7), as shown below:

$$\Delta J_{s\_max} = -3.19\% - 0.20\% \times \theta_{wood\_night} + 0.25\% \times \theta_{wood\_daytime}$$
$$(R^2 = 0.94; P < 0.01) \tag{3.5}$$

$$\Delta J_{s\_0} = -24.93\% - 0.62\% \times \theta_{wood\_night} + 0.84\% \times \theta_{wood\_daytime}$$
$$(R^2 = 0.91; P < 0.01) \tag{3.6}$$

$$r = 0.03\% - 0.00005\% \times \theta_{wood\_night}$$
$$(R^2 = 0.96; P < 0.01) \tag{3.7}$$

By inserting Eq. 3.5, 3.6 and 3.7 into Eq. 3.4, we derived an equation for correcting the previously discussed estimation biases. With this "correction equation", we thus corrected $J_{s\_bias}$ of the remaining 24 combinations of $\theta_{wood\_night}$ and $\theta_{wood\_daytime}$, for which the logistic regression had not worked. Before correction, $J_{s\_bias}$ was about 10% smaller than $J_s$ ($J_{s\_bias} = 0.90 \times J_s - 0.82; R^2 = 0.98; P < 0.01$; Appendix Fig. A.2), while corrected $J_{s\_bias}$ ($J_{s\_corrected}$) was much closer to actual $J_s$ ($J_{s\_corrected} = 1.01 \times J_s - 0.64; R^2 = 0.99; P < 0.01$; Appendix Fig. A.2).

# 3.4   Discussion

## 3.4.1   $\Delta T_{max}$ and $\theta_{wood}/\theta_{soil}$

Granier's formula for estimating $J_s$ with TDP method is based on the assumption that wood thermal properties are constant throughout the day, which results in one constant diurnal $\Delta T_{max}$ (Granier, 1987). However, $\Delta T_{max}$ actually changes as wood thermal properties fluctuate diurnally, which is not reflected when using a common $\Delta T_{max}$. This introduces estimation errors when calculating $J_s$ based on a common daily $\Delta T_{max}$ (Vergeynst et al., 2014). In our study, a dehydration experiment was conducted on segments of freshly sprouted bamboo culms. The results show that decreasing culm $\theta_{wood}$ led to increasing $\Delta T_{max}$ (Fig. 3.2 a). Similar results were found in a dehydration experiment on tree segments (Vergeynst et al., 2014). In trees, the fluctuation pattern of $\theta_{wood}$ contrasted the daily fluctuation pattern of transpiration. $\theta_{wood}$ reached peak values during the night, when $J_s$ was zero or marginal, and dropped to a minimum during the daytime (Hao et al., 2013; Sperling et al., 2015). On culms of the bamboo species *B. vulgaris*, a similar pattern of culm circumference was observed (Yang et al., 2015). Although Yang et al. (2015) did not perform direct measurements of $\theta_{wood}$, the daily dynamics of culm circumference can be expected to at least partly reflect changes in $\theta_{wood}$ (Köcher et al., 2013; Scholz et al., 2008). Based on our findings, such fluctuations of $\theta_{wood}$ between nighttime and daytime go along with corresponding fluctuations in $\Delta T_{max}$ (Fig. 3.2). In the bamboo culms used in our study, $\Delta T_{max}$ significantly decreased with increasing $\theta_{soil}$ (Fig. 3.3), which may be attributed to the corresponding changes of $\theta_{wood}$ caused by the dynamics of $\theta_{soil}$. For trees, close coupling of the $\theta_{wood}$-$\theta_{soil}$ relationship was reported for rainy days and sunny days and for different seasons; on rainy days or after irrigation, $\theta_{wood}$ was significantly increased and subsequently decreased during following sunny days (Hao et al., 2013; Holbrook et al., 1992; Wullschleger et al., 1996). Over the course of a growing season, variation in $\theta_{wood}$ of red maple was reported to be 39% between the dry and the wet season (Wullschleger et al., 1996). It has been put forward that dynamics in $\theta_{wood}$ may reflect changes in stem water storage (Sperling et al., 2015). Dynamics in stem water storage may thus be derived from changes in $\theta_{wood}$ among days, given that $\theta_{wood}$ is derived from the $\Delta T_{max}$-$\theta_{wood}$ relationship and dry weight or volume of the tree stems or bamboo culms are known.

The model-derived $\Delta T_{max}$-$\theta_{wood}$ relationship was based on an ideal assumption that the nighttime zero sap flow existed and lasted long enough to establish a one-to-one correspondence between $\Delta T_{max}$ and maximum $\theta_{wood}$. However, this ideal assumption may not always be met during experiments (Regalado and Ritter, 2007). As such, several studies have reported nighttime sap flow in different species, which was presumably related to atmospheric evaporative demand (Forster, 2014). Further, during dry periods the commonly high daytime transpiration in combination with relatively low soil water availability could potentially lead to more nighttime sap flow in the form of refilling the depleted stem water reservoirs (Wang et al., 2012). In some cases, this might mean that zero flow conditions are not met at all, not even during the night. Even when the stem is fully recharged and reaches its maximum water content, nighttime sap flow could still occur, e.g., in the form of guttation. In the wet season (approx. April to May), we observed guttation from midnight to approx. 6:00 in the morning on bamboos growing close to a river. During this time, or even in general, zero nighttime sap flux conditions might thus not have been met, which would consequently affect the derived $\Delta T_{max}$. In our study, $\Delta T_{max}$ thus could have potentially been affected (i.e. lowered) by water fluxes occurring for different reasons. Therefore, both changes in $\theta_{wood}$ and nighttime sap flow are likely to influence $\Delta T_{max}$ in the same direction. As to which proportion they contributed in our study can thus far not be disentangled. This will require further, more in-depths ecophysiological studies.

### 3.4.2 The influence of $\theta_{wood}$ on $J_s$

In our study, we numerically simulated the influence of $\theta_{wood}$ on TDP-derived $J_s$. The results pointed to a direct and quantifiable relationship between $\theta_{wood}$ and changes in $J_s$, and thus potential errors in previous studies assuming a static $\theta_{wood}$ (Vergeynst et al., 2014; Wullschleger et al., 2011). Wullschleger et al. (2011) simulated scenarios examining the impact of wood thermal conductivity on the relationship between $J_s$ and $k$ (= $\Delta T_{max}/\Delta T$ - 1). They found a negative relationship between $\Delta T$ and thermal conductivity and pointed out that the $J_s$-$k$ relationship might be influenced by several factors including $\theta_{wood}$, wood density, and thermal conductivity. Vergeynst et al. (2014) quantified the influence of $\theta_{wood}$ on $J_s$ by simulating possible temperature changes that were assumed to relate to $\theta_{wood}$. However, they did not find a direct relationship between $\theta_{wood}$ and errors in $J_s$. Our results supplement previous TDP error

analyses and point to a direct and quantifiable relationship between $\theta_{wood}$ and errors on $J_s$, which could potentially be corrected for e.g., with the mentioned model.

Using numerical simulations, we found increasing relative underestimations of $J_s$ for larger decrease of $\theta_{wood}$ from nighttime to daytime (Fig. 3.4), which may be due to depleted stem water storage. In previous studies on bamboos (Yang et al., 2015) and palms (Sperling et al., 2015), gradual decreases of $\theta_{wood}$ from sunrise to sunset were reported. Thus, $\theta_{wood}$ in the afternoon and especially at dusk was likely the lowest, which could introduce substantial bias into according estimates of $J_s$ (Fig. 3.4). Our results indicate that the magnitude of the relative underestimation of $J_s$ substantially differed with varying $J_s$: the relative error of $J_s$ (%) was largest at low $J_s$ and gradually became smaller, eventually approaching a stable value with increasing $J_s$ (Fig. 3.4). TDP-derived $J_s$ is thus influenced more profoundly by changing $\theta_{wood}$ in plants with generally low $J_s$ or when $J_s$ tends to be low (e.g., early morning, late afternoon). In contrast, for plants with generally high $J_s$ or at peak times of $J_s$ (e.g., around noon), the influence of changes in $\theta_{wood}$ would be smaller. Nevertheless, despite the relatively smaller errors at higher daytime $J_s$, they were responsible for causing most of the absolute underestimations of daily water use (Fig. 3.5).

Additional to varying for different $J_s$, the influence of $\theta_{wood}$ on TDP-derived $J_s$ may also differ with different water conditions of the soil due to different weather or management conditions, e.g., between rainy or sunny days or after irrigation. The applied model simulation indicated that, when $\theta_{wood}$ was reduced by the same ratio (e.g., half) from nighttime to daytime, higher nighttime $\theta_{wood}$ caused larger relative underestimation of $J_s$ (Fig. 3.6). High $\theta_{wood\_night}$ may occur during the wet season or during the growing period of a plant. This could potentially lead to estimation errors when calibrating the TDP method with other methods in situ. Consequently, calibration approaches conducted over short periods may not reflect medium- or long-term dynamics in $\theta_{wood}$. Similarly, one-time laboratory calibration experiments on tree or bamboo segments may also be prone to error due to potentially varying (or unknown) $\theta_{wood}$, e.g., because of varying soil water conditions at the time of stem harvest.

For TDP and other heat-based methods, influences or biases due to changes in $\theta_{wood}$ cannot fully be avoided (Vergeynst et al., 2014). Additional to calibration-based approaches to correct for such errors, other possible solutions may include new types of sensors, which already account for dynamic

changes of $\theta_{wood}$ when estimating $J_s$ (Trcala and Čermák, 2016; Vandege-huchte and Steppe, 2013). Decreasing the sensitivity of the heat domain by increasing the power supply (Tatarinov et al., 2005) may be a further option. However, this may lead to possible damages to the wood structure; including dynamic change of $\theta_{wood}$ into estimating $J_s$ thus seems to be a more promising approach. The model applied in our study to simulate the influence of changes in $\theta_{wood}$ on $J_s$ may be a first step to developing such a dynamic solution. In our study, the model was built under steady-state conditions, under which each simulation result was derived from the assumption of constant sap flow. These steady-state conditions may not (always) be met under field conditions, where sap flow is prone to external influences and may thus change frequently and not always predictably. For future studies, the application of the model in situ for simultaneous assessments of $\theta_{wood}$ and sap flow would be an interesting next step.

### 3.4.3 Correcting $J_{s\_bias}$

In our study, we numerically simulated the influence of $\theta_{wood}$ on TDP-derived $J_s$. The results point to a direct and quantifiable relationship between $\theta_{wood}$ and relative changes in $J_s$, and thus potential errors in previous studies when assuming a static $\theta_{wood}$ (Vergeynst et al., 2014; Wullschleger et al., 2011). Wullschleger et al. (2011) simulated scenarios examining the impact of $K_{wood}$ on the relationship between $J_s$ and $k$ (= $\Delta T_{max}/\Delta T$ - 1), and they pointed out that the $J_s$-$k$ relationship might be influenced by several factors including $\theta_{wood}$, wood density, and $K_{wood}$. Vergeynst et al. (2014) quantified the influence of $\theta_{wood}$ on $J_s$ by simulating possible temperature changes that were assumed to relate to $\theta_{wood}$. Our results supplement these previous TDP error analyses by building a direct and quantifiable relationship between $\theta_{wood}$ and $J_{s\_bias}$ with a numerical model. In our study, $J_{s\_bias}$ successfully corrected with our derived "correction equations" (Eq. 3.4, 3.5, 3.6 and 3.7). The four equations, which built upon 21 of the 45 sets of the simulated data, yielded satisfactory corrections of $J_{s\_bias}$ when applying them to the remaining 24 sets of data (Appendix Fig. A.2). Nonetheless, our correction approach still needs further improvements for future applicability.

Firstly, in our study, the model was built under steady-state conditions, under which each simulation result was derived from the assumption of constant $J_s$. These steady-state conditions may not (always) be met under

field conditions, where $J_s$ is prone to external influences and may thus change frequently and not always predictably. For future studies, a non-steady-state with varying $J_s$ should be considered, and an application of the model in situ for simultaneous assessments of $\theta_{wood}$ and $J_s$ would be needed. Additionally, the simulation in our study was mainly based on Eq. 3.1, derived by applying density and porosity of the bamboo species *B. vulgaris*. For other (bamboo) species, the parameters in the equations may thus differ. Further correction attempts could e.g., directly include the density and porosity of wood into the correction equations as further variables, making it more universally applicable. In addition, it has to be considered that nighttime sap flow may occur in some species and that "zero sap flow" conditions might thus not always be met. Our model-derived $\Delta T_{max}$-$\theta_{wood}$ relationship was based on the assumption that the nighttime zero sap flow existed and lasted long enough to established a one-to-one correspondence between $\Delta T_{max}$ and maximum $\theta_{wood}$. This ideal assumption may not always be met during field experiments (Regalado and Ritter, 2007). As such, several studies have reported nighttime sap flow in different species, which was presumably related to atmospheric evaporative demand (Forster, 2014). Further, during dry periods, the commonly high daytime transpiration in combination with relatively low soil water availability could potentially lead to more nighttime sap flow in the form of refilling depleted stem water reservoirs (Wang et al., 2012). In some cases, this might mean that zero flow conditions are not met at all, not even during the night. Even when the stem is fully recharged and reaches its maximum water content, nighttime sap flow could still occur, e.g., in the form of guttation. In this case, the $\Delta T_{max}$ might be derived under a non-zero sap flux conditions and might lead to underestimation of $J_s$. Therefore, both changes in $\theta_{wood}$ and nighttime sap flow are likely to influence $\Delta T_{max}$ in the same direction. It will require further, more in-depths ecophysiological studies to evaluate and correct the impact of nighttime sap flow as well as the coupled effects of both changes in $\theta_{wood}$ and nighttime sap flow on TDP-derived $J_s$.

For TDP and other heat-based methods, influences or biases due to changes in $\theta_{wood}$ cannot fully be avoided (Vergeynst et al., 2014). Decreasing the sensitivity of the heat domain by increasing the power supply (Tatarinov et al., 2005) may be an option. However, such operation may lead to possible damages to the wood structure. Additionally to calibration-based and mathematical approaches to correct for such errors due to changes in $\theta_{wood}$, other possible solutions, as previously explored by Vandegehuchte and Steppe (2012) and Trcala and Čermák (2016), may include new types of sensors that already

account for dynamic changes of $\theta_{wood}$ when estimating $J_s$. The model applied in our study to simulate the influence of changes in $\theta_{wood}$ on $J_s$ may be a possible reference for future studies to develop new models and for testing and further improving such new types of sensors.

## 3.5 Conclusions

In our study encompassing laboratory dehydration experiments and field monitoring, $\Delta T_{max}$, a core variable in calculating $J_s$ with the TDP method, was found to correlate negatively with both $\theta_{wood}$ in bamboo culms and with $\theta_{soil}$. By numerically simulating this negative $\Delta T_{max}$-$\theta_{wood}$ relationship for different scenarios of daily and seasonal changes in $\theta_{wood}$, the corresponding relative underestimation of $J_s$ was quantified. Keeping other controlling variables constant, large relative underestimation became apparent 1) for large decreases of $\theta_{wood}$ from nighttime to daytime, 2) at relatively low $J_s$, and 3) for relatively larger nighttime $\theta_{wood}$ when the ratio of decrease to the daytime (e.g., by half) was kept constant. Our findings indicate that TDP measurements can be profoundly influenced by diurnal changes in $\theta_{wood}$, particularly in species with low water consumption, in species with large diurnal changes in stem water storage (between nighttime and daytime), and between periods with strongly alternating soil water conditions (e.g., between sunny and rainy days). A mathematical correction equation was built with the simulated data by the steady-state numerical model, and it yielded acceptable corrected $J_s$. Interesting approaches for future studies include testing the here applied model in situ by simultaneously assessing dynamics in $\theta_{wood}$ and $J_s$, as well as further improving and developing heat-based methods to include the assumption of non-stable $\theta_{wood}$ at different temporal scales.

# Chapter 4

# Deuterium tracing for assessing water circulation in bamboos

Dongming Fang[1*], Tingting Mei[1,3,4], Alexander Röll[1], Hendrayanto[2], Dirk Hölscher[1]

[1] Tropical Silviculture and Forest Ecology, Georg-August-Universität Göttingen, Germany.
[2] Department of Forest Management, Institut Pertanian Bogor, Indonesia.
[3] State Key Laboratory of Subtropical Silvilculture, Zhejiang Agriculture and Forestry University, Lin'an 311300, Zhejiang province, China.
[4] Zhejiang Provincial Key Laboratory of Carbon Cycling in Forest Ecosystems and Carbon Sequestration, Zhejiang Agriculture and Forestry University, Lin'an 311300, Zhejiang province, China.

[*] Correspondence: Dongming Fang, Tropical Silviculture and Forest Ecology, Georg-August-Universität Göttingen, Büsgenweg 1, Göttingen, 37077, Germany. Email: dongmingf@gmail.com

# Abstract

Bamboos are woody monocots with a hollow culm and connected rhizomes. We assessed bamboo water circulation in three big clumpy bamboo species by deuterium tracing along with formerly calibrated thermal dissipation probes (TDP) in a common garden in Indonesia. The deuterium-derived sap velocities correlated with the TDP-derived velocities in two of three species. In all species, the deuterium residence time in bamboo culms was little influenced by the contribution of the culm water storage to transpiration as estimated by TDPs at different culm heights. Potential reasons include a small water storage volume in the culms, a low estimated contribution of the storage to transpiration and high sap flux densities. Daily culm water use rates estimated by the deuterium and the TDP approaches correlated linearly ($R^2 = 0.9$) but were by 70% in the deuterium estimates. After the experiment, culms were cut down and analyzed for residual deuterium, but concentrations were low which indicates that retention did not play a major role in causing errors of the deuterium tracing approach. In culms neighboring the deuterium labeled culms of *Bambusa vulgaris* and *Gigantochloa apus*, elevated deuterium concentrations were detected indicating water transfer between culms. Based on the differences in daily water use on labeled culms and the enhanced deuterium concentrations in neighboring culms of these two species, we inferred that five neighboring culms might receive water from the labeled culms. On contrast, in culms neighboring labeled *Dendrocalamus asper* culms, only slightly elevated deuterium concentrations were observed which implies a limited role by water transfer. However, incomplete mixing as indicated by high variation among three TDP sensors at breast height may be of particular importance for deuterium tracing in *D. asper*. In conclusion, species-specific differences among big clumpy bamboos are indicated and the deuterium tracing points to water transfer among culms.

**Keywords: error analysis, sap velocity, water residence time, water storage, water transfer, water use**

## 4.1   Introduction

Unidirectional water transport from the soil through plants to air was thought to be the general framework when studying plant water use (Goldsmith, 2013;

Philip, 1966). However, this framework has been enlarged gradually by the new findings, such as foliage water uptake from air into leaves (Goldsmith et al., 2013; Studer et al., 2015) and inverse flow from the leaves to soil (Eller et al., 2013; Goldsmith, 2013), soil water translocation by roots (Burgess et al., 2001b; Sakuratani et al., 1999; Smith et al., 1999), and water transfer among interconnected plants through roots or rhizomes (Adonsou et al., 2016; Zhao et al., 2016). Such these water use characteristics, in combination with the frequently studied internal water storage (James et al., 2003; Meinzer et al., 2006; Yang et al., 2015) and the most studied transpiration, seem to constitute a more complicated water circulation within and among the plants. Within the plants, the internal water circulation can be formed by water transport (sap flow) to canopy or soil, and by water exchange between conduits and storage compartments for water storage (James et al., 2003). Between the plants and the environment (air and soil) and among the plants, the outer water circulation can be composed by water uptake from soil or foliage, water translocation, and water transfer. These water circulations were important to stimulate and maintain some physiological processes, e.g., regulating stomatal closure by transporting the root-produced abscisic acid to leaves (Hartung et al., 2002), maintaining high transpiration rates with the temporally stored water in stems (Goldstein et al., 1998; James et al., 2003), or relieving water shortage by water redistribution among interconnected plants (Adonsou et al., 2016; Zhao et al., 2016). Therefore, exploring and monitoring these water circulations would deepen our understanding of plant physiology.

Bamboos, as fast growing monocots, may have unique characteristics of water circulation. Compared with trees, comparable (Dierick et al., 2010; Kume et al., 2010) or higher (Ichihashi et al., 2015; Mei et al., 2016) maximum sap flux densities were found on bamboo species in previous studies. High sap flux densities may be attributed to the large culm hydraulic conductivity and low sapwood capacitance, as sap velocity on trees was found positively correlated with stem hydraulic conductivity and negatively with sapwood capacitance (Meinzer et al., 2006). If such correlations applied to bamboos, it may mean that bamboos had low sapwood capacitance which could be implied by the short residence time of water in the stem (Meinzer et al., 2006). However, longer residence time on one bamboo species (*Bambusa blumeana*) than on the reference trees was found (Schwendenmann et al., 2010). The contradictory findings may be case-specific or common for bamboos, and therefore, the corresponding investigation needs to be done on more bamboo species. Another distinctive characteristic of water circulation on

bamboos is the water transfer among culms, due to the rhizomes which possibly provide passages for transporting water among culms (Stapleton, 1998). Water transfer among culms has been implied on *B. blumeana* by observing elevated deuterium ($D_2O$) concentrations on the leaves of the neighbor culms which were in the same clump of the $D_2O$ labeled culms (Dierick et al., 2010). Another investigation on Moso bamboo (*Phyllostachys pubescens*) also implied water transfer by finding 20% less water use on the rhizome-cut culms than on the regular culms (Zhao et al., 2016). These findings need to be further tested on more species with the directly connected culms and with no destructive operation.

Deuterium tracing method, due to its traceability, has been applied for measuring sap velocity and water residence time in the stems of trees (James et al., 2003; Meinzer et al., 2006), and for estimating daily water use rates (Calder, 1991; Dierick et al., 2010; Dye et al., 1992; Schwendenmann et al., 2010). In these studies, the $D_2O$ was first injected into the base stem of trees/bamboos (this operation is usually called labeling) and then the water transpired from leaves in the labeled trees/bamboos was periodically sampled to trace the $D_2O$ movement (Calder, 1991). Subsequently, the $D_2O$ concentration in the samples was used to estimate sap velocity, water residence time and daily water use rates (See details in Calder (1991) or Meinzer et al. (2006)). However, deuterium-derived water use rates were thought to be less reliable when two assumptions proposed by Calder (1991) for estimating the water use rates were violated (Schwendenmann et al., 2010). The two assumptions were: First, all the $D_2O$ injected into the base stem is taken up and transpired out from leaves without tracer loss in other forms; Second, the $D_2O$ is thoroughly mixed in the transpiration stream before water flowed into different regions of the crown (Calder, 1991). Compared with the other methods (e.g., thermal dissipation probe, TDP), both overestimation (Kalma et al., 1998; Marc and Robinson, 2004; Schwendenmann et al., 2010) and underestimation (Dye et al., 1992) on water use rates from deuterium tracing method were observed. On one bamboo species (*B. blumeana*), water use rates were found eight times higher with deuterium tracing method than with TDP method (Schwendenmann et al., 2010). The discrepancies could be attributed to several potential interference sources which may break the two assumptions, such as tracer loss due to retention of tracer in plants and water transfer among plants (Schwendenmann et al., 2010). Nevertheless, the discrepancies caused by the interference sources can also be estimated to explore the corresponding water circulation characteristics (e.g., water transfer). This process could be realized by monitoring tracer dynamics

on leaves, stem and the interconnected plants to address the difference in water use rates simultaneously derived with deuterium tracing method and a reference method.

Our objectives were applying $D_2O$: (1) to explore the water circulation characteristics of the bamboos, including sap velocities, water residence time, water use rates, and water transfer between culms, (2) and to evaluate the potential interference sources in $D_2O$-based daily water use estimates with referring to TDP method, such as $D_2O$ retention and transfer. To achieve the aims, we applied deuterium tracing method simultaneously with measurements of calibrated TDP sensors (Mei et al., 2016) on three tropical clumpy bamboo species in a common garden.

## 4.2   Materials and methods

### 4.2.1   Study site and species

The study was conducted in a common garden in Bogor, Indonesia (6°33'40" S, 106°43'27" E, 182 m asl). Bogor is a city with moderate temperature (average annual temperature 25.6 °C) and plenty of rainfall (annual precipitation 3978 mm) but has apparent wet and dry season (Van Den Besselaar et al., 2015). Three bamboo species (*Bambusa vulgaris*, *Gigantochloa apus* and *Dendrocalamus asper*) were selected for $D_2O$ labeling. For each species, the selected bamboo culms for $D_2O$ labeling were in one clump and located at the edge of the clump. The clump base areas were 18, 20 and 6 m$^2$, and the canopy areas were 346, 427 and 63 m$^2$ for *B. vulgaris*, *G. apus* and *D. asper*.

### 4.2.2   $D_2O$ tracing

Three to four culms per species were labeled (Table 4.1). The labeled culms were injected with $D_2O$ (99.90% D, euroiso-top, Gif sur Yvette, France) during 6:00-7:00 on 8$^{th}$ March 2013 (Fig. 4.1). The operation of injecting $D_2O$ into the studied bamboos followed Dierick et al. (2010). First, plastic tubes were fixed with an angle of 45° to the bamboo culms at the height of 50 cm above the ground. Four to six tubes (four tubes for *B. vulgaris* and *G. apus*; six tubes for *D. asper*) were fixed eventually around each labeled culm. The tubes were then filled with 40 mM KCl solution, and holes were drilled under water. After
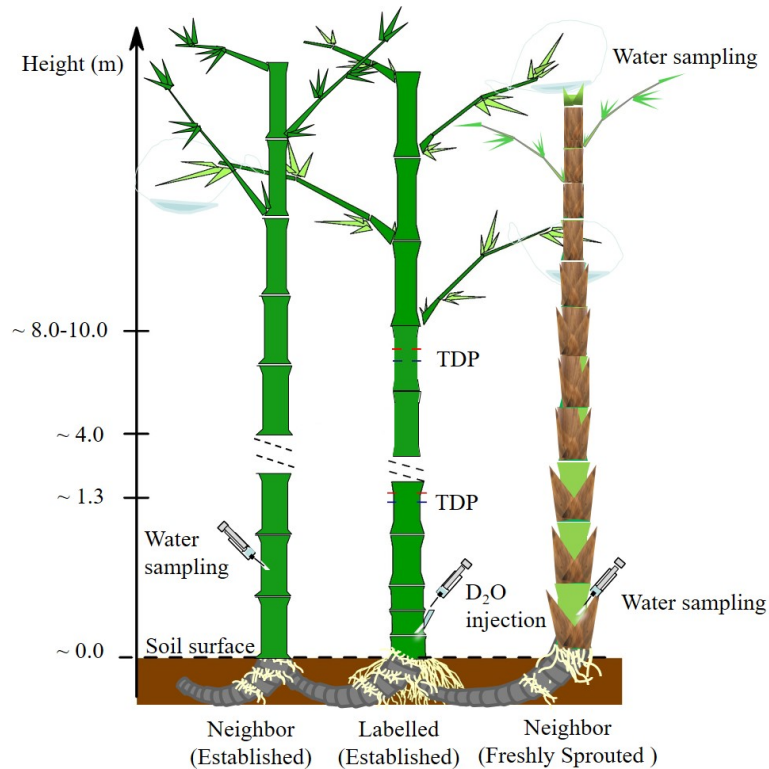
Fig. 4.1 Scheme of applying deuterium tracing and TDP methods.

that, holes were washed by injecting more solution, and the remaining solution in the holes were extracted by a syringe and replaced with 1.5 - 3 g $D_2O$ in each hole. The $D_2O$ was taken up by transpiration stream, and KCl solution was added into holes for several times afterward to make the residual $D_2O$ in the tubes/holes being taken up as much as possible. After sunset, water remained in the tubes and holes was collected and weighed, and then 1.5 ml of them was stored at 4 °C in the refrigerator and used for isotope analysis to measure the amount of remained $D_2O$.

Following the approach of Calder (1991), the $D_2O$ samples were collected from leaf condensate water by installing transparent bags. On each sampling day between 7:00 and 8:00, ten self-sealing transparent bags were installed on five different sun-exposed regions on each bamboo canopy (sealing 5 - 6 leaves per bag) and the bags were collected at the same time in the next day. All the ten condensate samples for a culm were totally combined to a mixed sample, and 1.5 ml of the mixed sample was transferred into a glass vial and stored as same as mentioned above. Sampling was conducted every day in the first ten days and 4 - 6 days' interval in the next three weeks.

Table 4.1 The information of studied bamboos and trees (3 culms per species but 4 culms of *B. vulgaris* used). The adjusted $WU_{D_2O}$ was $WU_{D_2O}$ adjusted with deuterium transfer on bamboos. The values were represented as the means(SD) which were in parenthesis.

| Species | Height (m) | DBH (cm) | $D_2O$ injected | $T_{arrival}$ | $T_{residence}$ |
|---|---|---|---|---|---|
| *B. vulgaris* | 17.9(0.8) | 7.0(0.4) | 5.8(1.6) | 1.5(1.0) | 5.5(1.3) |
| *D. asper* | 21.1(0.9) | 10.7(0.9) | 8.0(1.1) | 1.0(0.0) | 5.0(1.7) |
| *G. apus* | 16.2(2.7) | 7.9(1.1) | 5.7(0.1) | 1.0(0.0) | 6.3(0.6) |

To detect if there was $D_2O$ retention in the bamboos, on $16^{th}$, $17^{th}$ or $20^{th}$ April 2013, all the $D_2O$ labeled bamboos were harvested in early mornings (from 5:00 - 7:00). On each culm, three water samples (1.5 ml) were extracted from leaves, branches and rhizomes, and one sample was obtained from each culm segment every 2 m height. The sampling organs were sealed in the transparent plastic bags and left under the sunshine to make water transpired out, and water samples (1.5 ml) were collected in glass vials. Outside diameter, wall thickness and height of the segment were measured to calculate the fresh volume ($v_f$, $cm^3$). Samples collected from each organ were weighted ($w_f$, g) and dried with $100\,^{\circ}C$ in the oven for 24/48 hours (24 hours for leaves/branches, 48 hours for rhizomes and culms) to get dry weight ($w_d$, g) in the lab. The water content of each segment was then derived as ($w_f$ - $w_d$)/ $w_d$. The lowest $D_2O$ concentration in the collected samples was used as background values to calculate the mass of $D_2O$ retention in the bamboos.

To test for $D_2O$ transfer among bamboo culms, three established and three freshly sprouted neighbor culms, which were 30 - 50 cm distant to the $D_2O$ labeled culms, were sampled in 3 - 5 days' interval. The established culms were similar to the labeled ones. The young culms popped up 4 - 5 months before the tracer study began and had already reached a height of around 10 m or higher, but they still hold some brown sheaths attached to the culms and were not fully leafing. In approximately 6:00, small holes were drilled in the bamboo wall at around 1 m height, and water samples (1.5 ml) were collected directly from the holes (Fig. 4.1).

The $D_2O$ concentrations in the culm segments of the cut-down labeled culms were used as background values for correcting the $D_2O$ concentrations in the samples in the labeled and neighboring culms.

### 4.2.3    $D_2O$ analysis in the lab

The isotope analysis was carried out in the Center for Stable Isotope Research and Analysis (KOSI) at the University of Göttingen, Germany. The samples were measured in a Delta V Plus isotope ratio mass spectrometer (Thermo-Electron Cooperation, Bremen, Germany) coupled with a high-temperature conversion/elemental analyzer (TC/EA, Thermo Quest Finnigan, Bremen, Germany). The results with $2\permil$ measurement precision are expressed in delta notation in units of per mil ($\delta D$, $\permil$) as D/H of the sample ($R_{\text{sample}}$) relative to that of Vienna Standard Mean Ocean Water ($R_{\text{VSMOW}}$).

### 4.2.4    $D_2O$ arrival time, velocity and residence time

Three variables were used to describe the behavior of the $D_2O$ reflecting the water uptake and storage characteristics (Meinzer et al., 2006; Schwendenmann et al., 2010). First, arrival time ($T_{\text{arrival}}$, days) was defined as the time of leaf $D_2O$ concentration passing over 10% of the maximum $D_2O$ concentration for the first time. Second, tracer velocity ($V_{D_2O}$, m day$^{-1}$) was derived as the distance between sampling and injecting points over the arrival time. At last, tracer residence time ($T_{\text{residence}}$, days) was estimated as the time course when the $D_2O$ concentration was above 10% of the maximum $D_2O$ concentration.

To calculate water use estimated by deuterium tracing method, the notation of $D_2O$ ($\delta D$) values were converted to give a mass concentration of the tracer (Calder, 1991). The mean daily water use ($WU_{D_2O}$) over the experiment was calculated with the equation as below:

$$WU_{D_2O} = \frac{M}{\sum_{i=1}^{T} C_i \Delta t_i} \tag{4.1}$$

Where $C_i$ is the mass concentration (g kg$^{-1}$) in the $i^{th}$ time increment, $\Delta_{ti}$ is the duration of the $i^{th}$ time increment (days), and $T$ is the last time increment. This function is usually used under two assumed conditions as described in the introduction part (Calder et al., 1992).

### 4.2.5   Sap flow measurement and water use estimation by TDP method

On each labeled bamboo culm (three culms per species but four culms of *B. vulgaris* used), sap flux density ($J_s$, g cm$^{-2}$ h$^{-1}$) was measured by self-made 1 cm length TDP. The sensors were inserted into the bamboo culm at breast height (Mei et al., 2016) and below the lowest branches at around 7 m height. Three pairs of 1 cm length TDP were installed evenly apart from each other. From 8$^{th}$ March to 6$^{th}$ April 2013, the three TDP signal wires were connected in parallel to get an averaged voltage value. From 7$^{th}$ April 2013, to detect the circumferential variation of $J_s$, the three TDP sensors were installed separately to measure $J_s$ in three directions for at least one week. The TDP signals were sampled every 30 seconds and stored as 1-minute averages in data loggers and multiplexers (CR1000, AM16/32, Campbell Scientific Inc., USA). $J_s$ was calculated with species-specific calibrated formulas for these bamboos (Mei et al., 2016).

To compare with tracer velocity by deuterium tracing method ($V_{D_2O}$, m day$^{-1}$), daily accumulated $J_s$ ($J_{s\text{-}d}$, kg cm$^{-2}$ day$^{-1}$) derived from TDP method was converted into sap velocity ($V_{TDP}$, m day$^{-1}$) by the unit change. Water use (WU$_{TDP}$) of each bamboo was derived by multiplying $J_s$ with the culm wall cross-sectional area. Because WU$_{D_2O}$ was not arithmetic mean of daily water use during the experiment, mean TDP-derived WU and WU$_{D_2O}$ cannot be directly compared (Calder, 1991). Therefore, a weighted WU was introduced with the following equation with TDP method:

$$WU_{TDP} = \frac{\sum_1^T WU_i C_i}{\sum_1^T C_i} \tag{4.2}$$

Where WU$_i$ is the daily water use (kg d$^{-1}$) in the $i^{th}$ time period (day), and $C_i$ is the mean mass concentration of D$_2$O in condensate water in the $i^{th}$ time period.

To assess the influence of stem water storage on WU$_{D_2O}$, the relative contribution of stem water storage to transpiration ($C_{WS}$) was calculated following the procedure by Goldstein et al. (1998). The underlying assumption is that the daily water use measured at the lower (near breast height) and upper stems (under the crown) were equal in one day. First, adjusted half-hourly water use at the upper stem was derived by multiplying half-hourly water use at the upper stem with the ratio between the daily water use at the lower stem and at the upper stem. Second, the difference between the half-hourly water use at the

lower stem and the upper stem was calculated, and the positive difference in one day was integrated as water storage that contributed to daily transpiration. At last, water storage was divided by daily transpiration to get the $C_{WS}$.

### 4.2.6   Data analysis and statistics

Linear regressions were done on exploring relationships between $V_{D_2O}$ and $V_{TDP}$, between $T_{residence}$ and $V_{D_2O}$, $V_{TDP}$ or $C_{WS}$, and between $WU_{D_2O}$ and $WU_{TDP}$. The relative differences between $WU_{D_2O}$ and $WU_{TDP}$ (Dif$_{WU}$, %) was first calculated as the ratio of the difference between $WU_{D_2O}$ without considering any $D_2O$ loss and $WU_{TDP}$ to $WU_{TDP}$. In the following step, two interference sources relating $D_2O$ losses for bamboo $WU_{D_2O}$ were quantitatively assessed in our study: $D_2O$ retention in the labeled culms and $D_2O$ transfer to the neighbor culms. For each interference source (retention or transfer), the corresponding $D_2O$ losses were included into the Calder's equation (Calder, 1991) for calculating corrected $WU_{D_2O}$. Subsequently, the corresponding relative differences between the corrected $WU_{D_2O}$ and $WU_{TDP}$ were calculated. When assessing the influence of $D_2O$ transfer, the maximum amount of culms that may receive the transferred $D_2O$ from each labeled culm ($N_{max}$) was calculated under the assumption that the Dif$_{WU}$ was caused solely by $D_2O$ transfer. The distribution of the $N_{max}$ of all the labeled culms was subsequently plotted with histogram and kernel density distribution, from which a mode was derived. Thereafter, a corrected $WU_{D_2O}$ and a corresponding Dif$_{WU}$ were calculated with assumptions that water was transferred from each labeled culm to neighbor culms and that the amount of the receiving culms equaled to the mode value of the $N_{max}$ distribution. The newly derived Dif$_{WU}$ was further plotted with $CV_{J_s}$ with linear regression to assess the influence of incomplete mixing on $WU_{D_2O}$ estimation. All data analysis and figures were performed with SAS 9.3 (SAS Institute Inc., 2013).

## 4.3   Results

### 4.3.1   Tracer movement and sap velocity

On most of the studied bamboo culms, the $D_2O$ concentrations showed a two-peak pattern during the experiment, with a drop in the second day after
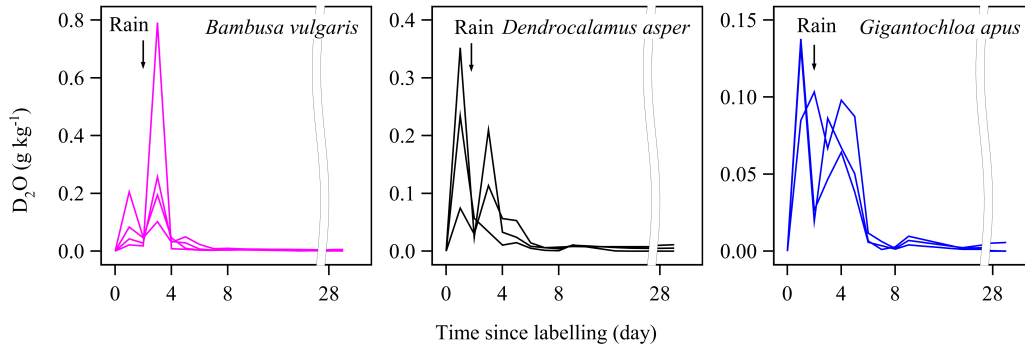
Fig. 4.2 Deuterium concentration ($D_2O$ g kg$^{-1}$ above background level) in transpired water of *B. vulgaris*, *G. apus* and *D. asper* over the course of the experiment. Day 0 is the day of deuterium injection.

Table 4.2 Deuterium signature ($\delta D$, ‰) in different bamboo organs (leaf, branch, stem at 0, 2, 6, 10 m height and rhizome) of the labelled bamboos (4 culms of *B. vulgaris* and 3 culms of *D. asper* and *G. apus*) which was harvested after about 40 days since labelling. The values were represented as the means (standard deviation).

| Species | Rhizome | Stem | | | | Branch | Leaf |
|---|---|---|---|---|---|---|---|
| | | 0 m | 2 m | 6 m | 10 m | | |
| *B. vulgaris* | -32.9(5.6) | -40.9(1.7) | -42.8(1.5) | -43.3(1.7) | -43.7(4.5) | -41.7(2.8) | -33.8(1.5) |
| *G. apus* | -38.5(0.8) | -42.4(2.5) | -44.3(3.0) | -43.1(2.3) | -41.7(3.0) | -38.4(3.0) | -30.2(1.1) |
| *D. asper* | -44.9(2.2) | -32.5(25.1) | -38.0(9.0) | -40.9(5.0) | -42.4(3.3) | -39.0(11.6) | -52.3(13.1) |

labeling, which was a rainy day (Fig. 4.2). $T_{arrival}$ from stem base to the crown was one day on most of the labeled bamboos, except 3 days on one culm of *B. vulgaris* (Table 4.1). The maximal $D_2O$ concentrations on the labeled culms appeared in 1-3 days and varied between 0.09 and 0.79 g kg$^{-1}$ for the three bamboo species (Fig. 4.2). Sap velocities derived from deuterium tracing method ($V_{D_2O}$) were on average 5.6 times higher than from the TDP method ($V_{TDP}$; 12.5 vs. 3.6, 13.3 vs. 3.2 and 16.1 vs. 1.3 m day$^{-1}$ on *B. vulgaris*, *G. apus* and *D. asper*, respectively).$V_{D_2O}$ was significantly correlated with $V_{TDP}$ among culms of *B. vulgaris* and *D. asper* ($R^2 = 0.78$; $P < 0.01$) but not in *G. apus* (Fig. 4.3).

### 4.3.2 Residence time and stem water storage

$T_{residence}$ varied between 5.5 and 6.3 days on average for the three studied bamboo species (Table 4.1). $T_{residence}$ seemed to decrease with increasing $V_{TDP}$
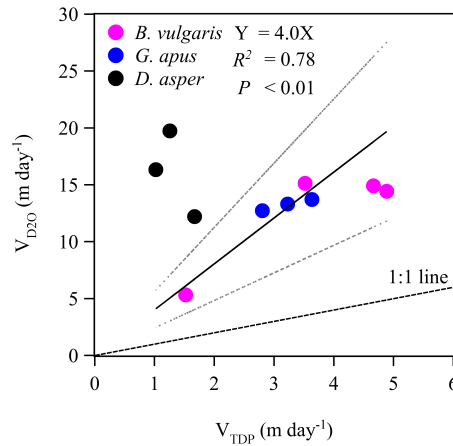
Fig. 4.3 Sap velocities (m day$^{-1}$) derived from deuterium tracing method ($V_{D_2O}$) in relation to the sap velocities obtained from TDP method ($V_{TDP}$). The two grey dot lines represent 95% confidence limits for the expected values. The black line accounts for a regression line.

and did not significantly correlate with culm water storage ($C_{WS}$; Fig. 4.4). During the experiment, $C_{WS}$ were 15%, 9% and 9% on average for *B. vulgaris*, *G. apus* and *D. asper*, respectively.

### 4.3.3 Water use rate

There was a significant correlation between $WU_{D_2O}$ and $WU_{TDP}$ estimates ($R^2$ = 0.94, $P < 0.05$; Fig. 4.5). However, the deuterium tracing method gave 70% on average higher values than the TDP method. $WU_{D_2O}$ and $WU_{TDP}$ were 11.3 vs. 8.1, 13.2 vs. 7.0 and 16.0 vs. 8.0 kg day$^{-1}$ for *B. vulgaris*, *G. apus* and *D. asper*, respectively

### 4.3.4 D$_2$O retention, transfer, incomplete mixing and their influence on deuterium derived water use rate

In the cut-down bamboo tissues, the D$_2$O concentration ($\delta$D, ‰) showed an increasing trend from stem base to leaves and root in *B. vulgaris* and *G. apus*, while not in *D. asper* (Table 4.2). In *B. vulgaris* and *G. apus*, the $\delta$D values were significantly higher on leaves than on stems ($P < 0.05$ with a t-test). The remained D$_2$O in each whole bamboo (including leaves, branches, culm and rhizome) varied between 0.005 to 0.075 g, which was negligible to the injected
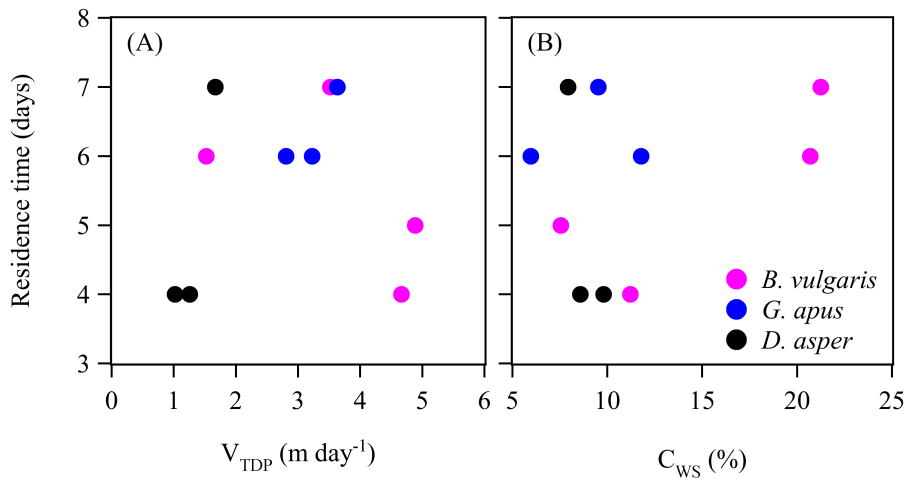
Fig. 4.4 Residence time in relation to (A) the sap velocity derived from thermal dissipation probe ($V_{TDP}$, m day$^{-1}$) and (B) the contribution of culm water storage to daily water use ($C_{WS}$, %).
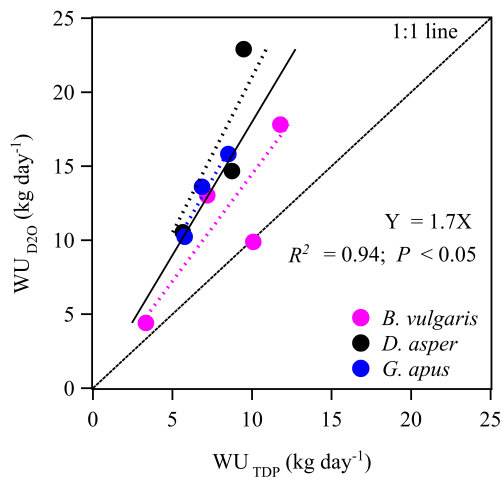


Fig. 4.5 Water use estimated by the TDP method (WU$_{TDP}$, kg day$^{-1}$) versus water use determined by deuterium tracing (WU$_{D_2O}$, kg day$^{-1}$) on bamboos. The solid line represents regression of all values of the three bamboo species. The dash lines represent species-specific regressions: *B. vulgaris*: $Y = 1.4X$, $R^2 = 0.95$, $P < 0.01$; *D. asper*: $Y = 2.0X$, $R^2 = 0.97$, $P < 0.01$; *G. apus*: $Y = 1.9X$, $R^2 = 0.99$, $P < 0.01$.
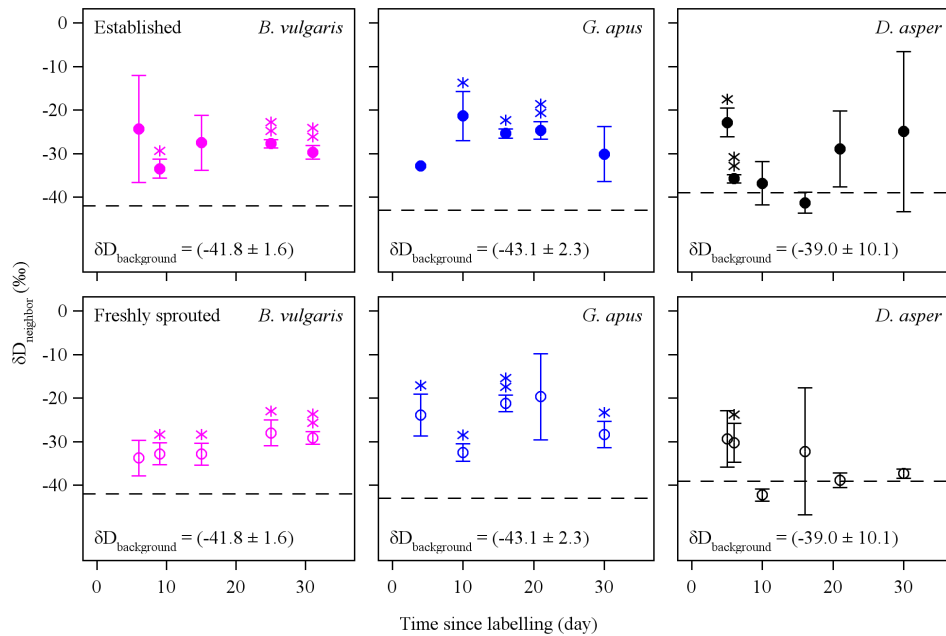
Fig. 4.6 Deuterium signature ($\delta$D, ‰) above the background values in xylem water in established (filled dots) and freshly sprouted (hollow dots) culms neighboring the labeled culms. Each dot (mean ± SD, N = 3 except one dot in established *G. apus*) stands for the mean values from each species (4 culms for *B. vulgaris* or 3 culms for *D. asper* and *G. apus*). The background values were derived from the stems of the cut-down labeled culms. The dashed line refers to background $\delta$D value that was derived by averaging the stem $\delta$D values of the cut-down labeled bamboos after about 40 days since labeling. The asterisks above the dots indicated significant (one asterisk) and extremely significant (two asterisks) difference between the $\delta$D values and the background values.

mass (Table 4.1) and produced only 1% on average higher values on $WU_{D_2O}$ referring to $WU_{TDP}$.

Compared with the background $\delta$D values, significant higher $\delta$D values were found in the transpiration stream of neighbor established and freshly sprouted bamboos almost over the 30 days on *B. vulgaris* and *G. apus*, while only in the first 6 days on *D. asper* ($P < 0.05$ with t-test; Fig. 4.6). Such elevated $\delta$D values may be related to water transfer through rhizomes between the labelled bamboos and neighbor ones. Based on the assumption that the water transfer existed continuously during the experiment, the total transferred $D_2O$ on one neighbor culm varied between 0.36 to 0.93 g, which accounted for 1.7 - 11.7% of the injected $D_2O$. As the $D_2O$ retention was negligible, the difference between $WU_{D_2O}$ and $WU_{TDP}$ was assumed mainly relating to tracer loss by water transfer among culms. Under such assumption, the amount of
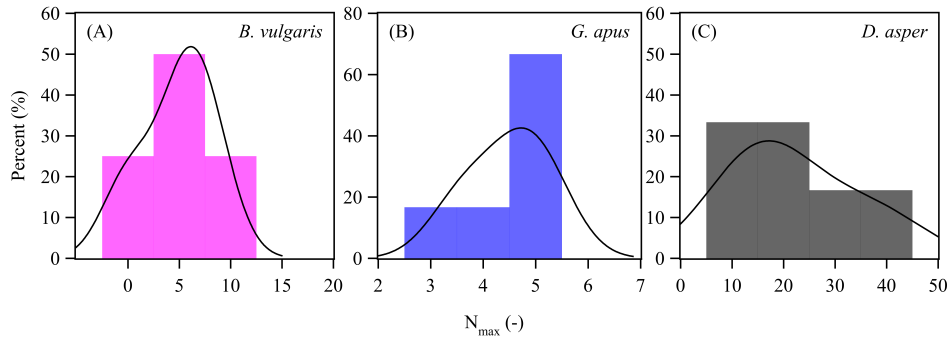
Fig. 4.7 The distribution of the maximal amount of neighboring culms ($N_{max}$) which may receive transferred water from the labeled culms (*B. vulgaris*, *G. apus* and *D. asper*). For each species, data of 3 established and 3 freshly sprouted culms were used. The black line represented fitted kernel distribution. The mode (at the most frequency) of the $N_{max}$ was 5.1, 4.5 and 22.0 on *B. vulgaris*, *G. apus* and *D. asper*, and the mode was 6.7 when pooling the three species together.

culms that may receive $D_2O$ transfer from the labeled culms ranged from 0 to 41 culms with the mode of 6 culms (Fig. 4.7).

We assumed the incomplete mix of $D_2O$ in sap flow was another interference source of $WU_{D_2O}$ estimation, which may be indicated by the different sap flux densities in different directions. Among the culms of each species, the averaged coefficients of variation of daily sap flux densities at breast height in three directions ($CV_{J_s}$) were 23%, 52% and 14% for *B. vulgaris*, *D. asper* and *G. apus* respectively. With the assumption that a labeled culm transferred $D_2O$ to 6 neighboring culms (Fig. 4.7), the calculated differences between the corrected $WU_{D_2O}$ and $WU_{TDP}$ was found significantly correlated with $CV_{J_s}$ (Fig. 4.8; $R^2 = 0.44$, $P < 0.05$).

## 4.4 Discussion

### 4.4.1 Sap velocity

Compared to *B. blumeana* in Philippine (Dierick et al., 2010; Schwendenmann et al., 2010), the three bamboo species (*B. vulgaris*, *G. apus* and *D. asper*; Table 4.1) in our study showed much smaller $T_{arrival}$ (1.5, 1.0, 1.0 vs. 3.1 days) and $T_{max}$ (2.5, 1.3, 1.7 vs. 4.8 days) while larger $V_{D_2O}$ (12.5, 13.3, 16.1 vs. 8.5 m day$^{-1}$) and $V_{TDP}$ (3.6, 3.2, 1.3 vs. 0.9 m day$^{-1}$). Such differences among

the bamboo species in the two studies may be attributed to the species-specific anatomical structures, different sampling methods or various environmental conditions in these sites. Bamboos had highly variable size and shape of vascular bundles among species (de Agrasar and Rodríguez, 2003) which may lead to different water transport velocities. Despite this, different sampling methods applied in our study and the study in Philippine might also contribute to the differences. In the Philippine study, leaves were collected twice a day (interval sampling) while we installed transparent bags on the branches to gather water for a whole day (Calder et al., 1986). The interval sampling may cause missing of the peak value that was used to derive the $T_{\text{arrival}}$ and $V_{\text{D}_2\text{O}}$.

The averaged $V_{\text{D}_2\text{O}}$ of the three bamboo species was 5.6 times higher than $V_{\text{TDP}}$. Such large differences between $V_{\text{D}_2\text{O}}$ and $V_{\text{TDP}}$ were also found in other studies (Dierick et al., 2010; James et al., 2003; Meinzer et al., 2006). Compared with $V_{\text{TDP}}$, higher $V_{\text{D}_2\text{O}}$ was found on one bamboo species (*Bambusa blumeana*) and five tropical tree species (Schwendenmann et al., 2010), and on temperate conifers (Meinzer et al., 2006). Meinzer et al. (2006) explained that sap velocity derived from sap flux density by the unit change were not the right sap velocity transported in the conduits and the fraction of the conduit area to the whole cross sectional area may influence the calculation. In an early study, Tatarinov et al. (2005) described sap flux density as the product of sap velocity, wood porosity, and water density. Therefore, following the work of Vandegehuchte and Steppe (2012), we calculated wood porosity from easily obtained factors such as dry wood density and fresh wood volume of a sample and got new $V_{\text{TDP}}$, which reduced the relative deviation of $V_{\text{D}_2\text{O}}$ to $V_{\text{TDP}}$ from 5.6 times to 0.86 times higher. Despite the new $V_{\text{TDP}}$ calculated in such way may also introduce errors, it did reduce the differences and may be improved with the more accurate calculation on porosity. The different measurement scales of the two methodologies could be another reason for the difference between $V_{\text{D}_2\text{O}}$ and $V_{\text{TDP}}$. $V_{\text{TDP}}$ only stand for the velocity between the installation heights of the TDPs while $V_{\text{D}_2\text{O}}$ is a mean value along the hydraulic path from stem base to the crown until water left the leaves.

Despite $V_{\text{D}_2\text{O}}$ was higher in our study and also the other previous studies, $V_{\text{D}_2\text{O}}$ could even be larger when $D_2O$ sampling was done at a higher frequency. The arrival time ($T_{\text{arrival}}$, 1 day for all but one) could be shorter if the tracer arrived at the crown within one day and strong water uptake occurred in daytime. The one-day sampling interval in the present study may be too coarse for a precise estimation of the arrival time. Therefore, $T_{\text{arrival}}$ was the maximal $D_2O$ transit time from base stem to canopy, and thus $V_{\text{D}_2\text{O}}$ derived

with $T_{\text{arrival}}$ and the transport pathway was minimum estimates of maximum sap velocity (James et al., 2003; Meinzer et al., 2006). In future studies, one should probably sample water from leaves with shorter intervals, such as 4 hours over the initial days.

### 4.4.2 D$_2$O residence time and water storage

$T_{\text{residence}}$ varied between 5.5 and 6.3 days on average for the three studied bamboo species (Table 4.1), while 11.5 days on another bamboo species - *B. blumeana* and 4.7 days on the five reference tree species (Schwendenmann et al., 2010). However, $T_{\text{residence}}$ on these bamboo species was shorter than the $\approx$ 20 days of two tropical tree species in Panama (James et al., 2003) and much shorter than the 36 - 79 days on two coniferous species in North America (Meinzer et al., 2006). $T_{\text{residence}}$ on trees was found positively correlating with the normalized maximum crown-base sap flow which implies the relative reliance of transpiration on water storage (James et al., 2003), and with sapwood capacitance which reflects the water exchange capacity between transporting lumens and surrounding tissues (Meinzer et al., 2006). Therefore, It was assumed that $T_{\text{residence}}$ could be an indicator of the relative reliance of transpiration on water storage (James et al., 2003). However, on the three studied bamboo species in our study, $T_{\text{residence}}$ was found not significantly related to the normalized maximum crown-base sap flow (data not show) nor with the daily $C_{\text{WS}}$ (Fig. 4.4 A). Such finding may be attributed to the limited support of the water storage to the relatively high daily transpiration, as the bamboo culms have much fewer volumes to store water than tree stems due to the thin culm wall and the hollow center. In the present study, during the experiment from $8^{th}$ March to $6^{th}$ April 2013, daily $C_{\text{WS}}$ were 15%, 9% and 9% on average for *B. vulgaris*, *D. asper* and *G. apus*, respectively. On contrast, on trees or palms, 10 - 50% of daily transpiration can be contributed by stem water storage (Carrasco et al., 2015; Goldstein et al., 1998; Holbrook et al., 1992; Scholz et al., 2008; Waring and Running, 1978). However, although $T_{\text{residence}}$ was not correlated with $C_{\text{WS}}$, it appeared to negatively correlate with $V_{\text{D}_2\text{O}}$ (Fig. 4.4 A). It may indicate that high axial water transport efficiency reduced the time of water staying in the bamboo culms. These findings seemed to verify the hypothesis that the trade-off of water transport efficiency and water storage capacity could contribute to a safe water status in the crown (Gleason et al., 2016; James et al., 2003). On bamboos, culm water storage may be less

important than the relatively high water transport efficiency on maintaining leaf water status, which could be indicated by the higher maximum sap flux densities on bamboo species than on the neighbored trees (Ichihashi et al., 2015; Mei et al., 2016).

### 4.4.3 Water use derived with deuterium tracing method

On most of the studied culms (90%) in our study, water use was higher by deuterium tracing method ($WU_{D_2O}$) compared to calibrated TDP method ($WU_{TDP}$). On average, the deuterium tracing method gave $41\pm35\%$, $99\pm38\%$ and $87\pm11\%$ higher values on *B. vulgaris*, *D. asper* and *G. apus* respectively. Higher values (11 - 43%) by $D_2O$ method was found on *Eucalyptus grandis* compared with Heat Pulse Method (Kalma et al., 1998), while lower values (7 - 26%) was also found in the same species with the same reference method by Dye et al. (1992). On the only studied bamboo species (*B. blumeana*) applied with $D_2O$ method (Schwendenmann et al., 2010), on average 813% higher water use was found compared with TDP. The discrepancy between $D_2O$ method and the reference methods were supposed to come from both of the methods (Kalma et al., 1998; Schwendenmann et al., 2010). Errors could be raised if the reference method was used violating its application conditions (Lu et al., 2004; Smith and Allen, 1996). Lower estimation (by 66% on average on four bamboo species) by uncalibrated TDP was found in situ when compared with stem heat balance method (Mei et al., 2016). Considering the errors associated with $D_2O$ method, two primary sources presumed mostly related to $D_2O$ method were tracer loss (retention in labeled plants or redistribution to soil or neighbor plants) and incomplete mixing of $D_2O$ in the stem before flowing to different branches or crown levels. Both of them could break the underlying assumptions of applying the $D_2O$ method (Kalma et al., 1998; Kline et al., 1970; Schwendenmann et al., 2010).

### 4.4.4 $D_2O$ retention and its influence on $WU_{D_2O}$

Remaining $D_2O$ were found in the labeled bamboos after 40 days since $D_2O$ injection, but it was insignificant to affect the water use estimation. The total remaining $D_2O$ in each bamboo culm was merely 1% on average of the injected $D_2O$, which could correspondingly lead to 1% higher estimate of the

$WU_{D_2O}$. It was thought that the plants would retain too little tracer to change the water use rates estimate after sampling for enough long time (James et al., 2003; Kline et al., 1970; Schwendenmann et al., 2010). James et al. (2003) found prominent tracers from all portions of the *Cordia alliodora* tree after eight days of $D_2O$ labeling and Schwendenmann et al. (2010) found the absent of $D_2O$ in branches after three weeks of labeling. Therefore, to exclude the influence from retention of $D_2O$, the sampling period should be long enough, and the time may differ on different species.

Although the remaining $D_2O$ was too little to influence water use estimated by the $D_2O$ method significantly, they showed arresting distribution within the labeled bamboos after the experiment. On *B. vulgaris* and *G. apus*, the remaining $D_2O$ were obviously more in leaves and roots than in stems, with smallest values appearing in $\approx 2$ m height (Table 4.2). This $D_2O$ distribution on the organs may indicate that the injected $D_2O$ was relocated upward and downward from the injected points. On leaves, the enrichment of $D_2O$ may be partly attributed to the element fractionation, which makes more $D_2O$ than hydrogen left in the leaves when water was transpired rapidly to the air during daytime (Roden and Ehleringer, 1999). While in roots, $D_2O$ could be transferred from injected points via phloem according to Münch flow-pressure theory (Münch, 1927). Inverse water flows through phloem was considered as a possible way to take tracers downwards (Choi and Aronoff, 1966; Dierick et al., 2010; Schwendenmann et al., 2010). On *Eucalyptus saligna* trees, $D_2O$ was observed exchanging between phloem and xylem through ray parenchyma (Pfautsch et al., 2015a,b). On bamboos, we assumed that the water exchange between phloem and xylem were much easier than trees, as the phloem and xylem stay closely to each other in vascular bundles (Grosser and Liese, 1971). Additionally, the inverse water flow may be more active when leaves were wet due to rain, fog or dew, as in this situation water potential gradient could be formed from leaves to roots (Goldsmith, 2013; Goldsmith et al., 2013). In our study, when rain occurred on the second day after $D_2O$ labeling, a clear drop of the $D_2O$ concentration was observed in most of the labeled bamboos (Fig. 5.2). The drop may also be possibly induced by the foliage water uptake that diluted $D_2O$ in the crown and stem.

### 4.4.5   D$_2$O transfer between culms and its influence on WU$_{D_2O}$

The water transported by inverse water flow may be released to soil from roots, or transferred to other trees or bamboo culms if the plants had connected rhizomes (Dierick et al., 2010; Kline et al., 1970; Marc and Robinson, 2004; Zhao et al., 2016). In this case, loss of D$_2$O occurred and led to overestimates of the water upward to the leaves. In the present study, water transfer was implied by the elevated D$_2$O concentration in the neighbor freshly sprouted and established bamboos (Fig. 4.6). The D$_2$O loss caused by the water transfer to one neighbor culm accounted for 1.7 - 11.7% of the injected D$_2$O on the labeled culms. However, the total D$_2$O loss caused by the water transfer would depend on how many culms the D$_2$O could be transferred to. Intuitively, one culm could be directly connected with at least two other culms: one mother culm and one (or more) son culm. However, as bamboos, especially clumpy bamboos, have a sophisticated interconnected rhizome system (Liese and Köhl, 2015; Stapleton, 1998), the water transfer could probably happen among more culms. In our study, the water transfer may probably happen among five culms on *B. vulgaris* and *G. apus* (Fig. 4.7). These findings indicated the bamboo culms might transport water downward to the underground rhizome system, and further redistribute this water to the other culms in a clump.

Additionally, the quantity of the transferred water was unclear. In another recent study on a running bamboo species (*P. pubescens*), the rhizome-cutting culms consumed $\approx$ 20% less water use than the intact culms and such difference was thought relating to water transfer through rhizomes from other culms or roots (Zhao et al., 2016). Furthermore, the reliance on the water transfer may differ upon the age of the culms. For example, freshly sprouted culms were thought more relied on rhizomes of mother culms than older ones (Liese and Köhl, 2015; Zhao et al., 2016). However, in our study on both freshly sprouted and established neighbor culms of the three studied bamboo species, significant higher $\delta$D values were observed ($P < 0.05$ with t-test; Fig. 4.6). This finding indicated that water transfer might be a typical water use characteristic at clump edges of bamboo culms regardless of their ages. The actual impact of water transfer from rhizomes may be more complex than our understanding due to the sophisticated rhizome system of bamboos (Stapleton, 1998).
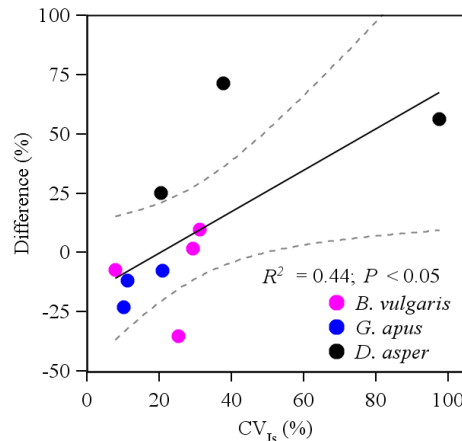
Fig. 4.8 The relative differences between the corrected $WU_{D_2O}$ and $WU_{TDP}$, in relation to coefficients of variation of daily sap flux densities at breast height ($CV_{J_s}$). The corrected $WU_{D_2O}$ was calculated based on the assumption that $D_2O$ transfer between one labeled culm and six neighboring culms, and the assumption was based on the mode of the distribution of the maximal amount of neighboring culms when pooling the three species together.

### 4.4.6 Variability of sap flux and incomplete mixing of $D_2O$

Besides the tracer loss due to retention and transfer, incomplete mixing of $D_2O$ may become another interference source to $WU_{D_2O}$. Unlike the direct influence on water use estimation from tracer loss, influence from incomplete $D_2O$ mixing was harder to detect and quantify. The injected $D_2O$ at the base of the culms could be transported axially and radially (James et al., 2003). Therefore, the $D_2O$ concentration in the leaves could be influenced by the speeds of the axial water transport and the radial water exchange between the xylem vessels and the surrounding tissues. In the present study, the $T_{residence}$ of the $D_2O$ appeared to correlate with $V_{D_2O}$ negatively. Such relationship may mean that if the water transport efficiency was different in the different directions, the $T_{residence}$ of the $D_2O$ injected in the different directions may vary accordingly and furtherly the mixing extent of the $D_2O$ was different. In our study, the averaged $CV_{J_s}$ at breast height were 14 - 52% on the three bamboo species, which may indicate incomplete $D_2O$ mixing according to the assumption mentioned above. Excluding the influence of water transfer on $WU_{D_2O}$ with assuming six culms receiving transferred $D_2O$ (Fig. 4.7), the differences between $WU_{D_2O}$ and $WU_{TDP}$ were correlated with the $CV_{J_s}$ significantly (Fig. 4.8). These findings indicated that except avoiding $D_2O$ loss in any form, we should also try to eliminate the influence of incomplete

$D_2O$ mixing when estimating water use rates with deuterium tracing method. Uniform sampling over the entire canopy could be a seemingly reasonable way. Additionally, drilling more holes around the culms for injecting $D_2O$ could be another way to reduce errors from incomplete mixing.

## 4.5   Conclusions

By applying the deuterium tracing method and the reference TDP method on three tropical clumpy bamboo species, we found some unique water circulation characteristics of bamboos and their impacts on the deuterium derived water use rates. Compared to one previous study on another bamboo species (*B. blumeana*), our studied bamboos had higher sap velocities which could be even higher if sampling at a higher frequency. The high sap velocities, in combination with the relative shorter residence time and the smaller contribution of the water storage to transpiration, may indicate the bamboo leaf water status rely more on the water transport efficiency than on the water storage. Bamboo culms can probably transfer water to the neighboring culms and influence significantly the accuracy of the deuterium derived water use rates on two of the three studied species. However, instead of water transfer, the sap flow variety around the culms could be responsible for the errors of the deuterium derived water use rates on the third species. The findings implied even among these big clumpy species, they show species-specific water circulation characteristics. In the present study can probably deepen our insight on the bamboo water circulations and provide a basis to improve the application of the deuterium tracing method on water circulations.

# Chapter 5

# Water transfer between bamboo culms in the period of sprouting

Dongming Fang[1]*, Tingting Mei[1,2,3], Alexander Röll[1], Dirk Hölscher[1]

[1] Tropical Silviculture and Forest Ecology, Georg-August-Universität Göttingen, Germany.
[2] State Key Laboratory of Subtropical Silvilculture, Zhejiang Agriculture and Forestry University, Lin'an 311300, Zhejiang province, China.
[3] Zhejiang Provincial Key Laboratory of Carbon Cycling in Forest Ecosystems and Carbon Sequestration, Zhejiang Agriculture and Forestry University, Lin'an 311300, Zhejiang province, China.

* Correspondence: Dongming Fang, Tropical Silviculture and Forest Ecology, Georg-August-Universität Göttingen, Büsgenweg 1, Göttingen, 37077, Germany. Email: dongmingf@gmail.com

# Abstract

Bamboo culms are often connected to neighboring culms via rhizomes, which may enable resource exchange between culms. One may assume that such an exchange is particularly important in the phases of vegetative reproduction, sprouting and early, fast, "explosive" growth of a new culm. Water exchange between bamboo culms has to our knowledge thus far not been addressed directly in any studies. In big, clumpy bamboos we assessed water transfer between established and neighboring freshly sprouted culms by thermal dissipation probes (TDP) inserted into culms and the rhizome, by deuterium tracing, and by a cutting experiment. During the early phase of sprouting, highest sap flux densities in culms were observed at night, whereas neighboring established culms had high sap flux rates during the daytime. After leaf flushing on freshly sprouted culms, the nighttime peaks disappeared and culms switched to the diurnal sap flux patterns with daytime maxima as commonly observed in established culms. Additionally, modified TDPs inserted into rhizomes indicated water flowing from the established to the freshly sprouted culms. In the early phases, rhizome-transferred water contributed an estimated 47% to daily sap flow rates of freshly sprouted culms. The deuterium tracing method also pointed to water transfer from established culms to freshly sprouted culms. A stable isotope mixing model (SIAR) suggests that one individuallylabeled, established culm contributed about 10% to the sap flow rates of a freshly sprouted culm, which further suggests that a given freshly sprouted culm receives water from more than one established culm, i.e. from five culms on average . In accordance with this, freshly sprouted culms without leaves reduced sap flow rates by 80% after the established culms of the clump were cut. Our findings thus suggest that bamboos exchange water via rhizomes, which is particularly important in the period of early growth of freshly sprouted culms. These freshly sprouted culms have very unusual temporal pattern of sap flux with nighttime maxima, and they receive significant volumes of their sap flow from more than one neighboring culm.

**Keywords: water transfer, bamboo shoots, TDP, deuterium tracing, clumpy bamboo, rhizome**

## 5.1 Introduction

In contrast to the typical, independently standing species, species with interconnected roots or rhizomes may have the possibility to share resources with each other directly (Baret and DesRochers, 2011). Resource allocation among interconnected individuals, refered to as "physiological integration" (Caraco and Kelly, 1991; Kroon et al., 1996; Lau and Young, 1988), has previously been intensively studied on herbaceous species (Alpert and Mooney, 1986; Chapman et al., 1992; Kroon et al., 1996; Lau and Young, 1988; Stuefer et al., 1996). In contrast, only the mechanism has only been studied in a few tree species in recent years, e.g., lodgepole pine (Fraser et al., 2006), aspen (Baret and DesRochers, 2011), and poplar (Adonsou et al., 2016). For these studied herbaceous and tree species, nutrient and carbohydrate transfer via interconnected roots or rhizomes was reported. The transferred amounts and the direction of transfer depended on the status of both the donor and the dependent individual (Adonsou et al., 2016; Kroon et al., 1996). As such, resource translocation can increase under conditions of increasing temporal variance in resource availability of the dependent individuals, while it can decrease when temporal variance in resource availability of donors increases (Caraco and Kelly, 1991). Such resource integration was shown to be of critical importance e.g., for new ramets grown from the parental root systems (Baret and DesRochers, 2011) or for young bamboo culms (Song et al., 2016).

As rhizomatous monocot species, bamboos are well known for their fast expansion via the underground rhizome system as well as the rapid growth rates of freshly sprouted culms (Liese and Köhl, 2015). After emerging from the soil, bamboo culms can attain their full heights within one or two months, with growth rates of up to 10 - 80 cm per day (Liese and Köhl, 2015; Song et al., 2016). Some species may even grow up to 1 m per day (Ueda, 1960). This leads to the obvious question of where developing culms with no leaves and only few roots get the resources to sustain such incredible growth rates. Important mechanisms could be nutrient storage in the rhizome system as well as resource translocation from attached mature culms that are neighboring the young, leafless culms (Li et al., 1998a,b; Liese and Köhl, 2015). A study on Moso bamboo (*Phyllostachys pubescens*) revealed that the content of non-structural carbohydrates in mature culms declined substantially during the "explosive growth" period of neighboring, young bamboo shoots; it was believed that this was due to translocation of carbohydrates from mature to young culms via the underground rhizomes (Song et al., 2016). According to

the widely accepted Münch theory (Münch, 1927), carbohydrate translocation in the phloem is always also accompanied by water translocation (Savage et al., 2016). Water transfer among bamboo culms might thus not just be an important drough-coping strategy particularly for freshly sprouted culms, but might also play a key role for carbohydrate-translocation mechanisms (Adonsou et al., 2016). Applying deuterium tracing on culms in a clump of *Bambusa blumeana*, Dierick et al. (2010) found higher deuterium concentration than the background values in neighboring culms close to the labeled culms. This elevated deuterium concentration was thought to imply the existence of water transfer among the culms via the underground rhizomes. In another study on Moso bamboo, some culms' rhizomes were purposfully cut and these culm thus disconnected from the rhizome network. The culms with cut rhizomes subsequently consumed 20% less water than the culms with intact rhizomes (Zhao et al., 2016, TDP). This reduction in water use was thought to relate to the disruption in rhizome connectivity.

Generally, deuterium tracing has the advantage of accurately tracing the actual movement of water, while combining rhizome cutting and TDP observations can help to quantify the amount of water transferred via rhizomes at a higher temporal resolution. Therefore, applying both methods together on bamboo culms could be a promising way to assess the water translocation among culms. Our aim in this study was 1) to explore if water transfer existed among established and freshly sprouted bamboo culms, and 2) to quantify the contribution of belowground water transfer from established culms to freshly sprouted culms.

## 5.2 Materials and methods

### 5.2.1 Study site and bamboos

The study site is located in a bamboo garden in Bogor, Indonesia (6°33'40" S, 106°43'27" E, 182 m asl). Rainfall in Bogor is 3978 mm per year and the mean annual temperature is 25.6 °C (Van Den Besselaar et al., 2015). The climate is characterized by alternative dry (June to September) and wet (October to May in next year) periods. Compared to the dry period, the wet period has much higher monthly precipitation (383 vs. 230 mm). During the wet periods, new shoots of bamboos sprout from the soil and grow to reach their full height. The three studied bamboo species (*Bambusa vulgaris*, *Gigantochloa apus*, and
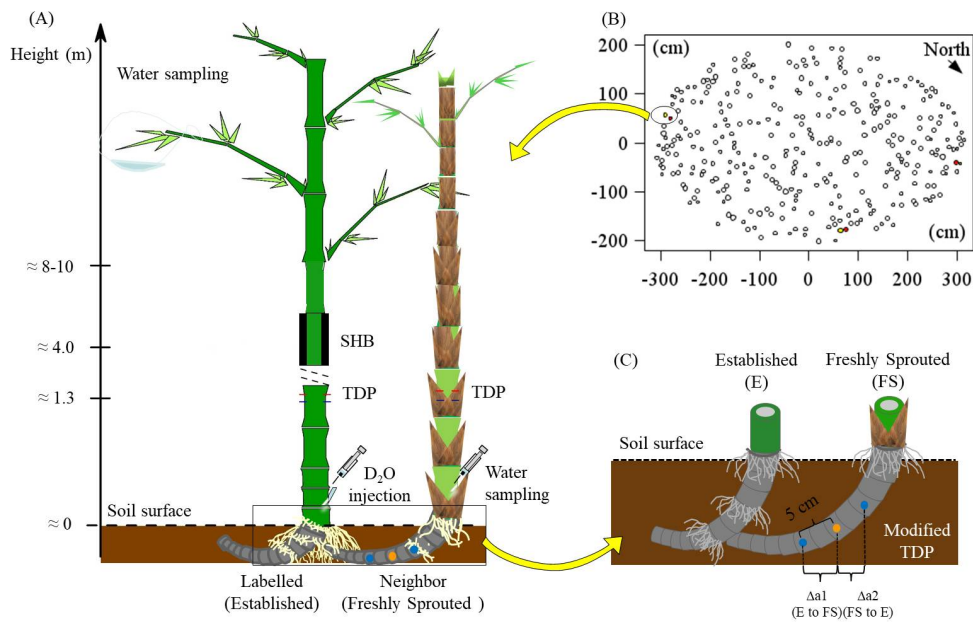
Fig. 5.1 (A) Experimental scheme for applying deuterium tracing and TDP methods; (B) the locations of labelled culms and their neighbor culms in a clump of *B. vulgaris* (n = 3 pairs of culms). The red, yellow and white filled circles represented the labelled established, the neighbor freshly sprouted and the other culms, respectively. (C) Setup of self-made thermal dissipation probes with two reference probes installed at equal distance from the central heating probe on the rhizome of *B. vulgaris*. The orange point represents the heating probe, the blue points are the unheated reference probes.

*Dendrocalamus asper*) are clumpy bamboo species. These clumpy species connect established culms to freshly sprouted culms via short rhizomes ($\approx 30$ to 50 cm length). Unlike the hollow culms of the bamboos, the rhizomes are solid. During the nearly four-month experimental period, the freshly sprouted culms went through three particular growing stages, here refered to as the "pre-leafing", "leafing" and "well-leafed" periods. In the pre-leafing period, freshly sprouted culms grew in height but were without any leaves; in the following leafing period, culm growth almost came to a halt while the leaves began to develop; in the final well-leafed period, both culm- and leaf-development were (nearly) completed.

## 5.2.2 Sap flow measurements with the TDP method

From the clump edge of *B. vulgaris*, we selected three pairs of established and attached freshly sprouted culms during the pre-leafing period and installed

TDP sensors on each of them (Fig. 5.1). Interconnectivity between established and freshly sprouted culms was verified by partially removing the topsoil and directly observing the rhizomes. On each culm, three TDP sensors (1 cm length) were inserted into the culm walls at the breast height. Each TDP sensor consisted of a heated and an unheated reference probe, and the heating probe was installed 10 cm above the reference probe. The heating probe was powered by 120 mA (Mei et al., 2016). The temperature differences between the two sensors (recorded as voltage signals) were used for calculating sap flux density ($J_s$, g cm$^{-2}$ h$^{-1}$). To capture potentially occuring circumferential variability of water use in bamboo culms, we installed three pairs of TDP evenly around the culm. The signals from the three sensors were averaged connecting the signal wires in parallel. Voltage signals were recorded every 30 seconds and averaged every 10 minutes with data loggers and multiplexers (CR1000, AM16/32, Campbell Scientific Inc., USA). The TDP voltage signals were used to calculate $J_s$ with the Granier's original TDP sap flux equation (Granier, 1987), which were subsequently corrected with available species-specific calibration parameters Mei et al. (2016). Sap flow rates (SF) per hour (g h$^{-1}$) were derived by multiplying corrected $J_s$ by the cross-section area of the culm walls at breast height. Daily SF was obtained by summing up the hourly SF of a day.

To measure $J_s$ and detect direction of sap flow in the rhizome between each pair of culms, we built self-made, modified TDP sensors with three probes instead of two. This modified TDP consisted of one central heating and two unheated reference probes. The heating probe was installed at the mid-point of the rhizome between the culms, and the two reference sensors were installed at 5 cm distance from the heated probe, one on each side. The temperature differences between each reference probe and heated probe were recorded as voltage signals and stored in the same way as described above for the "standard" TDP sensors for measurements of culm $J_s$. In the analysis, the two derived $J_s$ were compared, and the reference probe with the lower $J_s$ was assigned the downstream position (to determine direction of flow). This was based on the assumption that sap flow brought the heat energy to the downstream sensor and that this heat would increase the temperature of the downstream sensor. In this case, the signal value from the downstream sensor was smaller than that from the upstream sensor. To verify this assumption, we simulated the heat field around the heating sensor and the two reference sensors under different sap flow density with the ANSYS model (Academic version, CFX 17.0, ANSYS Inc., Pennsylvania, USA). The $J_s$ of the rhizome

Table 5.1 The information of studied bamboos and trees (3 culms per species but 4 culms of *B. vulgaris* used). The adjusted $WU_{D_2O}$ was $WU_{D_2O}$ adjusted with deuterium transfer on bamboos. The values were represented as the means(SD) which were in parenthesis.

| Species | Height (m) | DBH (cm) | $D_2O$ injected | $T_{arrival}$ | $T_{residence}$ |
|---|---|---|---|---|---|
| *B. vulgaris* | 17.9(0.8) | 7.0(0.4) | 5.8(1.6) | 1.5(1.0) | 5.5(1.3) |
| *D. asper* | 21.1(0.9) | 10.7(0.9) | 8.0(1.1) | 1.0(0.0) | 5.0(1.7) |
| *G. apus* | 16.2(2.7) | 7.9(1.1) | 5.7(0.1) | 1.0(0.0) | 6.3(0.6) |

was calculated with the same calibrated formulas as for culms, and hourly SF was derived as the product of $J_s$ and the cross-section area of the rhizomes. As for culms, daily SF of rhizomes was obtained by summing up the hourly SF of a day. The contribution of rhizomes to the freshly sprouted culms was calculated as a ratio of daily SF of the rhizomes to those of the freshly sprouted culms.

To explore how freshly sprouted culms were influenced when established culms were removed, we cut and removed all established culms in one clump and kept them in a different clump of *G. apus*. Culm $J_s$ of the left freshly sprouted culms was monitored by TDP in the same way as described above. The monitoring was conducted on five culms with an initial height of around 2 meters; it stopped after about one month due to the falling of the culms. Until then, the culms had reached 5 - 8 meters in height without any leaf development.

### 5.2.3 Deuterium tracing

To explore if there was water transferred from established culms to freshly sprouted culms (Fig. 5.1 C), we conducted a deuterium tracing experiment on three clumpy bamboo species (*B. vulgaris*, *G. apus* and *D. asper*) in the leafing and well-leafed periods of freshly sprouted culms. From the edge of the clumps, we selected four pairs of established and attached freshly sprouted culms for *B. vulgaris* and three pairs for *G. apus* and *D. asper* (Table 5.1). In the morning (6:00 - 7:00) on $8^{th}$ March 2013, we injected deuterium oxide ($D_2O$, 99.90% D, euroiso-top, Gif sur Yvette, France) into the established culms at a height of $\approx$ 50 cm. Before labeling, we glued four plastic tubes on each culm and filled them with 40 mM KCl solution. We then drilled holes into the tubes and replaced the solution with 1.5 - 3 g $D_2O$. The tubes were

refilled with KCl solution several times. The residual $D_2O$ in the tubes was collected with syringes after sunset.

Sampling was conducted on both the labeled established culms and the attached freshly sprouted culms. On each labeled established culm, we sampled from five regions of the crown, sealing five leaves each with one transparent plastic bag per leaf. The leaf condensate water from the leaves of one culm was collected and mixed at around 7:00 am every day of the first ten days and every 4 - 6 days for three weeks after that. On each attached freshly sprouted culm, we drilled holes on the culm and extracted water from the holes at around 6:00 in 3 - 5 day intervals. Additionally, after about 40 days since the deuterium labeling, all labeled established culms were harvested, and water samples were obtained from leaves, branches, culms and rhizomes. All water samples from both the labeled established culms and the attached freshly sprouted culms were kept in 1.5 ml glass vials which were stored in a refrigerator .

The water samples were analyzed in the Center for Stable Isotope Research and Analysis (KOSI) at the University of Göttingen, Germany. The analysis was conducted with a high-temperature conversion/elemental analyzer coupled via a ConFlo III interface to a Delta V Plus isotope ratio mass spectrometer (Thermo-Electron Cooperation, Bremen, Germany). The deuterium enrichment ($\delta$D, ‰) with 2‰ precision was derived as below ([Coplen, 1995](#)):

$$\delta D = (\frac{R_{sample}}{R_{VSMOW}} - 1) \times 1000 \qquad (5.1)$$

Where $R_{sample}$ is D/H in the water samples while $R_{VSMOW}$ is D/H in the Vienna Standard Mean Ocean Water.

### 5.2.4   Modeling water transfer from rhizome to culm with SIAR

For a specific single culm, water uptake by a culm was supposed to be composed of two parts: water absorbed from the soil and water transferred via rhizomes. However, in our study, an unlabeled target neighboring culm (established or freshly sprouted) close to the labeled culm was assumed to obtain water from three sources: soil, labeled culm and other unlabeled culms as a whole. Therefore, the contribution percentages of the three sources to the whole culm sap flow were summed up to 100%. To estimate the contribution of each part, an isotope mixing model (SIAR) was used ([Parnell et al., 2010](#),

Stable Isotope Analysis in R). The model was described by the following equation:

$$\delta D_{neighbor} = P_{soil} \times \delta D_{soil} + P_{label} \times \delta D_{label} + P_{otherunlabel} \times \delta D_{otherunlabel}$$

$$(5.2)$$

Where $\delta D_{neighbor}$ is the $\delta D$ values in the target neighbor culms that were close to the labeled ones; it was obtained from the fifth day since labeling, with 4 - 5 days intervals during the deuterium tracing period. $\delta D_{soil}$ is the $\delta D$ value in the soil, which was assumed to equal to and thus substituted with an averaged $\delta D$ value from the stems of the cut-down labeled culms of each species, with 3 - 4 culms per species). $\delta D_{label}$ is the $\delta D$ value in the labeled culms that was sampled from the leaves, from the fifth day since labeling to the $30^{th}$ day. $\delta D_{otherunlabel}$ is the $\delta D$ value in the other unlabeled culms, which should be in the range of the $\delta D$ values of all the sampled culms. $P_{soil}$, $P_{label}$, $P_{otherunlabel}$ are the contribution percentages of each source. The trophic enrichment factor was set to 0 for each source.

The SIAR model yielded the probability density distribution of each contribution percentage, and the low and high 95% highest density region was calculated. Additionally, the mode (with the highest density) of each contribution percentage was obtained and used for subsequent analysis.

### 5.2.5   Data analysis and statistics

All data analyses and plotting were performed with SAS 9.4.

## 5.3   Results

### 5.3.1   Culm sap flow patterns in established and freshly sprouted culms

In established culms, $J_s$ showed a typical diurnal pattern corresponding approximately to the diurnal patterns of radiation (PAR) and vapor pressure deficit. With rising PAR in the morning, $J_s$ started to increase until reaching its peak values around midday ($J_{s\_max}$; on average 56.4 cm$^{-2}$ h$^{-1}$). $J_s$ gradually decreased in the afternoon and remained close to zero during the nighttime. In contrast, $J_s$ of the freshly sprouted culms showed varying patterns over a
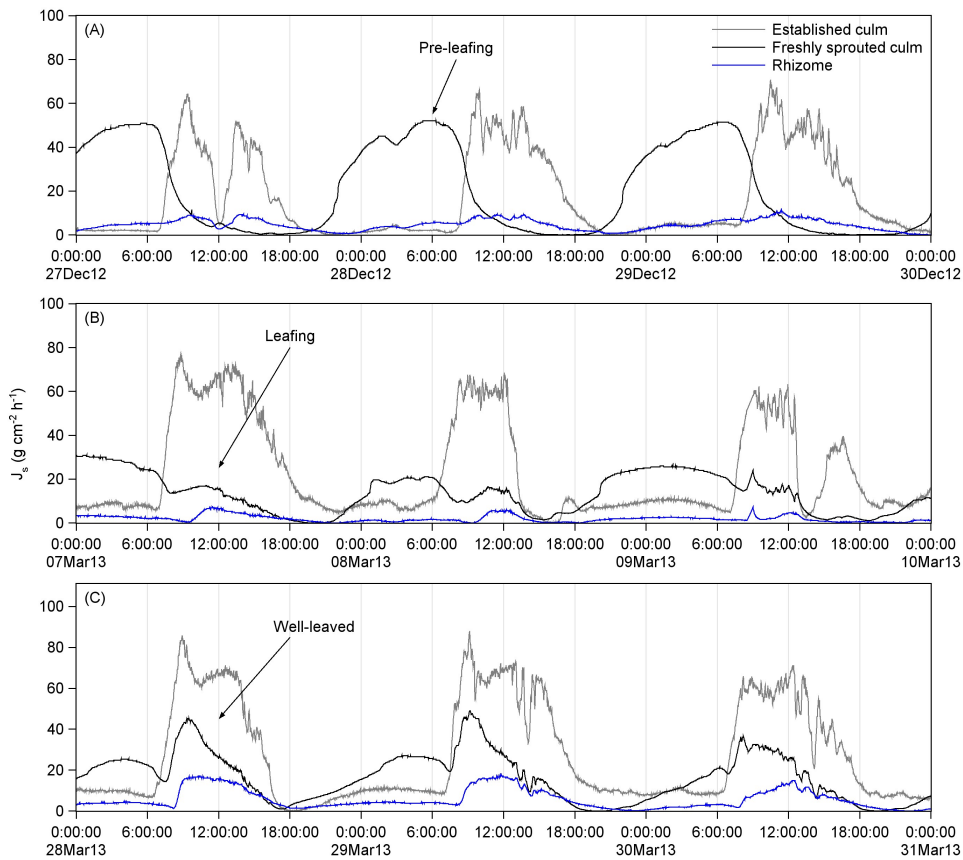
Fig. 5.2 Diurnal sap flux density ($J_s$) of rhizome, freshly sprouted and established culm of *Bambusa vulgaris* (Culm 1) in pre-leafing (A), leafing (B) and well-leafed (C) period.

three-month growing period. From their sprouting from the soil until the stage of leaf production (i.e. during the pre-leafing period), $J_s$ of freshly sprouted culms displayed a reverse pattern, with increasing Js from near zero at sunset time to its peak around sunrise (on average $J_{s\_max}$ = 43.6 g cm$^{-2}$ h$^{-1}$ of three culms; Fig. 5.2 A). With leaves emerging over the following several days (leafing period), the clear reverse pattern in young culms started to blurr into an intermediate pattern, with on average lower daytime $J_s$ (on average $J_{s\_max}$ = 25.5 g cm$^{-2}$ h$^{-1}$) than in established culms (on average $J_{s\_max}$ = 56.2 g cm$^{-2}$ h$^{-1}$) and with still quite active nighttime $J_s$ (on average $J_{s\_max}$ = 25.6 g cm$^{-2}$ h$^{-1}$; Fig. 5.2 B). However, after about 3 months since sprouting, $J_s$ of young culms was clearly higher during the daytime (on average $J_{s\_max}$ = 42.1 g cm$^{-2}$ h$^{-1}$ of three culms) than during the nighttime (on average $J_{s\_max}$ = 22.6 g cm$^{-2}$ h$^{-1}$ of three culms) and thus approached the pattern observed in mature, established culms (Fig. 5.2 C).

Table 5.2 $\delta$D values (means and standard deviations in brackets) in xylem water of freshly sprouted culms neighboring the labeled established culms. The dashed line refers to background deuterium values ($\delta$D, ‰) which were derived by averaging the stem $\delta$D values of the cut-down labeled bamboos after about 40 days since labeling. Note: * and ** represent significant differences (t-test) between values and the background values with $P < 0.05$ and $0.01$, respectively.

| Species | Background $\delta$D (‰) | $\delta$D (‰) after n days of labeling | | | | | |
|---|---|---|---|---|---|---|---|
| | | 5 days | 10 days | 15 days | 20 days | 25 days | 30 days |
| *B. vulgaris* | -42.2 | -33.7 (4.1)* | -32.8 (2.5)* | -32.8 (2.5)* | | -28.0 (2.9)* | -29.1 (1.4)** |
| *G. apus* | -43.1 | -23.4 (4.8)* | -32.5 (2.1)* | -21.2 (1.9)* | -19.7 (9.9)* | | -28.4 (3.0)* |
| *D. asper* | -39.0 | -29.3 (6.4)* | -42.2 (1.4) | -32.2 (14.5) | -38.8 (1.7) | | -37.3 (1.1) |

## 5.3.2 Rhizome sap flow between culms monitored with TDP

Based on the ANSYS simulation results and the observed voltage signals from self-made three-probe TDP sensors installed in the rhizomes between established culms and freshly sprouted culms (Appendix Fig. A.3 and A.4), , significant water flow from established to freshly sprouted culms via rhizome networks was observed.

During the pre-leafing period, Js patterns in rhizomes peaked around midday (on average $J_{s\_max} = 15.7$ g cm$^{-2}$ h$^{-1}$), corresponding to the $J_s$ peaks observed in established culms. However, there was also substantial $J_s$ in rhizomes during times of high $J_s$ in freshly sprouted culms (Fig. 5.2 A), pointing to the importance of water transfer from established to leafless young culms. The reduced sap flow observed in freshly sprouted culms during the days of leafing (see previous chapter) was also reflected in lower rhizome $J_s$. Rather than corresponding to the $J_s$ patterns in established culms, rhizome $J_s$ began to align with $J_s$ of young culms during the leafing period (Fig. 5.2 B). Once the leaves of young culms were well established (Fig. 5.2 C), $J_s$ patterns were synchronized in rhizomes, established and young bamboo culms, usually with peaks between 9 am and midday.

Generally, daily sap flow (SF) of the three freshly sprouted culms of *B. vulgaris* was positively correlated with SF of the rhizomes ($R^2 > 0.47$; $P < 0.01$; Fig. 5.3). The ratios between SF of the freshly sprouted culms and that of the rhizomes were 39.1%, 58.5% and 45.5% for the three culms, respectively. On average, the water flowing to the freshly sprouted culms via rhizomes from established culms contributed 47.7 ($\pm$9.9)% of daily SF of the freshly sprouted culms over the experiment period (Fig. 5.3).
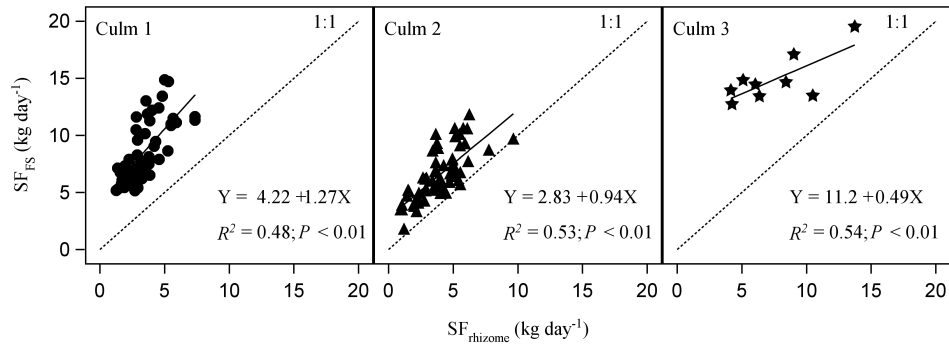
Fig. 5.3 Daily sap flow rates of freshly sprouted culm ($SF_{FS}$) of *Bambusa vulgaris* in relation to those of the corresponding rhizome ($SF_{rhizome}$).
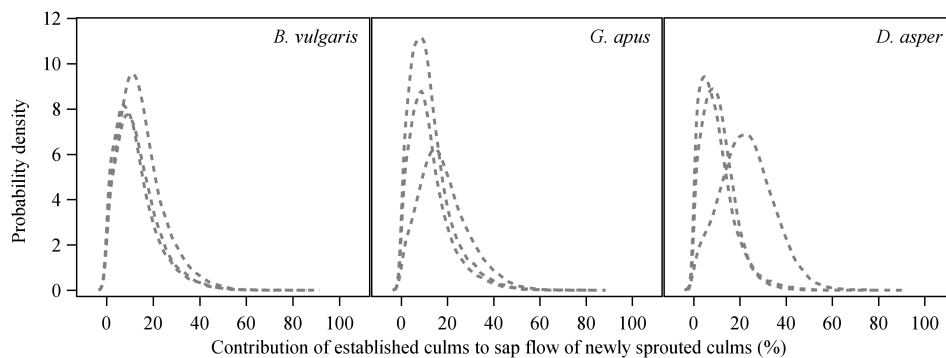


Fig. 5.4 Probability density distributions of the water contribution of labeled culm to water use (%) of neighbor freshly sprouted (dash line) culms of *B. vulgaris*, *G. apus* and *D. asper*, in which the highest probability of the water contribution (averaged in species) was 9%, 10% and 12% respectively.

### 5.3.3   Deuterium tracing between the freshly sprouted culm and the established culm

The deuterium tracing experiment showed a clear increase of deuterium concentration in freshly sprouted culms of three bamboo species including *B. vulgaris* (Table 5.2). This indicates that water was transferred from the labeled established culms to freshly sprouted culms via rhizomes. Results from the SIAR model suggest a considerable contribution of transferred water to daily transpiration of the freshly sprouted culms, i.e. on average 9%, 10% and 12% for *B. vulgaris*, *G. apus* and *D. asper*, respectively (Fig. 5.4).

### 5.3.4   Effect of removing established culms on freshly sprouted culms

As a surrogate for *B. vulgaris*, five freshly sprouted culms in a clump of *G. apus* where all established culms had been cleared were monitored. Established culms of *G. apus* transpired on average 63% of water of *B. vulgaris* per day, therefore the supposed $J_s$ of freshly sprouted culms of *G. apus* was calculated by multiplying that of *B. vulgaris* by 63% (Fig. 5.5). After removal of established culms, the daily sap flow of the freshly sprouted culms was estimated to be 79.3% lower than the corresponding values in another clump where established culms had not been removed.

The results indicate that established culms could support freshly sprouted culms not only by directly transferring water via rhizomes, but also via other (indirect) pathways such as, pumping up water from deeper soil layers and storing water in rhizome networks to facilitate accessibility for freshly sprouted culms.
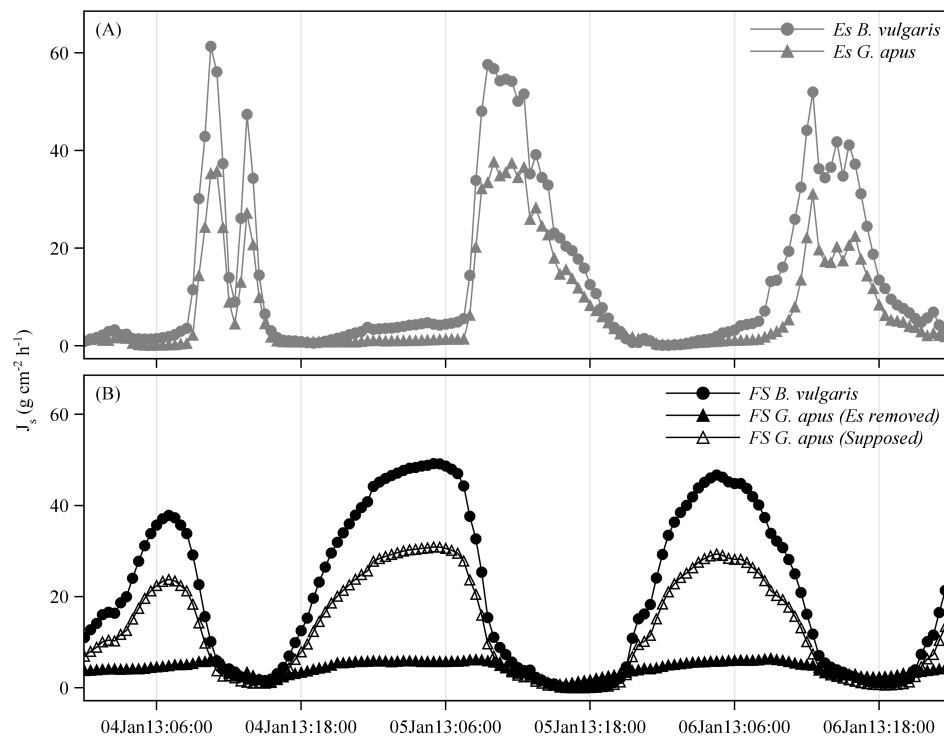
Fig. 5.5 Sap flux densities ($J_{\mathrm{s}}$, g cm$^{-2}$ h$^{-1}$) of (A) the established (Es) *G. apus* culms in a clump without clear-cut and a reference *B. vulgaris* and (B) $J_{\mathrm{s}}$ of the freshly sprouted (FS) *G. apus* culms in a different clump where all the established culms were cut, and in the reference *B. vulgaris* clump from which the baseline (non-clear-cut) scenario for *G. apus* was derived. This was done by multiplying $J_{\mathrm{s}}$ of freshly sprouted *B. vulgaris* by the mentioned ratio (0.63) of daily accumulated $J_{\mathrm{s}}$ in established *G. apus* vs. *B. vulgaris*.

## 5.4   Discussion

It is generally accepted that micrometeorological factors (e.g., solar radiation and vapor pressure deficit) are the main drivers of day-to-day fluctuations in tree water use and that limited soil water availability can constrain tree water use (Kume et al., 2007; O'Brien et al., 2004). However, water use patterns may vary under special circumstances, e.g., in freshly sprouted leafless bamboo culms. In our study, we found that diurnal $J_s$ patterns in freshly sprouted bamboo culms changed gradually, from the pre-leafing over the leafing to the well-leaved period (Fig. 5.2). During the pre-leafing period, diurnal $J_s$ patterns in freshly sprouted bamboo culms typically differed from patterns in neighboring established culms. The results imply that the $J_s$ pattern of freshly sprouted bamboo culms (nighttime maxima) was not always controlled by the classic micrometeorological drivers, particularly during the early growing stage when culms are still without leaves and branches (Liese and Köhl, 2015).The neighboring established culms most likely played an important supportive role for freshly sprouted culms. During the first four months since emerging, around 48% of the daily sap flow of freshly sprouted culms was provided by established culms via rhizomes (Fig. 5.3). Our findings further indicate that the water transfer via rhizomes into the freshly sprouted culms may come not only from the nearest direct connected established culms but also from more neighborhood culms via the interconnected underground rhizomes. For an individual freshly sprouted culm, water is probably provided by around 5 or 6 neighboring established culms (Fig. 5.4). However, the dependency of freshly sprouted culms may depend on their distance from established culms; as such, a previous study on poplar found that ramets benefited more from proximal root connection than from distal ones (Adonsou et al., 2016).

Despite previous evidence of water transfer via rhizomes in several species, many of the involved mechanisms still remain unclear. For bamboos, the drivers leading to the dynamic balance between the water use of the established donor culms and the water demand of the dependent freshly sprouted culms as well as the possibly involved trade-offs yet remains to be described. In our study, water use patterns were opposite between freshly sprouted and established culms, which may be an example for such a trade-off. Our results indicate that established donor culms reduced the water supply to the dependent freshly sprouted culms when their transpiration demand was high. As a result, water transfer to leafless freshly sprouted culms occurred mainly during the nighttime, when established culms transpire close to zero. According to

source-sink theory, resource translocation among connected herbaceous plants depends on resource availability; the resource is transferred from resource-abundant (source) to resource-scarce regions (sink, Marshall, 1996). The theory could explain the opposite water use patterns observed for freshly sprouted and established bamboo culms in our study. The established bamboo culms transpired a lot of water during daytime and were thought to withdraw water from the culm storage (Mei et al., 2016; Yang et al., 2015), which may lead to a large water demand. During the nighttime, along with the largely reduced transpirational pull and the refilling of the culm water storage via root pressure mechanisms (Cao et al., 2012; Yang et al., 2015), the water demand in established culms is largely reduced, while demand for water in freshly sprouted culms is growing more urgent. Such resource allocation relies largely on resource availability of the donor individuals, which can be simulated with models (Caraco and Kelly, 1991) and which has previously been observed in several tree (Adonsou et al., 2016; Baret and DesRochers, 2011; Fraser et al., 2006) and herbaceous species (Alpert and Mooney, 1986; Chapman et al., 1992; Kroon et al., 1996; Lau and Young, 1988; Stuefer et al., 1996; Wang et al., 2011b; Zhang et al., 2012). The dependency of freshly sprouted culms on established culms was largely relieved after they produced enough leaves (Fig. 5.2 C). However, water water transfer among the young culms and the interconnected established culms continued for several weeks after leaf flushing. The resource translocation could additionally be reactivated in case of resource stress of individual culms (Marshall, 1996). For example, differences in soil water availability, which have been reported even for small patches, could be balanced via interconnected rhizome networks (Hutchings et al., 1997; Wang et al., 2011a; Zhang et al., 2012).

According to the mentioned source-sink theory (Marshall, 1996), the discrepancy of the water potentials among culms may be the driving force of water translocation. During the daytime, due to limited culm water storage (approx. 10% of daily water use; Fang et al., unpublished data), established culms would face larger water stress and thus had a more negative water potential than leafless freshly sprouted culms with low transpiration during their early growing period. After the flushing of leaves, freshly sprouted culms can transpire water with their leaves during the daytime, which results in more negative water potentials to pull water up from the rhizomes. Another finding is that during the first four months since emergence, freshly sprouted culms kept active nighttime sap flow regardless of whether they were with or without leaves. Reduced competitive water uptake from rhizomes by the established

culms could be a potential reason, while another one may be carbohydrate translocation during the night.

Carbohydrate transport from the source (usually the leaves) to the sink (e.g., rhizome and freshly sprouted culm) is believed to be driven by hydrostatic pressure gradients in the phloem, according to the widely accepted Münch theory (Münch, 1927). In the carbohydrate transport process, the phloem has to withdraw water from the surrounding tissues (usually the xylem), which usually equilibrates the water potential between the phloem and the surrounding tissues (Hölttä et al., 2015; Thompson and Holbrook, 2003). It was found that drawing water from the xylem is more difficult when the water potential in the xylem is more negative. Carbohydrate transport in the phloem thus likely occurrs during the nighttime, when xylem water potential is less negative (Hölttä et al., 2015; Savage et al., 2016). Without substantial transpiration demand and with the water storage refilling via root pressure mechanisms, the less negative water potential in established culms during the night further promotes the phloem to draw water and transport carbohydrates to freshly sprouted culms. For Moso bamboos, non-structural carbohydrates in leaves, branches, culms, and rhizomes of established culms were significantly decreased, as they were transferred and used for the growth of freshly sprouted culms (Song et al., 2016).

## 5.5 Conclusions

Applying a deuterium tracing method and a modified TDP sap flux approach on three tropical bamboo species, we observed water transfer between established and freshly sprouted culms via rhizomes. The studied culms were located at bamboo clump edges, and the contribution of water transferred via rhizomes to daily sap flow of freshly sprouted culms was high. The observed water transfer to freshly sprouted culms could be explained with the source-sink theory, with differences in water potential and carbohydrate translocation via phloem among interconnected culms as potential driving forces. These previously postulated hypotheses could be further verified in our work. We also found indications that water transfer via rhizomes may be not merely constrained to directly neighboring culms, but that it may also exist among established culms, with distance being the major contrasting factor. Exploring the underlying mechanisms behind water translocation as observed in our study in future

works will be necessary to further deepen our insight into the explosive growth of bamboos at a young age.

# Chapter 6

# Water residence times in trees of a neotropical dry forest

Sophie Graefe[1]*, Dongming Fang[1], Philipp Butz[1], Dirk Hölscher[1]

[1] Tropical Silviculture and Forest Ecology, University of Goettingen, Germany.

Corresponding author, now at: University of Kassel, Organic Plant Production and Agroecosystems Research in the Tropics and Subtropics, graefe@uni-kassel.de

# Abstract

In tropical dry forests trees with different drought coping strategies co-exist among which leaf deciduous, stem succulent trees are very prominent. The actual role of stem succulence in tree water use is not fully understood and may differ under different moisture regimes. In a premontane dry forest of southern Ecuador, five tree species were studied in the rainy season including one stem succulent species (*Ceiba trichistandra*). All species were studied at the same site and some also across a soil moisture gradient. Deuterium tracing suggests species-specific mean residence times between 11 and 22 days. Mean residence times for Ceiba and two other deciduous tree species where about twice as high as those of evergreen tree species. Across species, residence times increased with tree diameter ($P < 0.05$). When synthesizing ours data and other reviewed data, residence times decreased significantly with wood density ($P < 0.05$). A difference between 19% and 34% in top soil moisture content did not significantly affect water residence times in the stem succulent Ceiba or reference species. Thus our data indicate that under the conditions studied, stem size was very important for tree water cycling but beyond stem succulence did not have much influence on daily transpiration.

**Keywords: Ecuador, deuterium tracing, stem succulence, tree size, evergreen, deciduous**

## 6.1   Introduction

Dryland forests cover a similar sized area as tropical moist forest, and nearly 20% of all forests in dryland areas are located in South America (Bastin et al., 2017). Nevertheless, Neotropical dry forests are considered to be at risk through conversion to other land uses, resulting in fragmented forest landscapes (Miles et al., 2006). A key characteristic of tropical dry forests is the low availability of water during several consecutive months, which has a profound influence on forest structure and physiological activities of trees, resulting in high phenological and functional diversity (Eamus, 1999). Most trees respond to drought through deciduousness, but also evergreen, brevideciduous and stem-succulent adaptation strategies co-exists (Borchert, 1994; Worbes et al., 2013). A principal determinant of functional types among dry forest trees is stem succulence, which enables flushing during or at the end of

the dry season (Borchert, 1994). It has been argued that the ability to maintain maximum rates of transpiration and carbon capture increases with increasing water storage capacity of trees (Goldstein et al., 1998).

Sap flux measurements with thermal dissipation probes (TDP) are one of the most widely used techniques for studying water use patterns of trees (Wullschleger et al., 1998), but this approach has only limited applicability to draw conclusions on stem water storage. In contrast, one of the main variables that can be assessed with deuterium ($D_2O$) tracing is the residence time of water, which makes deuterium tracing a promising method for better understanding the role of stem succulence and water storage. When water is only used for day to day transpiration, the residence time of a tracer is assumed to be rather short (a couple of days), whereas in the case of trees accessing internal water reserves for transpiration, tracer residence time will be longer (several weeks). James et al. (2003) was able to detect radial transport of $D_2O$ in several tree species of the seasonally dry tropics, which points to an exchange of water between stem storage compartments and the transpiration stream. In their study tracer residence time was positively correlated with diurnal water storage capacity.

The aim of the present study was to analyze water residence time by means of deuterium tracing in five tree species in a tropical dry forest of southern Ecuador. It was assumed that water residence time generally scales with tree size, but the study also aimed to shed light on other aspects beyond tree size that potentially influence water residence time in trees. The study was therefore conducted at different elevations to cover a soil moisture gradient. A special focus was put on the stem succulent species *Ceiba trichsitandra*, since the role of stored water in trees is still subject to discussion.

## 6.2   Materials and methods

### 6.2.1   Study site and tree species

The study was conducted in the protected forest reserve Laipuna, which is located in the Ecuadorian province of Loja and part of the Tumbesian dry forest ecoregion of northern Peru and southern Ecuador. The forest receives low annual rainfall with an average of 550 mm year$^{-1}$ (Spannl et al., 2016) and is characterized by an extended dry season of eight months. The Laipuna reserve has a size of 2100 ha and stretches over altitudes of 600 - 1400 m asl.

Precipitation input increases from low to high altitude (Spannl et al., 2016), resulting in a soil moisture gradient. For this study three sites were selected at 670 m, 860 m, and 1100 m asl respectively, to cover the moisture gradient. A total of 39 tree species were recorded in the forest, of which eight were evergreen species (Rodrigo et al., submitted). The majority of trees has a drought deciduous leaf phenology, and shed leaves with the onset of the dry season in May.

For the present study five tree species were selected (Table 6.1), of which two were evergreen (*Capparis scabrida*, *Geoffroea spinosa*) and three deciduous (*Ceiba trichistandra*, *Eriotheca ruizii*, *Erythrina velutina*). Whereas *E. velutina* is a drought deciduous species, *C. trichistandra* and *E. ruizii* are known to possess some succulent properties. *C. trichistandra* is a stem succulent with an outstanding shape and size, and is characterized by early leaf flush at the end of the dry season approximately one month earlier than the other species (Butz et al., 2016). Although not proven, *E. ruizii* is occasionally described as a root succulent, and its moist tubers are known to be used by farmers to feed cattle (Rodrigo et al., submitted). Overall, trees under this experiment covered DBH of 20 - 80 cm, and tree height of 6 - 16 m, whereby the distribution was species specific, with the evergreen *C. scabrida* displaying lowest and the deciduous succulent *C. trichistandra* highest values (Table 6.1).

### 6.2.2   Tracer application

On the three deciduous species, the deuterium tracing experiment was conducted during the rainy season in March 2015, which is a wet month with an average monthly precipitation of 110 mm (Butz et al. 2017). The deciduous species were originally studied with four replicates at each altitude, but the experiment did not yield usable data from all studied trees, resulting in only three replicates of certain species*altitude treatments (Table 6.1). During the 21 days of the experiment, mean soil water content (SWC) ranged from 19% at the lowest altitude to 34% at the highest altitude (Butz et al., in prep). The two evergreen species were not present in sufficient numbers at 860 m asl and completely absent at 1100 m asl. Thus they were only sampled at 670 m asl during the late wet season (from end of May to mid-June 2015) with four replicates per species. Mean monthly precipitation was 50 mm with an average SWC of 12% during that time at 670 m asl.

Table 6.1 Characteristics of tree species studied (mean with SD in brackets), wood density taken from Zanne et al. (2009).

| Species | Family | Phenology | n (trees) | DBH (cm) | Height (cm) | Wood density ($g\,cm^{-3}$) | $J_{s\_max}$ ($g\,cm^{-2}\,h^{-1}$)* |
|---|---|---|---|---|---|---|---|
| *Capparis scabrida* | Capparaceae | Evergreen | 4 | 19.7 (5.4) | 7.4 (1.5) | 0.69 | 12.1 (4.4) |
| *Geoffroea spinose* | Fabaceae | Evergreen | 3 | 27.7 (5.9) | 7.9 (0.8) | 0.75 | - |
| *Erythrina velutina* | Fabaceae | Brevi-deciduous | 9 | 27.9 (9.3) | 10.1 (3.6) | 0.2 | 8.2 (2.1) |
| *Eriotheca ruizii* | Malvaceae | Deciduous | 10 | 56.4 (17.3) | 13.1 (3.3) | 0.47 | 9.1 (3.5) |
| *Ceiba trichistandra* | Malvaceae | Deciduous (stem succulent) | 9 | 76.1 (14.7) | 15.0 (3.9) | 0.26 | 8.9 (3.6) |

Note: *$J_{s\_max}$ refers to the mean TDP-derived maximum sap flux density over the duration of the experiment

Deuterium oxide ($D_2O$, 99 atom% D, Sigma-Aldrich, Germany) was injected into the stems approximately 30 cm above ground through holes that were drilled at a distance of 5 cm around the trunk at an angle of $30°$. The holes had a depth of 7 cm and a diameter of 5 mm. The tracer was injected early in the morning immediately after drilling, identical volumes were applied to each hole, which were subsequently sealed with wood putty. *C. trichistandra*, *E. ruizii* and *E. velutina* received 0.5 ml $D_2O$ per cm diameter. This is about two third less than recommended by Meinzer et al. (2004), but was a result of tracer shortage. The two evergreen species received 0.5 ml $D_2O$ per cm sapwood circumference according to Meinzer et al. (2004).

Five leaves from the upper crown were collected at noon at daily intervals after tracer injection for the first seven days, and later on every three days until day 21 after tracer injection. Reference sample was taken at day zero before tracer application. The leaves were sealed in plastic bags and exposed to sunlight for 30 min (Meinzer et al., 2004). Condensed water was collected with a pipette, transferred into Eppendorf tubes, and stored at 4 °C until analysis. Additionally the baseline $D_2O$ signal in transpired was collected before injection from leaf samples through the same approach. The isotope signature was determined with a high-temperature element analyzer (TC/EA) which is coupled with an isotope ratio mass spectrometer (Delta V Plus, Thermo-Electron Cooperation, Bremen, Germany) at the Center for Stable Isotope Research and Analysis (KOSI) at the University of Göttingen.

### 6.2.3   Data analysis and statistics

Tracer arrival ($T_{\text{-arrival}}$, days) was defined as the time span that passed until the first sample exceeded 10% of maximum deuterium concentration, as described by Schwendenmann et al. (2010). $T_{\text{-max}}$ (days) refers to the point in time after tracer injection when maximum deuterium concentration was observed. Velocity of $D_2O$ transport ($V_{\text{-}D_2O}$, m day$^{-1}$) was estimated as tree height divided by number of days required to detect $D_2O$ tracer in transpired water. Tracer residence time ($T_{\text{-residence}}$, days) was estimated as the period when $D_2O$ concentration in leaves dropped below 10% of the maximum $D_2O$ concentration (Schwendenmann et al., 2010). When $T_{\text{-residence}}$ time exceeded 21 days (the lengths of the experiment), it was estimated by extrapolating deuterium concentration of the last three days to the 10% line (Meinzer et al., 2006).

Mean daily water use estimates obtained with $D_2O$ tracing ($WU_{-D_2O}$, kg day$^{-1}$) were derived according to Calder (1991) as follows:

$$WU_{D_2O} = \frac{M}{\sum_{i=1}^{T} C_i \Delta t_i} \tag{6.1}$$

Where $C_i$ is the mass concentration (g kg$^{-1}$) in the time increment, which was converted from the notation of $D_2O$ ($\delta D$, ‰) values, $\Delta_{ti}$ is the duration of the time increment (days), and $T$ is the total number of days of the experiment (= 21 days).

To make water use estimates from TDP ($WU_{TDP}$) comparable with $WU_{D_2O}$, $WU_{TDP}$ was converted to weighted values with the direct calculated values and the $D_2O$ concentrations as below (Calder, 1991):

$$WU_{TDP} = \frac{\sum_{1}^{T} WU_i C_i}{\sum_{1}^{T} C_i} \tag{6.2}$$

Where $WU_i$ is the daily water use (kg d$^{-1}$) measured with TDP in the $i^{th}$ day, $C_i$ is the mean mass concentration of $D_2O$ in condensated water in the $i^{th}$ day, and $T$ is the number of days of the experiment (= 21 days).

Linear and logarithmic regressions were used to explore relationships between tree structural parameters (DBH) and tracer velocity, residence time, and tree water use. Analysis of variance (ANOVA) was performed for the key parameters derived from the $D_2O$ tracing experiment ($T_{-arrival}$, $T_{-max}$, $T_{-residence}$, $V_{-D_2O}$, $WU_{-D_2O}$) within and across the tree types (deciduous and evergreen). All data analyses were performed with SAS 9.4 (SAS Institute Inc., 2013).

## 6.3 Results

Overall, the two evergreen species showed clearer tracer trajectories, higher peaks and less variability compared to the three deciduous species (Appendix Fig. A.7). In the three deciduous species (*C. trichistandra*, *E. ruizii*, *E. velutina*) the tracer was already detected one day after injection, whereas the two evergreen species (*C. scabrida*, *G. spinosa*) showed a slightly delayed tracer arrival. Maximum tracer values in transpired water were recorded after 2.3 - 4.4 days (Table 6.2). Tracer residence time varied between 11 - 22 days, with shortest residence time in the evergreen *G. spinosa*, and longest residence time in the deciduous stem-succulent *C. trichistandra*. Elevation was found to have no effect on tracer residence time (data not shown). Tracer velocities were

Table 6.2 Key results from the deuterium tracing experiment (mean with SD in brackets).

| Species | N (trees) | $T_{arrival}$ (days) | $T_{max}$ (days) | $T_{residence}$ (days) | $V_{D_2O}$ (m day$^{-1}$) | $WU_{D_2O}$ (kg day$^{-1}$) |
|---|---|---|---|---|---|---|
| *Capparis scabrida* | 4 | 1.3 (0.5)a | 2.8 (0.5)a | 14.3 (4.2)a | 6.3 (1.6)ab | 136.2 (56.7)a |
| *Geoffroea spinose* | 3 | 1.8 (1.0)b | 3.5 (1.0)a | 10.8 (6.3)a | 5.6 (2.7)b | 246.0 (89.2)b |
| *Erythrina velutina* | 9 | 1.0 (0)a | 4.4 (3.0)a | 19.2 (3.9)b | 10.1 (3.6)ac | 70.3 (46.0)a |
| *Eriotheca ruizii* | 10 | 1.0 (0)a | 2.3 (0.7)a | 18.8 (2.4)b | 13.1 (3.3)cd | 173.6 (47.4)ab |
| *Ceiba trichistandra* | 9 | 1.0 (0)a | 2.9 (2.0)a | 21.7 (1.7)b | 15.0 (3.9)d | 207.9 (71.6)b |
| Evergreen | 7 | 1.6 (0.5)A | 3.2 (0.6)A | 12.8 (2.1)A | 5.6 (1.0)A | 191.1 (77.6)A |
| Deciduous | 28 | 1.0 (0)A | 3.2 (1.1)A | 19.9 (1.5)B | 12.7 (2.5)B | 150.6 (71.6)A |

Note: $T$ = time, $V$ = velocity, WU = water use. Different lowercase letters indicate significant differences between species; different capital letters indicate significant difference between tree phenologies at $P < 0.05$.

observed in the range of 5.6 - 15.0 m day$^{-1}$, again with lowest values for *G. spinosa* and highest for *C. trichistandra* (Table 6.2). Overall the deciduous species displayed significantly higher tracer residence times and velocities compared to the evergreen species (Table 6.2). Highest water use estimates from D$_2$O tracing were obtained for *G. spinosa* and *C. trichistandra* with 246 and 208 kg day$^{-1}$ tree$^{-1}$, respectively. Lowest water use estimates were calculated for the brevi-deciduous *E. velutina* (70.3 kg day$^{-1}$ tree$^{-1}$; Table 6.2).

Both tracer velocity and tree water use showed a positive linear relationship with DBH at $P < 0.01$ (Fig. 6.1 a & b), whereby *C. trichistandra* and *E. ruizii* occupy the upper DBH range with 76.1 and 56.4 cm, respectively. The other three species had a mean DBH of < 30 cm (Table 6.1). A logarithmic relationship could be established between tracer residence time and DBH ($P < 0.01$, Fig. 6.1 c).
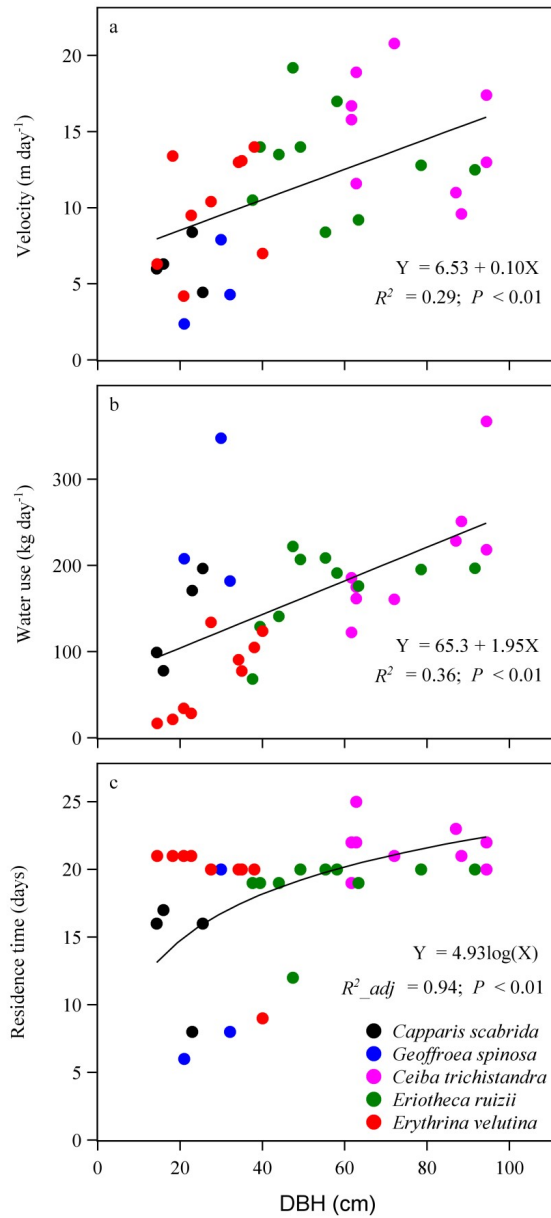
Fig. 6.1 (a) Tracer velocity (m day$^{-1}$), (b) water use (kg day$^{-1}$), and (c) tracer residence time (days) in relation to tree DBH (N = 35).
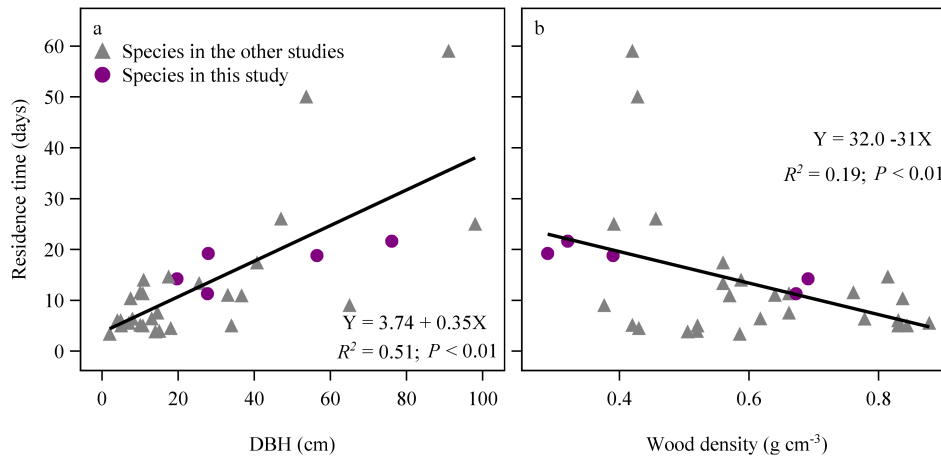
Fig. 6.2 Plant water residence time (days) estimated from deuterium tracing in relation to (a) tree DBH and (b) wood density in this study (n = 5) and from other studies (n = 25). See Appendix Table A.3 for a full list of cited studies and species. Wood density was taken from Zanne et al. (2009).

## 6.4 Discussion

Evergreen and deciduous species can be distinguished on the basis of ecophysiological traits, such as leaf-specific conductivity and stomatal sensitivity (Eamus, 1999; Worbes et al., 2013). Also regarding the dynamics of $D_2O$ tracer, trees from both phenological guilds reacted differently, i.e. tracer residence time and velocity were significantly lower in the two evergreen species compared to the three deciduous species in the present study. Tracer residence time can be regarded as an indicator of diurnal water exchange capacity (James et al., 2003), but was found to be highly variable in previous studies. A literature review of studies applying deuterium tracing on trees and other woody species found eleven studies from ten countries, which were conducted between 1986 and 2016 (Appendix Table A.3).

The present study yielded tracer residence times between 11 - 14 days for the two evergreen species (*C. scabrida*, *G. spinosa*), and 19 - 22 days for the three deciduous species (*C. trichsitandra*, *E. ruizii*, *E. velutina*). This is a lower range as reported by James et al. (2003), who found tracer residence times between 2 - 22 days in a seasonally dry forest in Panama, whereby the shortest residence time was reported for the deciduous species *Cordia alliodora*. Schwendenmann et al. (2010) recorded tracer residence times of 4.3 - 12.5 days in trees of a 12 years old reforestation stand in the Philippines. Longest tracer residence times were observed by Meinzer et al. (2006) on conifers in a temperate climate, which ranged between 36 - 79 days. Generally,

tracer residence time increased as tree diameter increased (Fig. 6.2 a), and relative water storage capacity was found to be highest in large trees (James et al., 2003; Meinzer et al., 2004). A similar trend was also revealed in the present study, with a positive relationship between residence time and tree size, and longest residence time in the stem succulent *C. trichistandra* (Fig. 6.1 c & 6.2 a).

In contrast to large diameter trees, a study conducted on tropical bamboos found tracer residence times in the range of 5.5 - 6.3 days only, with no clear relationship between culm water storage and bamboo diameter (Chapter 4). The relative shorter residence time on bamboos was attributed to the small volume of the hollow culms, which constrains water storage ability that was estimated to contribute only 10% to daily transpiration. These findings on bamboos reversely imply that the longer residence time of species in the present study might indicate larger water storage ability, which further explains their survival strategy in the extended dry periods.

The ability to store water in sapwood is an important function in the regulation of diurnal water deficits of trees from the seasonally dry tropics (Scholz et al., 2008). Especially during periods when the relation of water availability to transpiration demand is imbalanced, water storage was shown to be important for xylem safety of trees (Carrasco et al., 2015; Čermák et al., 2007a; Goldstein et al., 1998; Meinzer et al., 2006, 2010). Smaller trees have a faster internal water circulation to support the transpiration demand on a daily basis. Large trees in contrast store more water to buffer long-term seasonal drought to flush new leaves, as it was shown by Borchert (1994) and Butz et al. (unpublished data).

$D_2O$ tracer velocity as an estimate of maximum sap velocity depends on xylem hydraulic properties (James et al., 2003). Meinzer et al. (2006) found a positive linear relationship between tracer velocity and total daily sap flux in the outer sapwood. In a previously conducted experiment with the TDP method, maximum sap flux densities ($J_{s\_max}$) of 12.1 g cm$^{-2}$ h$^{-1}$ were recorded for the evergreen *C. scabrida*, whereas $J_{s\_max}$ ranged between 8 - 9 g cm$^{-2}$ h$^{-1}$ in the three deciduous species (Table 6.1). A correlation of $J_{s\_max}$ with tracer velocity was only observed when the three deciduous species were compared among each other. In this case, *C. trichistandra* displayed significantly higher tracer velocity and higher $J_{s\_max}$ compared to *E. velutina*.

Overall, tracer residence time significantly and negatively correlated with wood density, as it was shown for species from the present study and those from the literature survey (Fig. 6.2 b). Wood saturated water content was found

to be inversely related to wood density, and a species-independent scaling of sapwood capacitance with wood density could be established (Scholz et al., 2008; Stratton et al., 2000). Species with higher wood-saturated water content are expected to be more efficient with long distance water transport and have higher maximum photosynthetic rates. It further allows stem succulent species to produce new leaves when growing conditions are still unfavorable (Stratton et al., 2000). Water storage patterns of trees were previously assessed by comparing basal and crown sap flow when transpiration was increasing in the morning (Goldstein et al., 1998; James et al., 2003). In the study of Goldstein et al. (1998) from a seasonally dry forest in Panama, a linear relationship between diurnal storage capacity and basal sapwood area was observed, and the amount of water withdrawn from storage was estimated at 9 - 15% of total daily water loss. Daily changes in stem water storage can be also calculated from the difference between maximum and minimum stem volume per day derived from dendrometer measurements at the stem base and below the first branch (Dunisch and Morais, 2002). In their study from the Amazon region, diurnal changes in stem water storage of 0.6 - 2.5 l day$^{-1}$ were observed, and the significance of stem water fluctuations for the daily water balance strongly increased during drier periods (Dunisch and Morais, 2002). In the study of Butz et al. (2016), *C. trichistandra* was found to react most sensitive to fluctuating moisture availability with radial stem variation among the studied species. In the present study however, the deciduous *E. velutina* did not differ noticeable in tracer residence time from the stem succulent *C. trichistandra*, but Butz et al. (2016) could not observed a pronounced diurnal shrinking and swelling for this species as observed through dendrometer measurements. This indicates low internal water reserves in *E. velutina*, even so wood density of this species is with 0.2 g cm$^{-3}$ considerably low, despite being a legume tree, which are usually characterized by rather high wood densities (Powers and Tiffin, 2010; Zanne et al., 2009). Also *E. velutina* showed a fast re-flushing of leaves when environmental conditions became favorable (Butz et al., 2016), most likely a result of its low wood density and relatively long water residence time. For the evergreen species in contrast it seems to be advantageous to have a rather short stature and high wood density (e.g., 0.75 g cm$^{-3}$ for *G. spinosa* and 0.69 g cm$^{-3}$ for *C. scabrida*, Zanne et al., 2009), enabling a better adaptation to resist drought-induced embolism and efficient water transport under high demand (Hacke et al., 2001).

Although soil water content differed considerably between the lowest and highest study site (20% vs. 33%, data not shown), no significant difference in

residence time could be observed in the deciduous species that were studied across altitudes, including stem succulent *C. trichistandra*. Thus, there do not seem to be other factors apart of tree size and wood density influencing residence time, at least under non-limiting soil moisture levels during the rainy season. The question if water residence time is influenced by season, e.g., under water limiting conditions with the onset of the dry season when trees start shedding leaves, however, would require further study.

# Chapter 7

# Synthesis

Bamboos are characterized by hollow culms with abundant parenchyma and interconnected underground rhizome systems. As monocots, bamboos lack secondary growth, which means that unlike dicot trees they cannot produce new xylem. In bamboo culms, xylem and phloem form vascular bundles which are distributed over the abundant parenchyma (50% of the culms, Liese and Köhl, 2015). The parenchyma provides the potential to store water, which could subsequently be temporarily withdrawn by the xylem to contribute to transpiration in times of high evaporative demand. The rhizomes offers pathways for connected culms to redistribute water among each other. Such internal water storage in culms and water transfer among culms through external pathways could form water circulation that is specific to bamboos. The aim of this study was to assess water circulation in bamboos with respect to absolute water use rates, the contribution of internal stem water storage to transpiration, and the transfer of water between connected culms via rhizomes.
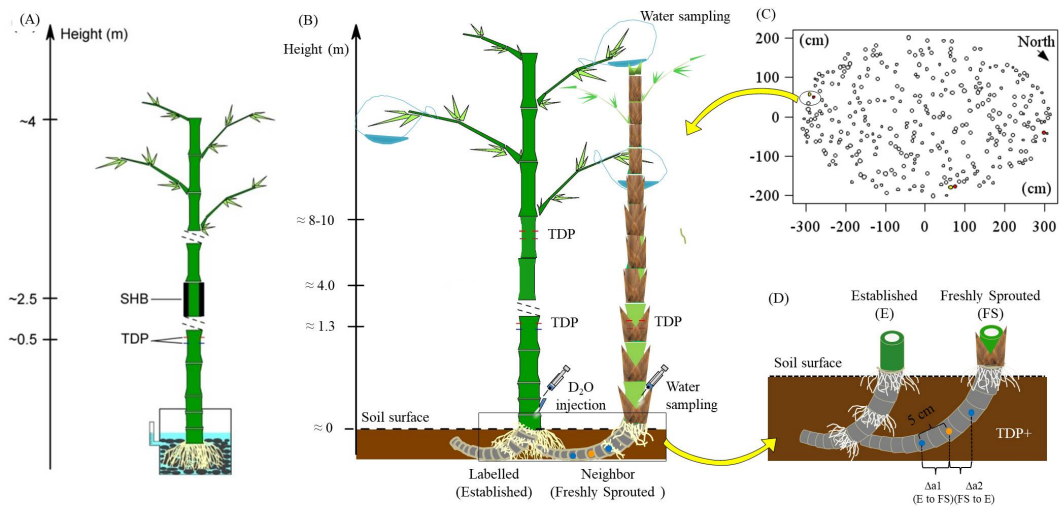
Fig. 7.1 Installation of thermal dissipation probe (TDP) and stem heat balance (SHB) sensors on bamboo culms for the calibration experiments on potted plants (A) and for the field calibration (B), and application of TDP and deuterium ($D_2O$) tracing on the culms at the edge of bamboo clumps (C) to explore water use, storage (B) and transfer (B, D).

# 7.1 How to measure water use characteristics of bamboos

To measure water circulation of bamboos, we need suitable and reliable methods. As bamboo culms are hollow and their culm walls are usually around 1 cm or less thick, they are suitable for measurements with wrapping or short-insertion techniques, or even for non-insertion methods. In this study, we applied two methods that have been widely used on trees but have been attempted few times on bamboos. One is the thermal dissipation probe (TDP; Granier, 1985) technique, which is easy to install and where probes can be self-made at low cost to fit bamboo culms of varying thicknesses. As suggested in various previous TDP-based studies (Lu et al., 2004; Vandegehuchte and Steppe, 2012; Wullschleger et al., 2011), we first tested and calibrated the method on potted and field bamboos in parallel to reference gravimetric and stem heat balance measurements (Sakuratani, 1981). The latter is a widely used wrapping technique, which was suggested to be suitable and reliable on bamboos (Dierick et al., 2010). We also explored the influence of stem water content on the accuracy of TDP measurements by numerical modeling. We further applied deuterium tracing (Calder, 1991) to allow for an estimation

of the water residence time in a certain culm and for the detection of water transfer among culms.

The pot and field calibration experiments (Fig. 7.1 A & B and Chapter 2) confirmed the previous suggestions that TDP needs calibration to yield reliable estimates of sap flow and thus water use rates (Lu et al., 2004; Smith and Allen, 1996; Vandegehuchte and Steppe, 2012; Wullschleger et al., 2011). The stem heat balance method is suggested as a feasible field-based method that does not require species-specific calibration. From linear relationships between estimates of the TDP and stem heat balance method, we derived species-specific in situ calibration parameters for the TDP method for each of the four bamboo species in our study (*Bambusa vulgaris*, *Dendrocalamus asper*, *Gigantochloa atroviolacea*, and *Gigantochloa apus*).

Along with daily dynamics of stem water storage, the wood's water content ($\theta_{wood}$) changed accordingly, and wood thermal conductivity ($K_{wood}$) could thus also be affected. Nonetheless, for TDP, a constant $K_{wood}$ was assumed when determining the maximal temperature difference between the heated and the reference sensors. In a dehydration experiment and numerical modeling (Chapter 3), we proved and quantified the underestimation of sap flux density ($J_s$) when ignoring these change of $\theta_{wood}$. Keeping other controlling variables constant, we found large relative underestimations 1) for large decreases of $\theta_{wood}$ from nighttime to daytime, 2) at relatively low $J_s$, and 3) for relatively larger nighttime $\theta_{wood}$ when the ratio of decline to the daytime (e.g., by half) was kept constant. Based on these results, a logistic-regression correcting equation to correct $J_s$ (Eq. 4 in Chapter 3) with three parameters related to nighttime and daytime $\theta_{wood}$ (Eq. 5, 6, 7 in Chapter 3) was developed.

The contribution of stem water storage to transpiration is often measured with TDP by monitoring the water use rates at the top and bottom positions of a stem (Carrasco et al., 2015; Köcher et al., 2013). It is commonly assumed that during times of diurnally high evaporative demand, water is withdrawn from the stem storage to contribute to transpiration, and is refilled later in the day (e.g., during the night). In our study, we estimated the contribution of stem water storage to daily water use of a culm to be on average 10%, i.e. relatively low. To examine the common assumption of the complete diurnal (e.g., nighttime) refilling of the depleted storage, we applied deuterium tracing to estimate average water residence times in bamboo culms, assuming that the water could certainly stay in the stem for more than one day. By injecting deuterium at the base of a culm and collecting and monitoring the deuterium concentration in the leaves, we estimated water residence times in different culms (Chapter

4). Stem water storage was thus assessed by TDP to quantify its contribution to transpiration, while deuterium was used to estimate the residence time. A combination of both methods was used to give complementary observations on water transfer among culms via underground rhizomes (Fig. 7.1 B & D). With deuterium tracing, we detected the direction and scales (how many culms) of water transfer, while modified three-probe TDP were used to monitor sap flow in rhizomes and further assess the contribution of underground water transfer to the receiving culms (Chapter 5). When only considering water use rates, TDP can be used in hourly, daily or even longer temporal scales, while deuterium tracing is limited to larger time steps, i.e. daily, depending on the sampling interval. Deuterium tracing thus seems less suitable to estimate water use rates on bamboos. However, it was an informative, complementary method to the TDP measurements when exploring water storage and transfer (Chapter 4, 5).

In dicot trees, xylem and phloem of a stem are typically separated into different layers around the stem and in charge of transporting water and photosynthates, respectively. Water use with TDP is measured in the sapwood, i.e., the xylem. In bamboos, however, xylem and phloem are intertwined and constitute vascular bundles distributed over the whole cross area of bamboo culms (Liese, 1985). This means that TDP in bamboos cannot solely measure water use rates in the xylems, but is always also affected by phloem activity. So far, we cannot determine if or to what extent sap transport in the phloem affects the accuracy of TDP measurements of water use. However, some methodological progress has been made. We found a reliable field method for calibrating TDP in bamboos and gained good insights into the importance of the stem water content on the accuracy of TDP measurements. We further developed a model which allows for corrections of water content related errors and thus made use of complementary insights that can be gained by combining independent methodological approaches.

To measure water transfer via rhizomes among culms, we used self-made modified three-probe TDP and tested them with numerical modeling to gain first fundamental insight into the water movements in bamboo rhizomes. Nonetheless, further tests and calibration experiments are needed with regard to probe design and resulting accuracy. In our study with deuterium tracing and the modified TDP, we found that the direction of water transfer was from established culms to freshly sprouted culms over the first four months of culm ontogeny. However, when considering more culms in a clump or more extended time periods (e.g., also encompassing water-limited condi-
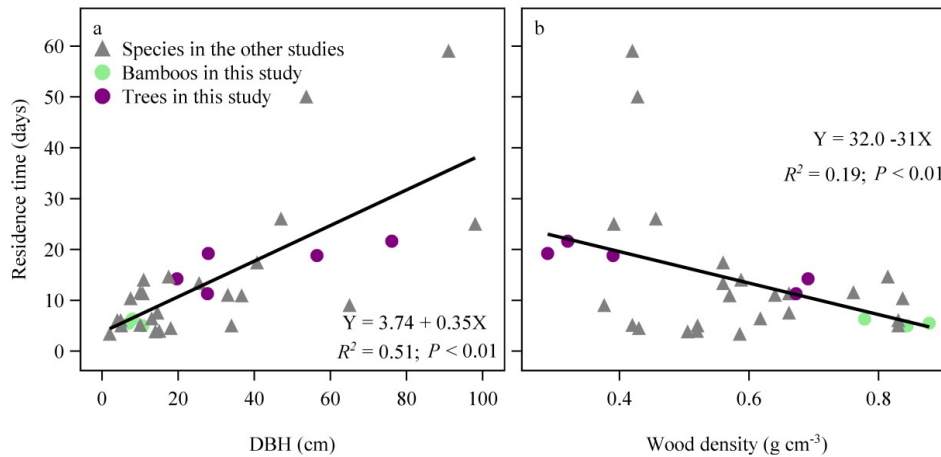
Fig. 7.2 Water residence time (days) of bamboos (N = 3) and trees (N = 5) in this study and the other 25 species in the previous studies (see the detailed list in the table 7.1) in relation to the diamter at breast height (DBH).

tions), multi-directional water transfer may also be possible. The heat ratio method (Burgess et al., 2001a) can be used to measure two directional water movements and thus could be a choice for applications on rhizomes of bamboos.

## 7.2 Water use characteristics of bamboos

For the studied bamboos (*Bambusa vulgaris*, *Dendrocalamus asper*, *Gigantochloa atroviolacea*, and *Gigantochloa apus*), we observed relatively higher maximal $J_s$ (21.6 - 70.5 g cm$^{-2}$ h$^{-1}$) compared to nearby tree species (10.5 - 23.3 g cm$^{-2}$ h$^{-1}$; *Gmelina arborea*, *Shorea leprosula* and *Hevea brasiliensis*). However, $J_s$ and the transpirational driving forces (e.g., vapor pressure deficit and radiation) were quickly decoupled, implying a rapid withdrawal of water from the stem in the morning, but with a relatively low overall contribution to daily transpiration (on average 10%, Chapter 2 and 4). Further, a relatively short water residence time in bamboo culms ($T_{residence}$; 5.5 - 6.3 days) was demonstrated by deuterium tracing. The result may imply either very little exchange between the conducting pathways and the storage compartments on bamboos, or a rapid exchange between them and a quick water withdrawal from the stem water storage. Either implication means that the water is not kept in the culms for a long time but is rather used for transpiration within a relatively short period. The quick decoupling between $J_s$ and the transpirational

driving forces exerted bamboos to avoid xylem cavitation, while nighttime root pressure could contribute to repairing embolized xylem and refilling the water withdrawn from the stem storage (Cao et al., 2012).

The deuterium tracing in this study proved the existence of water transfer among the culms within the same clump and the vital support to freshly sprouted culms by established culms (Chapter 4 and 5). Newly sprouted culms benefited substantially from interconnected nearby mature, established culms, with up to 48% of their sap flow provided by established neighboring bamboo culms (Chapter 5). When all established culms in a clump were removed, the sap flow of freshly sprouted culms decreased by 80% compared to a control clump (Chapter 5). The dependency of the freshly sprouted culms on established culms was largely relieved after they produced enough leaves, after a period of approx. four months. This, however, does not mean the termination of all water transfer among culms. The resource translocation could, e.g., be reactivated when culms face resource stress (Marshall 1996), as water availability for each culm even within small patch may differ substantially (Hutchings et al., 1997; Wang et al., 2011a; Zhang et al., 2012). Water transfer among bamboo culms may thus be a mechanism to secure the whole clump against potential drought conditions.

## 7.3  Stem water storage in bamboos and trees

Unlike the relatively small stems of bamboos, stem-succulent trees have quite big stems. In this study, we found a relatively longer $T_{residence}$ (21.7 days) of a deciduous stem-succulent tree species (*Ceiba trichistandra*) in contrast to two evergreen species (averaged 12.8 days) at the same sites in a tropical dry forest in Ecuador (Chapter 6). When synthesizing our observations of $T_{residence}$ of the bamboos and the trees with 11 previous studies on 25 species (Table 1), we found that the $T_{residence}$ was longer in larger-size and lower-wood-density species (Fig. 7.2 a & b). Among these species, two coniferous species (*Tsuga heterophylla* and *Pseudotsuga menziesii*) in North America have the longest $T_{residence}$ (59 and 50 days, respectively), and *T. heterophylla* has the highest height (53 m) among all the plotted species (Meinzer et al., 2006). Apart of these two conifers, the stem-succulent *C. trichistandra* from our study is near to the longest observed water residence time whereas the bamboos are near to the shortest observed water residence times. Across species, water residence

time increased with increasing diameter and decreased with increasing wood density (Fig. 7.2 a & b).

## 7.4 Outlook for the water circulation of bamboos and trees

Thus far, in many studies the estimation on the daily contribution of stem water storage to transpiration by TDP was based on the assumption that the depletion and refilling of stem water storage were achieved each day. However, observations from deuterium tracing point to several days of water residence time inside bamboo culms. Future work is needed to explore stem water storage mechanisms based on considerations of potentially incomplete diurnal refilling. For bamboos, water transfer could be explained by the hypothesis of the source-sink theory (Marshall, 1996) stating that water potential differences and carbohydrate transport via phloem among interconnected culms are coupled. Such assumptions will have to be verified further in future studies. Moreover, water transfer via rhizomes may be not constrained to freshly sprouted culms and the nearest directly connected established culm; it may also exist among established culms, with the distance among culms being a potentially limiting factor. Exploring the mechanisms behind water transfer in and among bamboo culms will further deepen our understanding of the mechanisms behind the extraordinary growth rates of many bamboos. For large and soft-wooded trees, stem water storage may be critical for their daily or long-term water use and other eco-physiological processes. For these species, water storage could be further explored with multiple methodologies, e.g., deuterium tracing, sap flow methods and the recently-attempted frequency domain reflectometry technique.

Table 7.1 Overview and key findings of studies applying deuterium tracing.

| Species | Location | N | DBH (cm) | Height (m) | $T_{-arrival}$ (days) | $T_{-residence}$ (days) | $V_{-D_2O}$ (m day$^{-1}$) | Reference |
|---|---|---|---|---|---|---|---|---|
| *B. vulgaris* | Indonesia | 4 | 7.0 (0.4) | 17.9 (0.8) | 1.5 (1.0) | 5.5 (1.3) | 12.5 (4.8) | This study |
| *G. apus* | Indonesia | 4 | 7.9 (1.1) | 16.2 (2.7) | 1.0 (0.0) | 6.3 (0.6) | 13.3 (0.6) | This study |
| *D. asper* | Indonesia | 4 | 10.7 (0.9) | 21.1 (0.9) | 1.0 (0.0) | 5.0 (1.7) | 16.1 (3.8) | This study |
| *Capparis scabrida* | Ecuador | 4 | 19.7 (5.4) | 7.4 (1.5) | 1.3 (0.5) | 14.3 (4.2) | 6.3 (1.6) | This study |
| *Geoffroea spinosa* | Ecuador | 4 | 28.2 (4.9) | 7.9 (0.6) | 1.8 (1.0) | 10.8 (6.3) | 5.6 (2.7) | This study |
| *Erythrina velutina* | Ecuador | 9 | 27.9 (9.3) | 10.1 (3.6) | 1.0 (0) | 19.2 (3.9) | 10.1 (3.6) | This study |
| *Eriotheca ruizii* | Ecuador | 10 | 56.4 (17.3) | 13.1 (3.3) | 1.0 (0) | 18.8 (2.4) | 13.1 (3.3) | This study |
| *Ceiba trichistandra* | Ecuador | 11 | 77.9 (13.7) | 15.5 (4.6) | 1.0 (0) | 19.5 (3.9) | 15.5 (4.6) | This study |
| *Eucalyptus teretecornis* | Southern India | 2 | 4.9 (0.0) | 7.0 (0.0) | 1.0 (0.0) | 6.0 (0.0) | 7.0 (0.0) | Calder et al. 1986 |
| *Eucalyptus teretecornis* | Southern India | 2 | 4.0 (1.0) | | 1.5 (0.7) | 6.0 (1.4) | | Calder et al. 1992 |
| *Eucalyptus gunnii* | UK | 1 | 5.0 (.) | 2.5 (.) | 1.0 (.) | 5.0 (.) | 2.5 (.) | Dugas et al. 1993 |
| *Prunus serrulata* | UK | 3 | 2.0 (0.0) | 2.0 (0.0) | 1.3 (0.6) | 3.3 (0.6) | 1.7 (0.6) | Dugas et al. 1993 |
| *Eucalyptus grandis* | South Africa | 2 | 14.5 (4.9) | 15.7 (10.6) | 0.8 (0.4) | 7.5 (6.2) | 19.8 (4.8) | Dye et al. 1992 |
| *Acer saccharum* | USA | 2 | 25.5 (10.6) | 14.6 (3.0) | 4.1 (2.8) | 13.3 (4.9) | 1.5 (0.3) | Gaines et al. 2016 |
| *Carya tomentosa* | USA | 3 | 33.0 (11.1) | 19.9 (0.3) | 2.3 (2.2) | 11.0 (1.5) | 8.6 (8.2) | Gaines et al. 2016 |
| *Quercus prinus* | USA | 3 | 36.7 (10.6) | 18.3 (1.4) | 3.3 (2.1) | 10.9 (9.3) | 4.9 (2.7) | Gaines et al. 2016 |
| *Quercus rubra* | USA | 3 | 40.7 (10.1) | 17.0 (2.6) | 3.5 (3.0) | 17.4 (5.0) | 6.1 (3.4) | Gaines et al. 2016 |
| *Anacardium excelsum* | Panama | 1 | 98.0 (.) | 38.0 (.) | 3.0 (.) | 25.0 (.) | 12.7 (.)(.) | James et al. 2003 |
| *Cordia alliodora* | Panama | 1 | 34.0 (.) | 26.0 (.) | 1.0 (.) | 5.0 (.) | 26.0 (.) | James et al. 2003 |
| *Ficus insipida* | Panama | 1 | 65.0 (.) | 28.0 (.) | 2.0 (.) | 9.0 (.) | 14.0 (.) | James et al. 2003 |
| *Schefflera morototoni* | Panama | 1 | 47.0 (.) | 22.0 (.) | 5.0 (.) | 26.0 (.) | 4.4 (.) | James et al. 2003 |
| *Eucalyptus grandis* | Australia | 3 | 10.7 (3.5) | 10.1 (4.8) | 1.7 (0.6) | 11.3 (4.0) | 5.8 (1.1) | Kalma et al. 1998 |
| *Ceriops tagal* | Mayotte Island | 3 | 7.5 (0.9) | 2.9 (0.3) | 2.4 (0.3) | 10.4 (1.2) | 1.2 (0.2) | Lambs et al. 2011 |
| *Rhizophora mucronata* | Mayotte Island | 2 | 17.5 (6.4) | 6.3 (1.8) | 3.3 (0.1) | 14.6 (3.0) | 1.7 (0.5) | Lambs et al. 2011 |
| *Fagus sylvatica* | France | 3 | 10.9 (4.1) | 6.5 (1.0) | 4.0 (0.0) | 14.0 (1.0) | 1.6 (0.3) | Marc and Robinson 2004 |
| *Pseudotsuga menziesii* | USA | 6 | 53.7 (56.2) | 27.7 (22.0) | 6.3 (5.1) | 50.0 (19.2) | 4.6 (0.8) | Meinzer et al. 2006 |
| *Tsuga heterophylla* | USA | 2 | 91.0 (2.8) | 53.0 (4.2) | 19.0 (2.8) | 59.0 (2.8) | 2.8 (0.6) | Meinzer et al. 2006 |
| *Bambusa blumeana* | Philippines | 4 | 10.0 (1.0) | 19.8 (0.7) | 3.1 (1.4) | 11.5 (4.3) | 8.5 (6.4) | Schwendenmann et al. 2010 |
| *Gliricidia sepium* | Indonesia | 6 | 13.0 (2.0) | 10.6 (3.3) | 1.7 (0.8) | 6.4 (0.8) | 6.3 (2.6) | Schwendenmann et al. 2010 |
| *Shorea contorta* | Philippines | 5 | 18.0 (7.0) | 16.1 (3.5) | 0.9 (0.0) | 4.5 (0.3) | 18.1 (4.0) | Schwendenmann et al. 2010 |
| *Shorea polysperma* | Philippines | 5 | 14.0 (2.0) | 13.3 (1.7) | 0.9 (0.0) | 3.8 (0.6) | 14.9 (2.0) | Schwendenmann et al. 2010 |
| *Swietenia macrophylla* | Philippines | 5 | 15.0 (1.0) | 14.2 (1.5) | 0.9 (0.0) | 3.9 (0.3) | 15.9 (1.7) | Schwendenmann et al. 2010 |
| *Theobroma cacao* | Indonesia | 6 | 10.0 (1.0) | 4.2 (0.6) | 1.7 (0.5) | 5.1 (0.9) | 2.5 (0.6) | Schwendenmann et al. 2010 |

# Bibliography

Adonsou, K. E., DesRochers, A., and Tremblay, F. (2016). Physiological integration of connected balsam poplar ramets. *Tree Physiology*, 36(7):797–806.

Alpert, P. and Mooney, H. A. (1986). Resource sharing among ramets in the clonal herb, fragaria chiloensis. *Oecologia*, 70(2):227.

Baker, J. and Bavel, C. v. (1987). Measurement of mass flow of water in the stems of herbaceous plants. *Plant, Cell & Environment*, 10(9):777–782.

Balakrishnan (1992). *Handbook of the logistic distribution /.* Dekker,.

Baret, M. and DesRochers, A. (2011). Root connections can trigger physiological responses to defoliation in nondefoliated aspen suckers. *Botany-botanique*, 89(89):753–761.

Bastin, J. F., Berrahmouni, N., Grainger, A., Maniatis, D., Mollicone, D., Moore, R., Patriarca, C., Picard, N., Sparrow, B., and Abraham, E. M. (2017). The extent of forest in dryland biomes. *Science*, 356(6338):635.

Baum, D. (1996). The ecology and conservation of the baobabs of madagascar. *Primate Report*, 46(1):311–327.

Borchert, R. (1994). Soil and stem water storage determine phenology and distribution of tropical dry forest trees. *Ecology*, 75(5):1437–1449.

Bovard, B., Curtis, P., Vogel, C., Su, H.-B., and Schmid, H. (2005). Environmental controls on sap flow in a northern hardwood forest. *Tree Physiology*, 25(1):31–38.

Burgess, S. S., Adams, M. A., Turner, N. C., Beverly, C. R., Ong, C. K., Khan, A. A., and Bleby, T. M. (2001a). An improved heat pulse method to measure low and reverse rates of sap flow in woody plants. *Tree Physiology*, 21(9):589–598.

Burgess, S. S., Adams, M. A., Turner, N. C., White, D. A., and Ong, C. K. (2001b). Tree roots: conduits for deep recharge of soil water. *Oecologia*, 126(2):158–165.

Bush, S. E., Hultine, K. R., Sperry, J. S., and Ehleringer, J. R. (2010). Calibration of thermal dissipation sap flow probes for ring-and diffuse-porous trees. *Tree Physiology*, 30(12):1545–1554.

Butz, P., Raffelsbauer, V., Graefe, S., Peters, T., Cueva, E., Hölscher, D., and Bräuning, A. (2016). Tree responses to moisture fluctuations in a neotropical dry forest as potential climate change indicators. *Ecological Indicators*.

Calder, I., Narayanswamy, M., Srinivasalu, N., Darling, W., and Lardner, A. (1986). Investigation into the use of deuterium as a tracer for measuring transpiration from eucalypts. *Journal of Hydrology*, 84(3-4):345–351.

Calder, I. R. (1991). Implications and assumptions in using the 'total counts' and convection-dispersion equations for tracer flow measurements-with particular reference to transpiration measurements in trees. *Journal of Hydrology*, 125(1):149–158.

Calder, I. R., Kariyappa, G., Srinivasalu, N., and Murty, K. S. (1992). Deuterium tracing for the estimation of transpiration from trees part 1. field calibration. *Journal of Hydrology*, 130(1-4):17–25.

Cao, K.-F., Yang, S.-J., Zhang, Y.-J., and Brodribb, T. J. (2012). The maximum height of grasses is determined by roots. *Ecology Letters*, 15(7):666–672.

Caraco, T. and Kelly, C. K. (1991). On the adaptive value of physiological integraton in colonal plants. *Ecology*, 72(1):81–93.

Carrasco, L. O., Bucci, S. J., Di Francescantonio, D., Lezcano, O. A., Campanello, P. I., Scholz, F. G., Rodríguez, S., Madanes, N., Cristiano, P. M., Hao, G.-Y., et al. (2015). Water storage dynamics in the main stem of subtropical tree species differing in wood density, growth rate and life history traits. *Tree Physiology*, 35(4):354–365.

Carslaw, H. S. and Jaeger, J. C. (1959). *Conduction of heat in solids*. Oxford: Clarendon Press.

Čermák, J., Kučera, J., Bauerle, W. L., Phillips, N., and Hinckley, T. M. (2007a). Tree water storage and its diurnal dynamics related to sap flow and changes in stem volume in old-growth douglas-fir trees. *Tree Physiology*, 27(2):181–198.

Čermák, J., Kucera, J., Bauerle, W. L., Phillips, N., and Hinckley, T. M. (2007b). Tree water storage and its diurnal dynamics related to sap flow and changes in stem volume in old-growth douglas-fir trees. *Tree Physiology*, 27(2):181.

Chapman, D. F., Robson, M. J., and Snaydon, R. W. (1992). Physiological integration in the clonal perennial herb trifolium repens l. *Oecologia*, 89(3):338–347.

Chapotin, S. M., Razanameharizaka, J. H., and Holbrook, N. M. (2006a). Baobab trees (adansonia) in madagascar use stored water to flush new leaves but not to support stomatal opening before the rainy season. *New Phytologist*, 169(3):549–559.

Chapotin, S. M., Razanameharizaka, J. H., and Holbrook, N. M. (2006b). Water relations of baobab trees (adansonia spp. l.) during the rainy season: does stem water buffer daily water deficits? *Plant, Cell & Environment*, 29(6):1021–1032.

Chen, X., Zhang, X., Zhang, Y., Booth, T., and He, X. (2009). Changes of carbon stocks in bamboo stands in china during 100 years. *Forest Ecology and Management*, 258(7):1489–1496.

Choi, I. C. and Aronoff, S. (1966). Photosynthate transport using tritiated water. *Plant Physiology*, 41(7):1119–1129.

Clearwater, M. J., Meinzer, F. C., Andrade, J. L., Goldstein, G., and Holbrook, N. M. (1999). Potential errors in measurement of nonuniform sap flow using heat dissipation probes. *Tree Physiology*, 19(10):681–687.

Cochard, H., Ewers, F., and Tyree, M. (1994). Water relations of a tropical vine-like bamboo (*Rhipidocladum racemiflorum*): root pressures, vulnerability to cavitation and seasonal changes in embolism. *Journal of Experimental Botany*, 45(8):1085–1089.

Constantz, J. and Murphy, F. (1990). Monitoring moisture storage in trees using time domain reflectometry. *Journal of Hydrology*, 119(1):31–42.

Coplen, T. B. (1995). Reporting of stable hydrogen, carbon, and oxygen isotopic abundances (technical report). *Pure & Applied Chemistry*, 24(5–6):707–712.

de Agrasar, Z. R. and Rodríguez, M. F. (2003). Culm anatomy of native woody bamboos in argentina and neighboring areas: cross section. *Bamboo Science and Culture: Journal of the American Bamboo Society*, 17:28–43.

Dierick, D. and Hölscher, D. (2009). Species-specific tree water use characteristics in reforestation stands in the philippines. *Agricultural and Forest Meteorology*, 149(8):1317–1326.

Dierick, D., Hölscher, D., and Schwendenmann, L. (2010). Water use characteristics of a bamboo species (*Bambusa blumeana*) in the philippines. *Agricultural and Forest Meteorology*, 150(12):1568–1578.

Do, F. and Rocheteau, A. (2002). Influence of natural temperature gradients on measurements of xylem sap flow with thermal dissipation probes. 1. field observations and possible remedies. *Tree Physiology*, 22(9):641–648.

Dransfield, S. and Widjaja, E. (1995). Bamboos-plant resources of southeast asia, no. 7. *Prosea. Bogor, Indonesia*.

Dunisch, O. and Morais, R. R. (2002). Regulation of xylem sap flow in an evergreen, a semi-deciduous, and a deciduous meliaceae species from the amazon. *Trees*, 16(6):404–416.

Dye, P. and Olbrich, B. (1993). Estimating transpiration from 6-year-old *Eucalyptus grandis* trees: development of a canopy conductance model and comparison with independent sap flux measurements. *Plant, Cell & Environment*, 16(1):45–53.

Dye, P., Olbrich, B., and Calder, I. (1992). A comparison of the heat pulse method and deuterium tracing method for measuring transpiration from *Eucalyptus grandis* trees. *Journal of Experimental Botany*, 43(3):337–343.

Eamus, D. (1999). Ecophysiological traits of deciduous and evergreen woody species in the seasonally dry tropics. *Trends in Ecology & Evolution*, 14(1):11.

Edwards, W. and Warwick, N. (1984). Transpiration from a kiwifruit vine as estimated by the heat pulse technique and the penman-monteith equation. *New Zealand Journal of Agricultural Research*, 27(4):537–543.

Eller, C. B., Lima, A. L., and Oliveira, R. S. (2013). Foliar uptake of fog water and transport belowground alleviates drought effects in the cloud forest tree species, drimys brasiliensis (winteraceae). *New Phytologist*, 199(1):151–162.

FAO (2010). Global forest resources assessment 2010: main report, fao forestry paper, 0258-6150; 163.

Forster, M. A. (2014). How significant is nocturnal sap flow? *Tree Physiology*, 34(7):757–765.

Fraser, E. C., Lieffers, V. J., and Landhäusser, S. M. (2006). Carbohydrate transfer through root grafts to support shaded trees. *Tree Physiology*, 26(8):1019.

Gaines, K. P., Meinzer, F. C., Duffy, C. J., Thomas, E. M., and Eissenstat, D. M. (2016). Rapid tree water transport and residence times in a pennsylvania catchment. *Ecohydrology*, 9(8):1554–1565.

Gleason, S. M., Westoby, M., Jansen, S., Choat, B., Hacke, U. G., Pratt, R. B., Bhaskar, R., Brodribb, T. J., Bucci, S. J., Cao, K.-F., et al. (2016). Weak tradeoff between xylem safety and xylem-specific hydraulic efficiency across the world's woody plant species. *New Phytologist*, 209(1):123–136.

Goldsmith, G. R. (2013). Changing directions: the atmosphere–plant–soil continuum. *New Phytologist*, 199(1):4–6.

Goldsmith, G. R., Matzke, N. J., and Dawson, T. E. (2013). The incidence and implications of clouds for cloud forest plant water relations. *Ecology Letters*, 16(3):307–314.

Goldstein, G., Andrade, J., Meinzer, F., Holbrook, N., Cavelier, J., Jackson, P., and Celis, A. (1998). Stem water storage and diurnal patterns of water use in tropical forest canopy trees. *Plant, Cell & Environment*, 21(4):397–406.

Granier, A. (1985). Une nouvelle méthode pour la mesure du flux de sève brute dans le tronc des arbres. *Annales des Sciences forestières*, 42(2):193–200.

Granier, A. (1987). Evaluation of transpiration in a douglas-fir stand by means of sap flow measurements. *Tree Physiology*, 3(4):309–320.

Grime, V. and Sinclair, F. (1999). Sources of error in stem heat balance sap flow measurements. *Agricultural and Forest Meteorology*, 94(2):103–121.

Grosser, D. and Liese, W. (1971). On the anatomy of asian bamboos, with special reference to their vascular bundles. *Wood Science and technology*, 5(4):290–312.

Hacke, U., Sperry, J., Pockman, W., Davis, S., and McCulloh, K. (2001). Trends in wood density and structure are linked to prevention of xylem implosion by negative pressure. *Oecologia*, 126(4):457.

Hao, G.-Y., Wheeler, J. K., Holbrook, N. M., and Goldstein, G. (2013). Investigating xylem embolism formation, refilling and water storage in tree trunks using frequency domain reflectometry. *Journal of Experimental Botany*, 64(8):2321–2332.

Hartung, W., Sauter, A., and Hose, E. (2002). Abscisic acid in the xylem: where does it come from, where does it go to? *Journal of Experimental Botany*, 53(366):27–32.

Hernández-Santana, V., David, T., and Martínez-Fernández, J. (2008). Environmental and plant-based controls of water use in a mediterranean oak stand. *Forest Ecology and Management*, 255(11):3707–3715.

Holbrook, N. M., Burns, M., and Sinclair, T. (1992). Frequency and time-domain dielectric measurements of stem water content in the arborescent palm, sabal palmetto. *Journal of Experimental Botany*, 43(1):111–119.

Holbrook, N. M. and Sinclair, T. R. (1992). Water balance in the arborescent palm, sabal palmetto. ii. transpiration and stem water storage. *Plant, Cell & Environment*, 15(4):401–409.

Hölttä, T., Linkosalo, T., Riikonen, A., Sevanto, S., and Nikinmaa, E. (2015). An analysis of granier sap flow method, its sensitivity to heat storage and a new approach to improve its time dynamics. *Agricultural and Forest Meteorology*, 211-212:2–12.

Horna, V., Schuldt, B., Brix, S., and Leuschner, C. (2011). Environment and tree size controlling stem sap flux in a perhumid tropical forest of central sulawesi, indonesia. *Annals of forest science*, 68(5):1027–1038.

Hutchings, Michael, J., Wijesinghe, and Dushyantha, K. (1997). Patchy habitats, division of labour and growth dividends in clonal plants. *Trends in Ecology & Evolution*, 12(10):390.

Ichihashi, R., Komatsu, H., Kume, T., Onozawa, Y., Shinohara, Y., Tsuruta, K., and Otsuki, K. (2015). Stand-scale transpiration of two moso bamboo stands with different culm densities. *Ecohydrology*, 8(3):450–459.

Inagaki, T., Ahmed, B., Hartley, I. D., Tsuchikawa, S., and Reid, M. (2014). Simultaneous prediction of density and moisture content of wood by terahertz time domain spectroscopy. *Journal of Infrared, Millimeter, and Terahertz Waves*, 35(11):949–961.

INBAR (2014). International trade in bamboo and rattan 2012. beijing: International network for bamboo and rattan.

James, S. A., Meinzer, F. C., Goldstein, G., Woodruff, D., Jones, T., Restom, T., Mejia, M., Clearwater, M., and Campanello, P. (2003). Axial and radial water transport and internal water storage in tropical forest canopy trees. *Oecologia*, 134(1):37–45.

Jarvis, N. (1989). A simple empirical model of root water uptake. *Journal of Hydrology*, 107(1-4):57–72.

Johnson, D., McCulloh, K., Meinzer, F., Woodruff, D., and Eissenstat, D. (2011). Hydraulic patterns and safety margins, from stem to stomata, in three eastern us tree species. *Tree Physiology*, 31(6):659–668.

Jung, E., Otieno, D., Lee, B., Lim, J., Kang, S., Schmidt, M., and Tenhunen, J. (2011). Up-scaling to stand transpiration of an asian temperate mixed-deciduous forest from single tree sapflow measurements. *Plant Ecology*, 212(3):383–395.

Kalma, S. J., Thorburn, P. J., and Dunn, G. M. (1998). A comparison of heat pulse and deuterium tracing techniques for estimating sap flow in *Eucalyptus grandis* trees. *Tree Physiology*, 18(10):697–705.

Kline, J., Martin, J., Jordan, C., and Koranda, J. (1970). Measurement of transpiration in tropical trees with tritiated water. *Ecology*, 51(6):1068–1073.

Köcher, P., Horna, V., and Leuschner, C. (2013). Stem water storage in five coexisting temperate broad-leaved tree species: significance, temporal dynamics and dependence on tree functional traits. *Tree Physiology*, 33(8):817–832.

Köhler, M., Dierick, D., Schwendenmann, L., and Hölscher, D. (2009). Water use characteristics of cacao and gliricidia trees in an agroforest in central sulawesi, indonesia. *Ecohydrology*, 2(4):520–529.

Köhler, M., Schwendenmann, L., and Hölscher, D. (2010). Throughfall reduction in a cacao agroforest: tree water use and soil water budgeting. *Agricultural and Forest Meteorology*, 150(7):1079–1089.

Kollman, F. F. and Côté, W. (1968). Principles of wood science and technology, vol i.

Komatsu, H., Onozawa, Y., Kume, T., Tsuruta, K., Kumagai, T., Shinohara, Y., and Otsuki, K. (2010). Stand-scale transpiration estimates in a moso bamboo forest: Ii. comparison with coniferous forests. *Forest Ecology and Managemen*, 260(8):1295–1302.

Kroon, H. D., Fransen, B., Rheenen, J. W. A. V., Dijk, A. V., and Kreulen, R. (1996). High levels of inter-ramet water translocation in two rhizomatous carex species, as quantified by deuterium labelling. *Oecologia*, 106(1):73.

Kubota, M., Tenhunen, J., Zimmermann, R., Schmidt, M., Adiku, S., and Kakubari, Y. (2005). Influences of environmental factors on the radial profile of sap flux density in fagus crenata growing at different elevations in the naeba mountains, japan. *Tree Physiology*, 25(5):545–556.

Kume, T., Onozawa, Y., Komatsu, H., Tsuruta, K., Shinohara, Y., Umebayashi, T., and Otsuki, K. (2010). Stand-scale transpiration estimates in a moso bamboo forest: (i) applicability of sap flux measurements. *Forest Ecology and Management*, 260(8):1287–1294.

Kume, T., Takizawa, H., Yoshifuji, N., Tanaka, K., Tantasirin, C., Tanaka, N., and Suzuki, M. (2007). Impact of soil drought on sap flow and water status of evergreen trees in a tropical monsoon forest in northern thailand. *Forest Ecology and Management*, 238(1):220–230.

Lau, R. R. and Young, D. R. (1988). Influence of physiological integration on survivorship and water relations in a clonal herb. *Ecology*, 69(1):215–219.

Li, R., Werger, M. J. A., During, H. J., and Zhong, Z. C. (1998a). Biennial variation in production of new shoots in groves of the giant bamboo phyllostachys pubescens in sichuan, china. *Plant Ecology*, 135(1):103–112.

Li, R., Werger, M. J. A., During, H. J., and Zhong, Z. C. (1998b). Carbon and nutrient dynamics in relation to growth rhythm in the giant bamboo phyllostachys pubescens. *Plant & Soil*, 201(1):113–123.

Liese, W. (1985). Anatomy and properties of bamboo. *Proceedings of the International Bamboo Workshop*, pages 196–208.

Liese, W. and Köhl, M. (2015). *Bamboo: the plant and its uses*, volume 10. Springer.

Liese, W. and Weiner, G. (1996). Ageing of bamboo culms. a review. *Wood Science and Technology*, 30(2):77–89.

Lin, J., He, X., Hu, Y., Kuang, T., and Ceulemans, R. (2002). Lignification and lignin heterogeneity for various age classes of bamboo (*Phyllostachys pubescens*) stems. *Physiologia Plantarum*, 114(2):296–302.

Lu, P., Urban, L., and Zhao, P. (2004). Granier's thermal dissipation probe (tdp) method for measuring sap flow in trees: theory and practice. *Acta Botanica Sinica-English Edition-*, 46(6):631–646.

Marc, V. and Robinson, M. (2004). Application of the deuterium tracing method for the estimation of tree sap flow and stand transpiration of a beech forest (*Fagus silvatica L.*) in a mountainous mediterranean region. *Journal of Hydrology*, 285(1):248–259.

Marshall, C. (1996). Sectoriality and physiological organisation in herbaceous plants: an overview. *Vegetatio*, 127(1):9–16.

Mei, T.-T., Fang, D.-M., Röll, A., Niu, F.-R., Hendrayanto, and Hölscher, D. (2016). Water use patterns of four tropical bamboo species assessed with sap flux measurements. *Frontiers in plant science*, 6:1202.

Meinzer, F. (2002). Co-ordination of vapour and liquid phase water transport properties in plants. *Plant, Cell & Environment*, 25(2):265–274.

Meinzer, F., Brooks, J., Domec, J.-C., Gartner, B., Warren, J., Woodruff, D., Bible, K., and Shaw, D. (2006). Dynamics of water transport and storage in conifers studied with deuterium and heat tracing techniques. *Plant, Cell & Environment*, 29(1):105–114.

Meinzer, F., Goldstein, G., and Andrade, J. (2001). Regulation of water flux through tropical forest canopy trees: do universal rules apply? *Tree Physiology*, 21(1):19–26.

Meinzer, F. C., James, S. A., and Goldstein, G. (2004). Dynamics of transpiration, sap flow and use of stored water in tropical forest canopy trees. *Tree Physiology*, 24(8):901.

Meinzer, F. C., Mcculloh, K. A., Lachenbruch, B., Woodruff, D. R., and Johnson, D. M. (2010). The blind men and the elephant: the impact of context and scale in evaluating conflicts between plant hydraulic safety and efficiency. *Oecologia*, 164(2):287–296.

Miles, L., Newton, A. C., Defries, R. S., Ravilious, C., May, I., Blyth, S., Kapos, V., and Gordon, J. E. (2006). A global overview of the conservation status of tropical dry forests. *Journal of Biogeography*, 33(3):491–505.

Mohmod, A. L. and Mustafa, M. T. (1992). Variation in anatomical properties of three malaysian bamboos from natural stands. *Journal of Tropical Forest Science*, 5(1):90–96.

Münch, E. (1927). Versuche über den saftkreislauf. *Berichte der Deutschen Botanischen Gesellschaft*, 45(6):340–356.

Nadler, A., Raveh, E., Yermiyahu, U., Lado, M., Nasser, A., Barak, M., and Green, S. (2008). Detecting water stress in trees using stem electrical conductivity measurements. *Soil Science Society of America Journal*, 72(4):1014–1024.

Nilsen, E. T., Sharifi, M. R., Rundel, P. W., Forseth, I. N., and Ehleringer, J. R. (1990). Water relations of stem succulent trees in north-central baja california. *Oecologia*, 82(3):299–303.

Niu, F., Röll, A., Hardanto, A., Meijide, A., Köhler, M., Hölscher, D., et al. (2015). Oil palm water use: calibration of a sap flux method and a field measurement scheme. *Tree Physiology*, 35(5):563–573.

O'Brien, J. J., Oberbauer, S. F., and Clark, D. B. (2004). Whole tree xylem sap flow responses to multiple environmental variables in a wet tropical forest. *Plant, Cell & Environment*, 27(5):551–567.

Parnell, A. C., Inger, R., Bearhop, S., and Jackson, A. L. (2010). Source partitioning using stable isotopes: coping with too much variation. *Plos One*, 5(3):e9672.

Pereira, H. and Hosegood, P. (1962). Comparative water-use of softwood plantations and bamboo forest. *Journal of Soil Science*, 13:299–313.

Peters, E. B., McFadden, J. P., and Montgomery, R. A. (2010). Biological and environmental controls on tree transpiration in a suburban landscape. *Journal of Geophysical Research: Biogeosciences*, 115(G4):2156–2202.

Petit, G., DeClerck, F. A., Carrer, M., and Anfodillo, T. (2014). Axial vessel widening in arborescent monocots. *Tree Physiology*, 34(2):137–145.

Pfautsch, S., Höltta, T., and Mencuccini, M. (2015a). Hydraulic functioning of tree stems-fusing ray anatomy, radial transfer and capacitance. *Tree Physiology*, 35(7):706–722.

Pfautsch, S., Renard, J., Tjoelker, M. G., and Salih, A. (2015b). Phloem as capacitor: radial transfer of water into xylem of tree stems occurs via symplastic transport in ray parenchyma. *Plant Physiology*, 167(3):963–971.

Philip, J. R. (1966). Plant water relations: some physical aspects. *Annual Review of Plant Physiology*, 17(1):245–268.

Phillips, N. G., Ryan, M. G., Bond, B. J., Mcdowell, N. G., Hinckley, T. M., and Čermák, J. (2003). Reliance on stored water increases with tree size in three species in the pacific northwest. 23(4):237–245.

Phillips, N. G., Scholz, F. G., Bucci, S. J., Goldstein, G., and Meinzer, F. C. (2009). Using branch and basal trunk sap flow measurements to estimate whole-plant water capacitance: comment on burgess and dawson (2008). *Plant & Soil*, 315(1–2):315–324.

Powers, J. S. and Tiffin, P. (2010). Plant functional type classifications in tropical dry forests in costa rica: leaf habit versus taxonomic approaches. *Functional Ecology*, 24(4):927–936.

Regalado, C. M. and Ritter, A. (2007). An alternative method to estimate zero flow temperature differences for granier's thermal dissipation technique. *Tree Physiology*, 27(8):1093–1102.

Renninger, H. J. and Phillips, N. (2010). Intrinsic and extrinsic hydraulic factors in varying sizes of two amazonian palm species (iriartea deltoidea and mauritia flexuosa) differing in development and growing environment. *American journal of botany*, 97(12):1926–1936.

Roden, J. S. and Ehleringer, J. R. (1999). Observations of hydrogen and oxygen isotopes in leaf water confirm the craig-gordon model under wide-ranging environmental conditions. *Plant Physiology*, 120(4):1165–1174.

Roderick, M. L. and Berry, S. L. (2001). Linking wood density with tree growth and environment: a theoretical analysis based on the motion of water. *New Phytologist*, 149(3):473–485.

Röll, A., Niu, F., Meijide, A., Hardanto, A., Knohl, A., Hölscher, D., et al. (2015). Transpiration in an oil palm landscape: effects of palm age. *Biogeosciences*, 12(19):5619–5633.

Saha, S., Holbrook, N. M., Montti, L., Goldstein, G., and Cardinot, G. K. (2009). Water relations of chusquea ramosissima and merostachys claussenii in iguazu national park, argentina. *Plant Physiology*, 149(4):1992–1999.

Sakuratani, T. (1981). A heat balance method for measuring water flux in the stem of intact plants. *Journal of Agricultural Meteorology*, 37(1):9–17.

Sakuratani, T., Aoe, T., and Higuchi, H. (1999). Reverse flow in roots of sesbania rostrata measured using the constant power heat balance method. *Plant, Cell & Environment*, 22(9):1153–1160.

Savage, J. A., Clearwater, M. J., Haines, D. F., Klein, T., Mencuccini, M., Sevanto, S., Turgeon, R., and Zhang, C. (2016). Allocation, stress tolerance and carbon transport in plants: how does phloem physiology affect plant ecology? *Plant Cell & Environment*, 39(4):709.

Scholz, F. C., Bucci, S. J., Goldstein, G., Meinzer, F. C., Franco, A. C., and Miralles-Wilhelm, F. (2008). Temporal dynamics of stem expansion and contraction in savanna trees: withdrawal and recharge of stored water. *Tree Physiology*, 28(3):469–480.

Schwendenmann, L., Dierick, D., Köhler, M., and Hölscher, D. (2010). Can deuterium tracing be used for reliably estimating water use of tropical trees and bamboo? *Tree Physiology*, 30(7):886–900.

Schwinning, S. and Ehleringer, J. R. (2001). Water use trade-offs and optimal adaptations to pulse-driven arid ecosystems. *Journal of Ecology*, 89(3):464–480.

Smith, D. and Allen, S. (1996). Measurement of sap flow in plant stems. *Journal of Experimental Botany*, 47(12):1833–1844.

Smith, D., Jackson, N., Roberts, J., and Ong, C. (1999). Reverse flow of sap in tree roots and downward siphoning of water by *Grevillea robusta*. *Functional Ecology*, 13(2):256–264.

Song, X., Peng, C., Zhou, G., Gu, H., Li, Q., and Zhang, C. (2016). Dynamic allocation and transfer of non-structural carbohydrates, a possible mechanism for the explosive growth of moso bamboo (*Phyllostachys heterocycla*). *Scientific reports*, 6.

Spannl, S., Volland, F., Pucha, D., Peters, T., Cueva, E., and Bräuning, A. (2016). Climate variability, tree increment patterns and enso-related carbon sequestration reduction of the tropical dry forest species loxopterygium huasango of southern ecuador. *Trees*, 30(4):1–14.

Sperling, O., Shapira, O., Schwartz, A., and Lazarovitch, N. (2015). Direct in vivo evidence of immense stem water exploitation in irrigated date palms. *Journal of Experimental Botany*, 66(1):333–338.

Stapleton, C. (1998). Form and function in the bamboo rhizome. *Journal of American Bamboo Society*, 12(1):21–29.

Steppe, K., De Pauw, D. J., Doody, T. M., and Teskey, R. O. (2010). A comparison of sap flux density using thermal dissipation, heat pulse velocity and heat field deformation methods. *Agricultural and Forest Meteorology*, 150(7):1046–1056.

Stratton, L., Goldstein, G., and Meinzer, F. C. (2000). Stem water storage capacity and efficiency of water transport: their functional significance in a hawaiian dry forest. *Plant Cell & Environment*, 23(1):99–106.

Studer, M., Siegwolf, R., Leuenberger, M., and Abiven, S. (2015). Multi-isotope labelling of organic matter by diffusion of $^2$h/$^{18}$o-h$_2$o vapour and $^{13}$c-co$_2$ into the leaves and its distribution within the plant. *Biogeosciences*, 12(6):1865–1879.

Stuefer, J. F., Hde, K., and During, H. J. (1996). Exploitation of environmental heterogeneity by spatial division of labour in a clonal plant. *Functional Ecology*, 10(3):328–334.

Tang, J., Bolstad, P. V., Ewers, B. E., Desai, A. R., Davis, K. J., and Carey, E. V. (2006). Sap flux–upscaled canopy transpiration, stomatal conductance, and water use efficiency in an old growth forest in the great lakes region of the united states. *Journal of Geophysical Research: Biogeosciences*, 111(G2).

Tatarinov, F. A., Kučera, J., and Cienciala, E. (2005). The analysis of physical background of tree sap flow measurement based on thermal methods. *Measurement Science and Technology*, 16(5):1157.

Thompson, M. V. and Holbrook, N. M. (2003). Scaling phloem transport: water potential equilibrium and osmoregulatory flow. *Plant Cell & Environment*, 26(9):1561–1577.

Trcala, M. and Čermák, J. (2016). A new heat balance equation for sap flow calculation during continuous linear heating in tree sapwood. *Applied Thermal Engineering*, 102:532–538.

Tyree, M. T. and Sperry, J. S. (1988). Do woody plants operate near the point of catastrophic xylem dysfunction caused by dynamic water stress? answers from a model. *Plant Physiology*, 88(3):574–580.

Tyree, M. T. and Yang, S. (1990). Water-storage capacity of thuja, tsuga and acer stems measured by dehydration isotherms. *Planta*, 182(3):420–6.

Uchimura, E. (1994). Invitation to bamboos: Wonder of biology. *Tokyo, Kenseisha*, 188.

Ueda, K. (1960). Studies on the physiology of bamboo, with reference to practical application. *Bulletin of the Kyoto university forests*, 30:1–167.

Van Den Besselaar, E. J., Klein Tank, A. M., Van Der Schrier, G., Abass, M. S., Baddour, O., Van Engelen, A. F., Freire, A., Hechler, P., Laksono, B. I., Jilderda, R., et al. (2015). International climate assessment & dataset: climate services across borders. *Bulletin of the American Meteorological Society*, 96(1):16–21.

Vandegehuchte, M. W. and Steppe, K. (2012). Improving sap flux density measurements by correctly determining thermal diffusivity, differentiating between bound and unbound water. *Tree Physiology*, 32(7):930–942.

Vandegehuchte, M. W. and Steppe, K. (2013). Corrigendum to: Sap-flux density measurement methods: working principles and applicability. *Functional Plant Biology*, 40(10):1088–1088.

Vergeynst, L. L., Vandegehuchte, M. W., McGuire, M. A., Teskey, R. O., and Steppe, K. (2014). Changes in stem water content influence sap flux density measurements with thermal dissipation probes. *Trees*, 28(3):949–955.

Wang, H., Zhao, P., Hölscher, D., Wang, Q., Lu, P., Cai, X. A., and Zeng, X. P. (2012). Nighttime sap flow of acacia mangium and its implications for nighttime transpiration and stem water storage. *Journal of Plant Ecology*, 5(3):294–304.

Wang, Y. H., Dong, M., Yu, F. H., Jiang, H., Yu, S. Q., Lin, X. Q., and He, W. M. (2011a). Mechanical shaking and soil water affect the growth of psammochloa villosa in the mu us sandland. *Journal of Arid Environments*, 75(10):974–977.

Wang, Z., Li, Y., During, H. J., and Li, L. (2011b). Do clonal plants show greater division of labour morphologically and physiologically at higher patch contrasts? *Plos One*, 6(9):e25401.

Waring, R. and Running, S. (1978). Sapwood water storage: its contribution to transpiration and effect upon water conductance through the stems of old-growth douglas-fir. *Plant, Cell & Environment*, 1(2):131–140.

Waring, R. H., Whitehead, D., and Jarvis, P. G. (1979). The contribution of stored water to transpiration in scots pine. *Plant, Cell & Environment*, 2(4):309–317.

Wickens, G. E. (1982). The baobab: Africa's upside-down tree. *Kew Bulletin*, 37(2):173–209.

Worbes, M., Blanchart, S., and Fichtler, E. (2013). Relations between water balance, wood traits and phenological behavior of tree species from a tropical dry forest in costa rica–a multifactorial study. *Tree Physiology*, 33(5):527.

Wullschleger, S. D., Childs, K. W., King, A. W., and Hanson, P. J. (2011). A model of heat transfer in sapwood and implications for sap flux density measurements using thermal dissipation probes. *Tree Physiology*, 31(6):669–679.

Wullschleger, S. D., Hanson, P. J., and Todd, D. E. (1996). Measuring stem water content in four deciduous hardwoods with a time-domain reflectometer. *Tree Physiology*, 16(10):809–815.

Wullschleger, S. D., Meinzer, F. C., and Vertessy, R. A. (1998). A review of whole-plant water use studies in tree. *Tree physiology*, 18(8–9):499.

Wullschleger, S. D. and Norby, R. J. (2001). Sap velocity and canopy transpiration in a sweetgum stand exposed to free-air co2 enrichment (face). *New Phytologist*, 150(2):489–498.

Yang, S.-J., Zhang, Y.-J., Goldstein, G., Sun, M., Ma, R.-Y., and Cao, K.-F. (2015). Determinants of water circulation in a woody bamboo species: afternoon use and night-time recharge of culm water storage. *Tree Physiology*, 35(9):964–974.

Yang, S.-J., Zhang, Y.-J., Sun, M., Goldstein, G., and Cao, K.-F. (2012). Recovery of diurnal depression of leaf hydraulic conductance in a subtropical woody bamboo species: embolism refilling by nocturnal root pressure. *Tree Physiology*, 32(4):414–422.

Zanne, A. E., Lopez-Gonzalez, G., Coomes, D. A., Ilic, J., Jansen, S., Lewis, S. L., Miller, R. B., Swenson, N. G., Wiemann, M. C., and Chave, J. (2009). Global wood density database. *Plant Economics*.

Zhang, Y., Zhang, Q., and Marek, S. (2012). Physiological integration ameliorates negative effects of drought stress in the clonal herb fragaria orientalis. *Plos One*, 7(9):e44221.

Zhao, X.-H., Zhao, P., Zhang, Z.-Z., Zhu, L.-W., Niu, J.-F., Ni, G.-Y., Hu, Y.-T., and Ouyang, L. (2016). Sap flow-based transpiration in *Phyllostachys pubescens*: applicability of the tdp methodology, age effect and rhizome role. *Trees*, pages 1–15.

Zimmermann, M. H. and Tomlinson, P. B. (1972). The vascular system of monocotyledonous stems. *Botanical Gazette*, 133(2):141–155.

# List of figures

# List of tables

**Appendix**

**Appendix Chapter 2**

Table A.1 The influence of the three factors formula type, time step and formula specificity on the performance of the linear calibration model. Results of multi-ANOVA of the three factors against normalized Root-Mean-Square Error (nRMSE).

| Source | DF | Type SS | Mean Square | F value | $P$ |
|---|---|---|---|---|---|
| Formula type | 1 | 0.0046 | 0.0046 | 0.68 | 0.4093 |
| Time step | 3 | 0.0046 | 0.0015 | 0.23 | 0.8777 |
| Formula specificity | 2 | 7.7675 | 3.8838 | 577.54 | <0.0001 |

Note: nRMSE, calculated by normalizing the RMSE with the observed range of sap flux densities from stem heat balance (SHB) measurements; RMSE derived from SHB measurements vs. model-predicted values of each day. Data of 63 days were used. $P < 0.01$ indicates significant difference.

Table A.2 Performance of culm-specific vs. species-specific vs. common linear formulas for a simple linear field calibration of the thermal dissipation probe (TDP) method with the stem heat balance (SHB) method on four bamboo species Normalized Root-Mean-Square Errors (nRMSE) and passing rates of the Wilcoxon Signed-Rank test for each species and formula specificity type.

| Species | Formula specificity | nRMSE | Passing rate (%) |
|---|---|---|---|
| *B. vulgaris* | common | $0.11^a$ | $83^a$ |
| | culm | $0.04^a$ | $94^a$ |
| | species | $0.10^a$ | $84^a$ |
| *G. apus* | common | $0.12^a$ | $77^a$ |
| | culm | $0.06^a$ | $90^a$ |
| | species | $0.10^a$ | $81^a$ |
| *D. asper* | common | $0.18^a$ | $74^a$ |
| | culm | $0.04^a$ | $94^a$ |
| | species | $0.18^a$ | $70^a$ |
| *G. atroviolacea* | common | $0.13^a$ | $74^a$ |
| | culm | $0.06^a$ | $89^a$ |
| | species | $0.12^a$ | $74^a$ |

Note: Superscripted letters indicate significant differences between nRMSEs and passing rates, respectively, within each species (Tukey's test, $P < 0.05$).

# Appendix Chapter 3

The thermal conductivity of the sample segments was calculated following the work of Vandegehuchte and Steppe (2013) who introduced a corrected thermal conductivity on the axial direction ($K_a$, W m$^{-1}$ K$^{-1}$) as shown in the following equation (Eq. 1).

$$K_a = K_w(\theta_{wood} - \theta_{wood-FSP})\frac{\rho_{dry}}{\rho_w} + 0.04186 \times (21.0 - 20.0 \times F_{v-FSP}) \quad (1)$$

Where $K_w$ is thermal conductivity of water (0.6 W m$^{-1}$ K$^{-1}$), $\theta_{wood-FSP}$ is $\theta_{wood}$ at fiber saturation point, $\rho_{dry}$ and $\rho_w$ are the density of dry wood and water (1000 kg m$^{-3}$), $F_{v-FSP}$ is a void fraction of wood at fiber saturation point (Eq. 2) according to Vandegehuchte and Steppe (2013):

$$F_{v-FSP} = 1 - G_b(\rho_w\rho_{cw}^{-1} + \theta_{wood-FSP}) \quad (2)$$

Where $F_{v-FSP}$ is void fraction of the wood at fiber moisture saturation point, $\rho_{cw}$ is the density of cell wall (1530 kg m$^{-3}$, Kollman and Côté, 1968; Vandegehuchte and Steppe, 2013), $G_b$ is the basic specific gravity as the function of weight of dry mass per fresh volume divided by the density of water. $\theta_{wood-FSP}$ (Eq. 3) refers to (Roderick and Berry, 2001):

$$\theta_{wood-FSP} = 0.2(\rho_d\rho_w^{-1})^{-\frac{1}{2}} \quad (3)$$

Where $\rho_{ovend}$ is the density of oven dried wood (Eq. 4) refers to (kg m$^{-3}$, Inagaki et al., 2014):

$$\rho_d = \rho_{air}(1 - F_{ovencw}) + \rho_{ovencw}F_{ovencw} \quad (4)$$

Where $\rho_{air}$ is the density of air at 20 °C (1.2 kg m$^{-3}$), $\rho_{ovencw}$ is the density of oven dried cell wall (1400 kg m$^{-3}$). $F_{ovencw}$ is the volume fraction of the oven dried cell wall (Eq. 5).

$$F_{ovencw} = w_{ovencw}\rho_{ovencw}^{-1}v_{fresh}^{-1} \quad (5)$$

Where $w_{ovencw}$ is the weight of oven-dried cell wall (kg). In this study, we assumed $w_{ovencw}$ approximately equal to the weight of oven-dried wood. $v_{fresh}$ is the volume of the fresh wood (m$^3$). The specific heat capacity of the fresh

wood was calculated following (Burgess et al., 2001a) as shown below (Eq. 6).

$$c = \frac{w_{dry}c_{dry} + c_w(w_{fresh} - w_{dry})}{w_{fresh}} \tag{6}$$

Where $c$ is heat capacity of fresh wood (J kg$^{-1}$ K$^{-1}$). $c_{dry}$ and $c_w$ are heat capacity of dry wood (1200 J kg$^{-1}$ K$^{-1}$) and water (4186 J kg$^{-1}$ K$^{-1}$) at 20 °C (Edwards and Warwick, 1984), and $w_{fresh}$ and $w_{dry}$ are weights of fresh and dry wood. Because the wood domain contains wood matrix and sap (approximately equal to water in physical properties), heat transfer in such porous media directly depends on the contact surface between the two phases. Such heat transfer is characterized by interfacial area density (IFA, Eq. 7) which is defined as the surface area per unit volume (m$^{-1}$).

$$IFA = \frac{\sqrt{4\pi P F_{v-FSP}}}{100} \tag{7}$$

Where $P$ is the number of conduits in 1 cm$^2$ of the wood which is approximately 250 for bamboos according to Mohmod and Mustafa (1992).
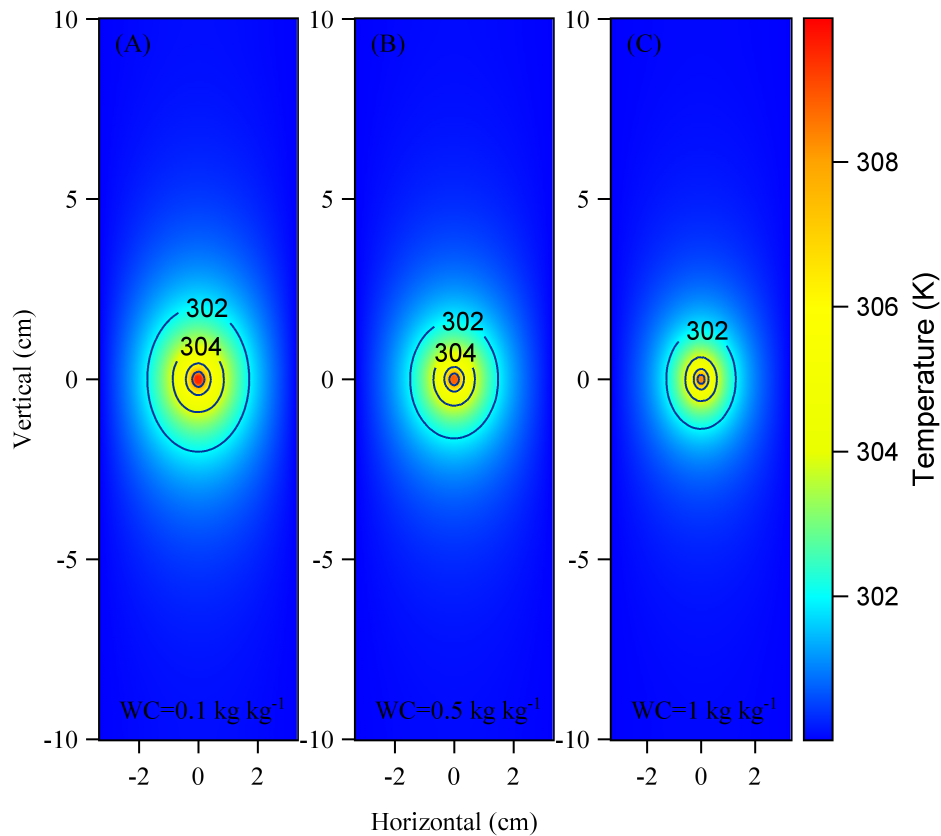
Fig. A.1 The temperature contours around the heating probe under zero sap flow conditions. The simulated bamboo segments had different water contents of 0.1 (A), 0.5 (B) and 1 kg kg$^{-1}$ (C), respectively. The ambient temperature in the model was set to 300 K. The legend shows the increase of temperature after reaching steady-state thermal conditions. The geometry and physical properties applied in the model were based on a mature culm segment of *B. vulgaris*, extracted from a culm at breast height.

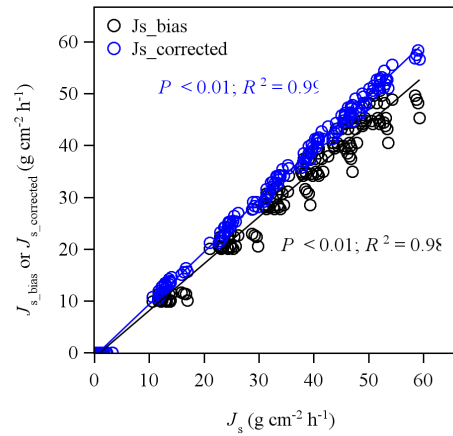Fig. A.2 The sap flux density ($J_s$) in comparison with $J_s$ calculated with the mismatched $\Delta T_{max}$ ($J_{s\_mis}$, g cm$^{-2}$ h$^{-1}$) and $J_{s\_mis}$ corrected with the correcting equation ($J_{s\_corrected}$).

# Appendix Chapter 5
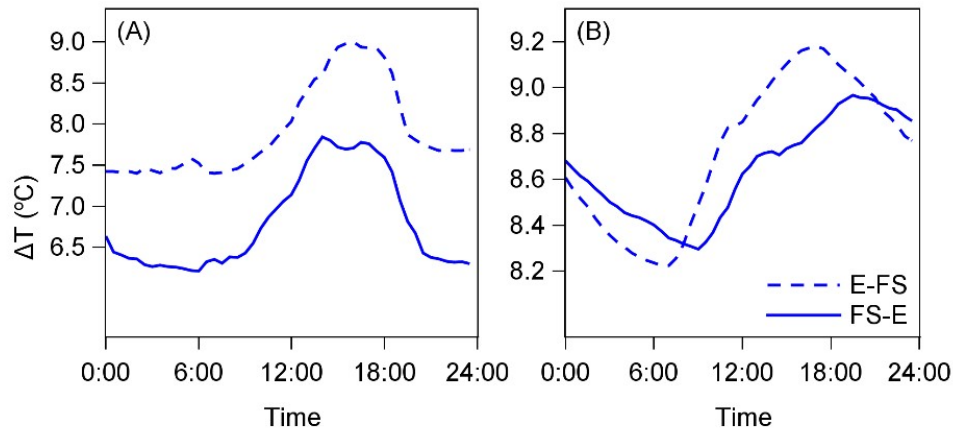
Fig. A.3 Typical diurnal patterns of temperature differences of upstream probes ($\Delta T_{E\text{-}FS}$) and downstream probes ($\Delta T_{FS\text{-}E}$) from rhizome: (A), temperature difference of downstream probes were lower than that of upstream probes ($\Delta T_{E\text{-}FS} > \Delta T_{FS\text{-}E}$); (B), temperature difference of downstream probes lagged behind that of upstream probes ($\Delta T_{E\text{-}FS}$ earlier than $\Delta T_{FS\text{-}E}$). Both scenarios implied flowing from established culm to freshly sprouted culm.



Fig. A.4 The simulated increased temperature fields ($K$) with different sap flux densities (from left to right: 0, 5, 10, 15, 20 g m$^{-2}$ s$^{-1}$). The values on x and y axis stand for the distances from the heating probe in tangential and axial directions, respectively.

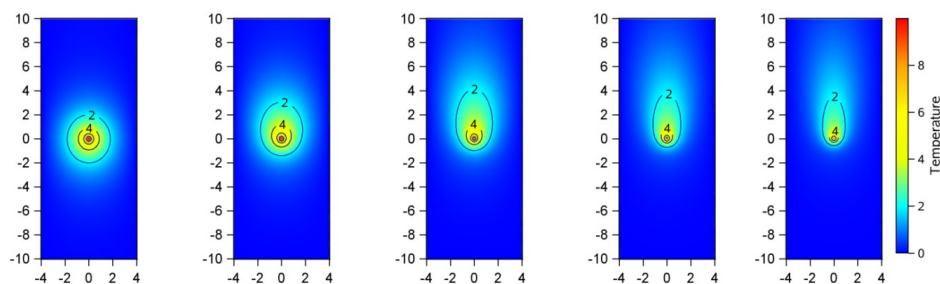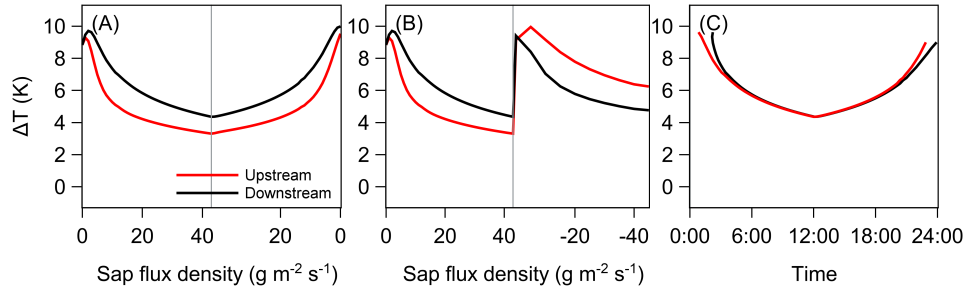Fig. A.5 Temperature difference ($\Delta T_{up}$ and $\Delta T_{down}$) with different sap flux densities (A) increasing from 0 to 43 g m$^{-2}$ s$^{-1}$ and then dropping down to 0 g m$^{-2}$ s$^{-1}$, (B) increasing from 0 to 43 g m$^{-2}$ s$^{-1}$ and then dropping suddenly down to 0 and increasing from 0 to 43 g m$^{-2}$ s$^{-1}$ in reverse direction, and (C) the proposed lagging patterns of temperature difference ($\Delta T_{up}$ and $\Delta T_{down}$) in scenarios (3).



Fig. A.6 The height of three monitored freshly sprouted culms of *B. vulgaris*. (B) The growth rates of the three monitored freshly sprouted culms of *B. vulgaris* in daytime vs. nighttime.

# Appendix Chapter 6

Fig. A.7 Deuterium concentration in transpired water over the duration of the experiment.

Table A.3 Overview and key findings of studies applying deuterium tracing.

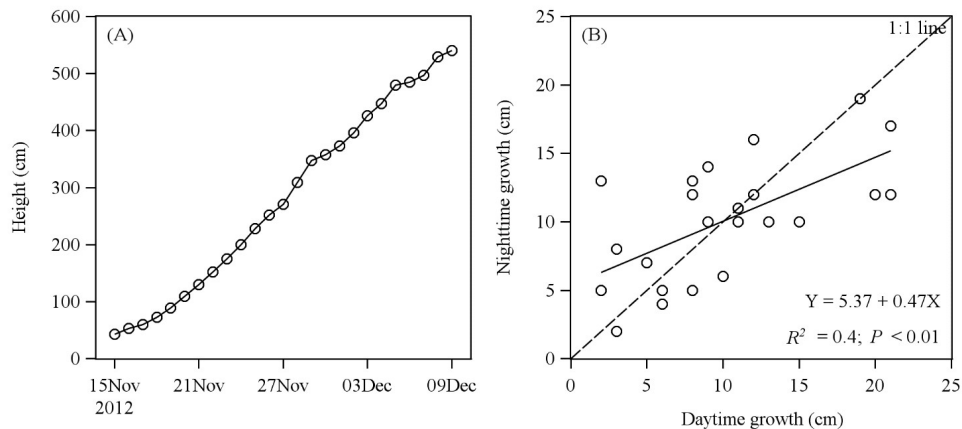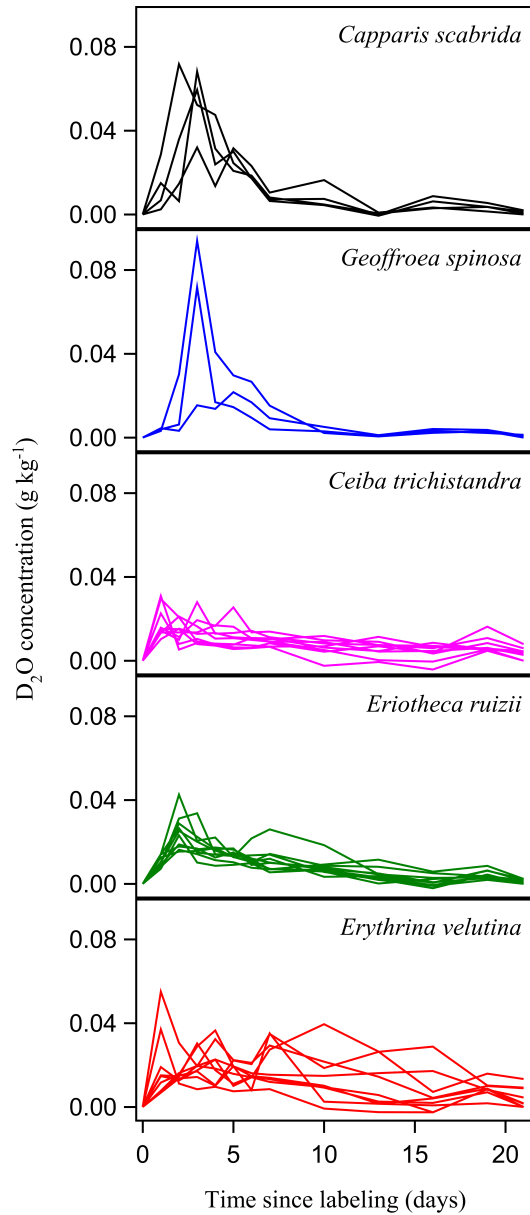| Species | Location | N | DBH (cm) | Height (m) | Injected $D_2O$ (g tree⁻¹) | $T_{arrival}$ (days) | $T_{max}$ (days) | $T_{residence}$ (days) | $V_{D_2O}$ (m day⁻¹) | $WU_{D_2O}$ (kg day⁻¹) | $J_s$ (g cm⁻² day⁻¹) | Reference |
|---|---|---|---|---|---|---|---|---|---|---|---|---|
| *Capparis scabrida* | Ecuador | 4 | 19.7 (5.4) | 7.4 (1.5) | 30.9 (8.4) | 1.3 (0.5) | 2.8 (0.5) | 14.3 (4.2) | 6.3 (1.6) | 136.2 (56.7) | 12.1 (4.4) | This study |
| *Geoffroea spinosa* | Ecuador | 4 | 28.2 (4.9) | 7.9 (0.6) | 44.3 (7.7) | 1.8 (1.0) | 3.5 (1.0) | 10.8 (6.3) | 5.6 (2.7) | 300.4 (130.9) | | This study |
| *Erythrina velutina* | Ecuador | 9 | 27.9 (9.3) | 10.1 (3.6) | 13.9 (4.6) | 1.0 (0) | 4.4 (3.0) | 19.2 (3.9) | 10.1 (3.6) | 71.5 (48.0) | 8.2 (2.1) | This study |
| *Eriotheca ruizii* | Ecuador | 10 | 56.4 (17.3) | 13.1 (3.3) | 28.2 (8.7) | 1.0 (0) | 2.3 (0.7) | 18.8 (2.4) | 13.1 (3.3) | 173.6 (47.4) | 9.1 (3.5) | This study |
| *Ceiba trichistandra* | Ecuador | 11 | 77.9 (13.7) | 15.5 (4.6) | 38.9 (6.9) | 1.0 (0) | 2.6 (2.0) | 19.5 (3.9) | 15.5 (4.6) | 270.4 (170.7) | 8.9 (3.6) | This study |
| *Eucalyptus teretecornis* | Southern India | 2 | 4.9 (0.0) | 7.0 (0.0) | 2.3 (1.1) | 1.0 (0.0) | 2.3 (0.5) | 6.0 (0.0) | 7.0 (0.0) | 3.7 (0.0) | | Calder et al. 1986 |
| *Eucalyptus teretecornis* | Southern India | 2 | 4.0 (1.0) | | 18.6 (8.9) | 1.5 (0.7) | 2.5 (0.7) | 6.0 (1.4) | | 4.6 (1.8) | | Calder et al. 1992 |
| *Eucalyptus gunnii* | UK | 1 | 5.0 (.) | 2.5 (.) | 4.0 (.) | 1.0 (.) | 2.0 (.) | 5.0 (.) | 2.5 (.) | 2.5 (.) | | Dugas et al. 1993 |
| *Prunus serrulata* | UK | 3 | 2.0 (0.0) | 2.0 (0.0) | 1.0 (0.0) | 1.3 (0.6) | 2.0 (0.0) | 3.3 (0.6) | 1.7 (0.6) | 0.9 (0.2) | | Dugas et al. 1993 |
| *Eucalyptus grandis* | South Africa | 2 | 14.5 (4.9) | 15.7 (10.6) | 18.6 (8.9) | 0.8 (0.4) | 1.5 (0.8) | 7.5 (6.2) | 19.8 (4.8) | 80.5 (19.1) | | Dye et al. 1992 |
| *Acer saccharum* | USA | 2 | 25.5 (10.6) | 14.6 (3.0) | 39.8 (16.5) | 4.1 (2.8) | 9.5 (3.5) | 13.3 (4.9) | 1.5 (0.3) | | | Gaines et al. 2016 |
| *Carya tomentosa* | USA | 3 | 33.0 (11.1) | 19.9 (0.3) | 51.8 (16.9) | 2.3 (2.2) | 3.7 (2.3) | 11.0 (1.5) | 8.6 (8.2) | | | Gaines et al. 2016 |
| *Quercus prinus* | USA | 3 | 36.7 (10.6) | 18.3 (1.4) | 57.6 (16.8) | 3.3 (2.1) | 4.3 (2.1) | 10.9 (9.3) | 4.9 (2.7) | | | Gaines et al. 2016 |
| *Quercus rubra* | USA | 3 | 40.7 (10.1) | 17.0 (2.6) | 64.1 (16.2) | 3.5 (3.0) | 3.7 (2.9) | 17.4 (5.0) | 6.1 (3.4) | | | Gaines et al. 2016 |
| *Anacardium excelsum* | Panama | 1 | 98.0 (.) | 38.0 (.) | 120.0 (.) | 3.0 (.) | 4.0 (.) | 25.0 (.) | 12.7 (.) | | 114.0 (.) | James et al. 2003 |
| *Cordia alliodora* | Panama | 1 | 34.0 (.) | 26.0 (.) | 45.0 (.) | 1.0 (.) | 2.0 (.) | 5.0 (.) | 26.0 (.) | | 66.0 (.) | James et al. 2003 |
| *Ficus insipida* | Panama | 1 | 65.0 (.) | 28.0 (.) | 125.0 (.) | 2.0 (.) | 4.0 (.) | 9.0 (.) | 14.0 (.) | | 107.0 (.) | James et al. 2003 |
| *Schefflera morototoni* | Panama | 1 | 47.0 (.) | 22.0 (.) | 65.0 (.) | 5.0 (.) | 8.0 (.) | 26.0 (.) | 4.4 (.) | | 72.0 (.) | James et al. 2003 |
| *Eucalyptus grandis* | Australia | 3 | 10.7 (3.5) | 10.1 (4.8) | 1.4 (1.1) | 1.7 (0.6) | 3.7 (1.5) | 11.3 (4.0) | 5.8 (1.1) | 14.2 (8.3) | | Kalma et al. 1998 |
| *Ceriops tagal* | Mayotte Island | 3 | 7.5 (0.9) | 2.9 (0.3) | 2.8 (0.3) | 2.4 (0.3) | 5.6 (2.1) | 10.4 (1.2) | 1.2 (0.2) | 8.6 (1.3) | | Lambs et al. 2011 |
| *Rhizophora mucronata* | Mayotte Island | 2 | 17.5 (6.4) | 6.3 (1.8) | 4.5 (0.7) | 3.3 (0.1) | 7.1 (0.0) | 14.6 (3.0) | 1.7 (0.5) | 14.2 (4.9) | | Lambs et al. 2011 |
| *Fagus sylvatica* | France | 3 | 10.9 (4.1) | 6.5 (1.0) | 4.0 (0.6) | 4.0 (0.0) | 5.7 (0.6) | 14.0 (1.0) | 1.6 (0.3) | 9.9 (6.6) | | Marc and Robinson 2004 |
| *Pseudotsuga menziesii* | USA | 6 | 53.7 (56.2) | 27.7 (22.0) | 78.7 (82.5) | 6.3 (5.1) | 9.0 (6.4) | 50.0 (19.2) | 4.6 (0.8) | 87.5 (18.9) | | Meinzer et al. 2006 |
| *Tsuga heterophylla* | USA | 2 | 91.0 (2.8) | 53.0 (4.2) | 134.0 (1.4) | 19.0 (2.8) | 25.0 (7.1) | 59.0 (2.8) | 2.8 (0.6) | 43.5 (23.3) | | Meinzer et al. 2006 |
| *Bambusa blumeana* | Philippines | 4 | 10.0 (1.0) | 19.8 (0.7) | 10.0 (0.0) | 3.1 (1.4) | 4.8 (1.6) | 11.5 (4.3) | 8.5 (6.4) | 63.0 (29.1) | 90.0 (37.0) | Schwendenmann et al. 2010 |
| *Gliricidia sepium* | Indonesia | 6 | 13.0 (2.0) | 10.6 (3.3) | 29.3 (6.6) | 1.7 (0.8) | 2.3 (0.8) | 6.4 (0.8) | 6.3 (2.6) | 95.0 (33.5) | 146.0 (39.0) | Schwendenmann et al. 2010 |
| *Shorea contorta* | Philippines | 5 | 18.0 (7.0) | 16.1 (3.5) | 28.0 (11.0) | 0.9 (0.0) | 0.9 (0.1) | 4.5 (0.3) | 18.1 (4.0) | 185.0 (146.9) | 115.0 (42.0) | Schwendenmann et al. 2010 |
| *Shorea polysperma* | Philippines | 5 | 14.0 (2.0) | 13.3 (1.7) | 20.0 (0.0) | 0.9 (0.0) | 1.1 (0.0) | 3.8 (0.6) | 14.9 (2.0) | 74.1 (25.6) | 75.0 (13.0) | Schwendenmann et al. 2010 |
| *Swietenia macrophylla* | Philippines | 5 | 15.0 (1.0) | 14.2 (1.5) | 20.0 (0.0) | 0.9 (0.0) | 0.9 (0.0) | 3.9 (0.3) | 15.9 (1.7) | 162.2 (23.2) | 173.0 (20.0) | Schwendenmann et al. 2010 |
| *Theobroma cacao* | Indonesia | 6 | 10.0 (1.0) | 4.2 (0.6) | 14.3 (2.8) | 1.7 (0.5) | 2.3 (0.5) | 5.1 (0.9) | 2.5 (0.6) | 27.6 (4.4) | 135.0 (32.0) | Schwendenmann et al. 2010 |

# Declaration

I hereby declare that I am the sole author of this dissertation entitled "WATER USE, STORAGE AND TRANSFER IN TROPICAL BAMBOOS". All the references and data sources that were used in this dissertation have been acknowledged. I further declare that this work has never been submitted in any forms as part of any other dissertation procedure.

Göttingen, December 2017 _____

submitted by
Dongming Fang
December 2017

# Acknowledgements

First and foremost, I want to give my highest gratitude to my supervisor Prof. Dr. Dirk Hölscher for his selfless, patient guidance and generous support on my doctoral study. With his ingenious design and continuous endeavor, I can overcome the difficulties to finish the fieldwork in Indonesia, and the analysis and publication work in Göttingen. I learned a lot from him either on how to work or on how to live.

Many thanks to our considerate department secretary Eva Siegelkow for her every help on each administrative thing, and also our warmhearted technician Mr. Reinhard köpp for his timely and professional technical support on everything I needed. Thanks to all the current and former (Niu, Hombe, Afik, Hong, ...) colleagues in the department of tropical silviculture and forest ecology for all the help and accompanying over the last four years. Particularly, I want to thank my friend and also close collaborator - Alexander Röll, for all the selfless, timely and professional help in the field work and the revising on paper-writing.

I also want to thank Prof. Dr. Hendrayanto from Faculty of Forestry in Bogor Agriculture University, and his smart and hard-working student - Wahyu Iskandar. Without their close collaboration, I cannot fulfill the experiments in IPB so smoothly. Only with their help, we can resolve the difficulties in the laboratory and field supporting equipment and find the capable workers: Maksum, Manda, Popi, Nizar, Yanuar, Soni, Dina.

Thanks to all the friends either in Göttingen or in China, with your accompanying and encouragement, I have been very enjoyable during these years.

I am grateful to my father and parents-in-law and siblings for your emotional support all the time. Special to my forever hopeful and optimistic late mom Shuzhen Song: she always asked me to be calm and concentrated under any circumstance.

At last, I want to give my heartfelt gratefulness to my beloved wife, Tingting Mei. Without you, I will never understand so profoundly and thoroughly

on how vital the mutual support is for spouses; without you, I could not get through all the difficult time I have met in China, Indonesia and Göttingen, especially the time when my mom passed away. Now I can say that we can realize the initial goal - harvesting the doctorate together. I'd like to keep going with you for the rest of my life.

# Curriculum vitae

**Dongming Fang**

## *Basic information*

| | |
|---|---|
| Gender | Male |
| Email | dongmingf@gmail.com |
| Date of birth | 09 Dec. 1984 |
| Place of birth | Hebei, China |
| Citizenship | Chinese |

## *High educations*

PhD (2013.10-)  *Plant Ecophysiology*, Department of Tropical Silviculture and Forest Ecology, Georg-August-Universität Göttingen.

Master (2008.09-2011.07)  *Global ecology*, Institute of Botany, Chinese Academy of Sciences, Beijing, China.

Bachelor (2004.09-2008.07)  *Forestry*, College of Forestry, Northeast Forestry University, Harbin, China.

## *Publications*

Tingting Mei, **Dongming Fang**[†], Alexander Röll, Dirk Hölscher (2017) The influence of bamboo culm water content on sap flux measurements by thermal dissipation probes: observations and modeling. *Trees*, DOI: 10.1007/s00468-017-1641-4 ([†] Shared first authorship)

Tingting Mei, **Dongming Fang**[†], Alexander Röll, Furong Niu, Hendrayanto, Dirk Hölscher (2016) Water Use Patterns of Four Tropical Bamboo Species

Assessed with Sap Flux Measurements. *Frontiers in plant science*, 6, 1202.
($^\dagger$ Shared first authorship)

**Dongming Fang**, Guangsheng Zhou, Yanling Jiang, Bingrui Jia, Zhenzhu Xu,
Xinghua Sui (2012) Impact of fire on carbon dynamics of Larix gmelinii
forest in Daxing'an mountains of northeast China: A simulation with CEN-
TURY model. *Chinese journal of applied ecology*, 23(9): 2411-2421. (In
Chinese)